

APPENDIX B

- (i) Pulse Velocity of Concrete
- (ii) Hardened Air Content of Concrete
- (iii) Deicer Penetration Profile in Concrete Using Disc Samples
- (iv) Freeze-Thaw Performance of Concrete
- (v) Reactivity of Aggregates from Airfield Pavements

Appendix B: Physical Properties of Cores

Part 1: Pulse Velocity

Introduction

The pulse velocity part of this study was done in order to determine the consistency of the cores with respect to density and strength on a comparative scale between the eight different airfield pavements.

Method

Pulse Velocity readings were taken on all airfield cores upon arrival to Clemson University. All of these readings were taken according to ASTM C 597 the *Standard Test Method for Pulse Velocity Through Concrete*. A solid bar of aluminum having the dimensions of 3"x 3" x 11 1/4" was used as a calibration standard and was tested prior to all readings to make sure the unit was acting in a consistent manner. The coupling agent used was petroleum jelly. The readings were taken across the diameter of the core at two-inch increments for the full length of the core sample. If the sample was an unbroken cylinder and the top and bottom surface were flat and parallel then lengthwise readings were taken.

Results

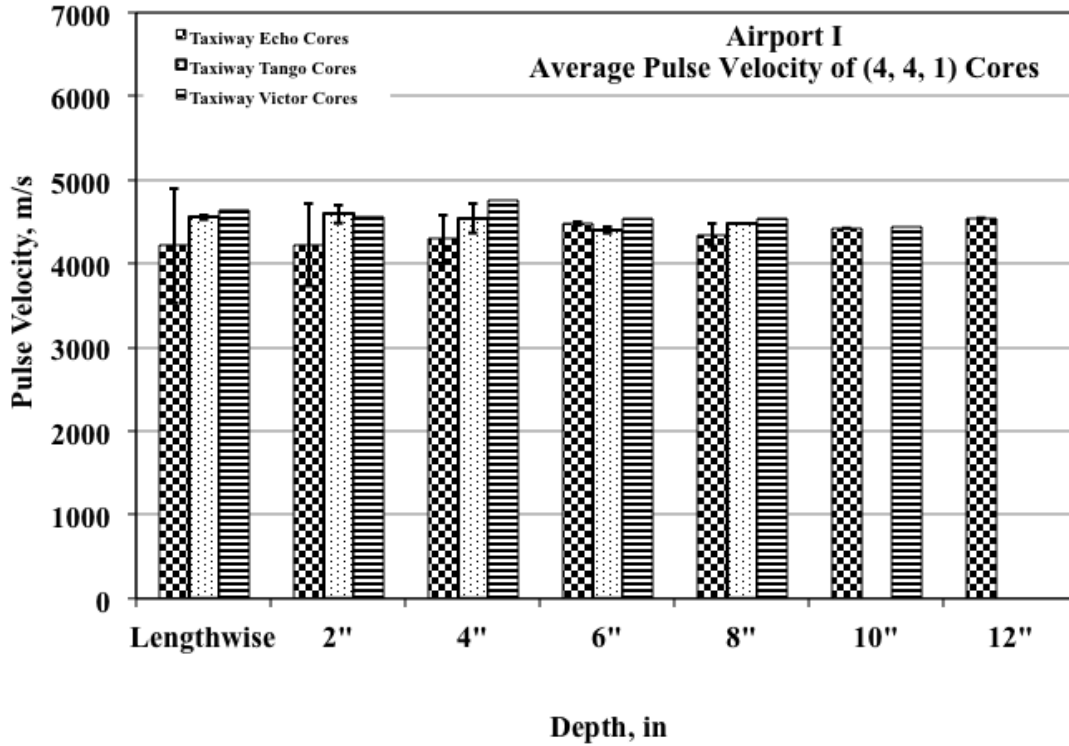


Figure 1: Pulse Velocity Results for Airport I

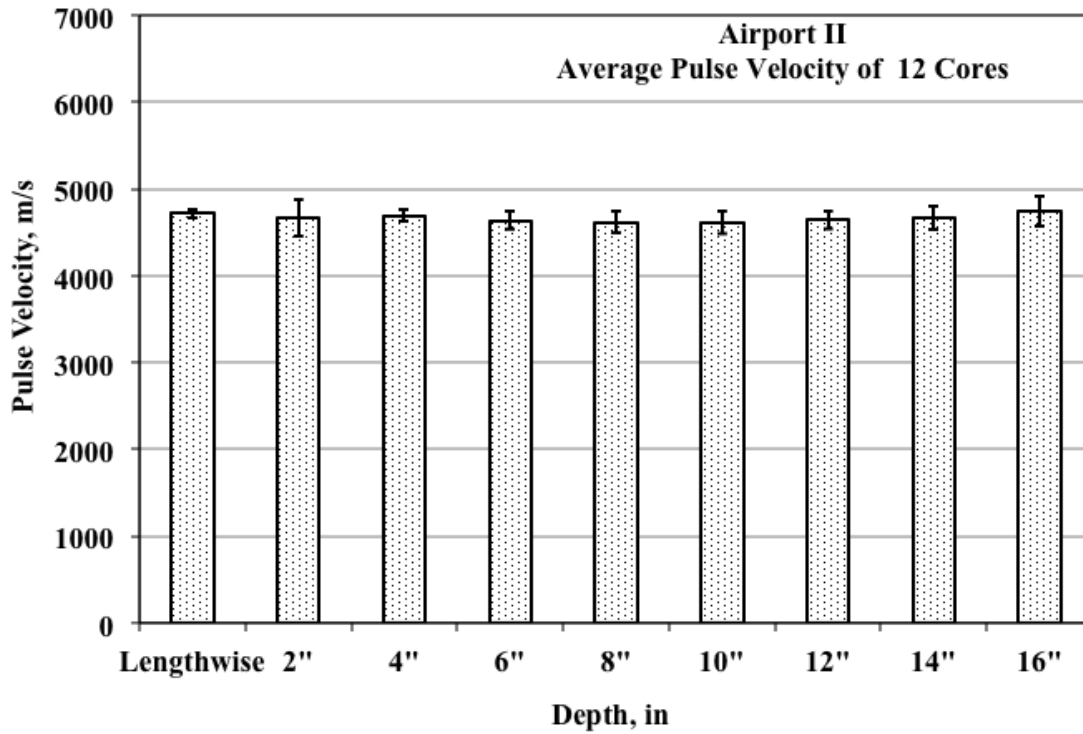


Figure 2: Pulse Velocity Results for Airport II

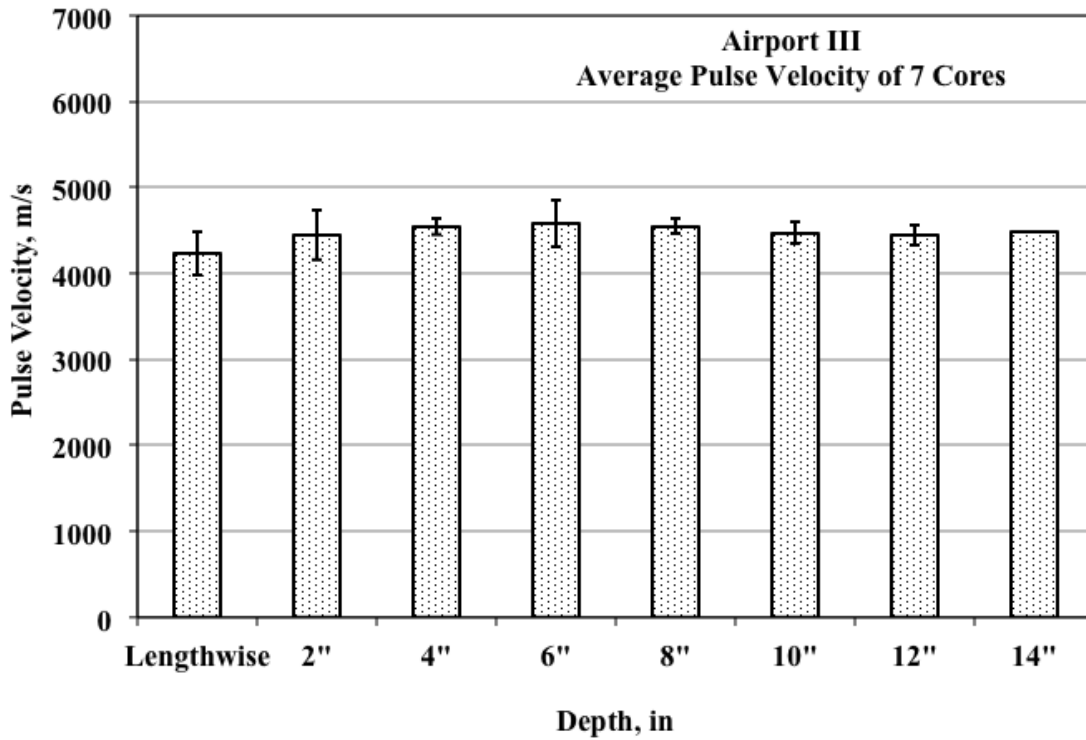


Figure 3: Pulse Velocity Results for Airport III

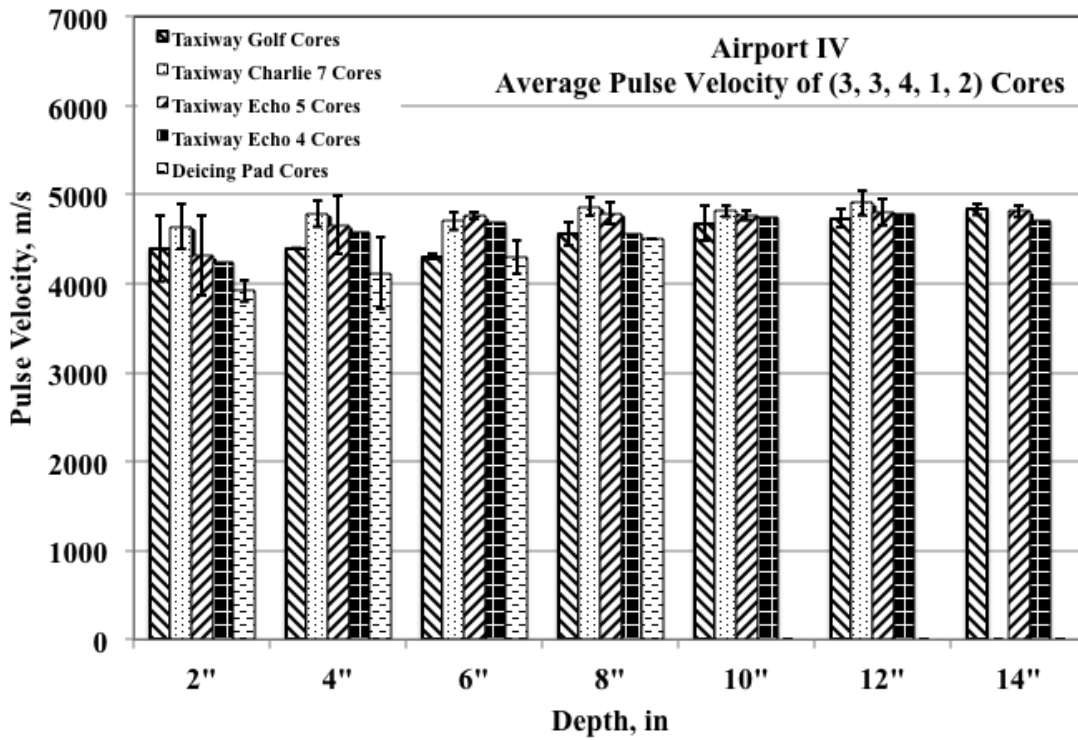


Figure 4: Pulse Velocity Results for Airport IV

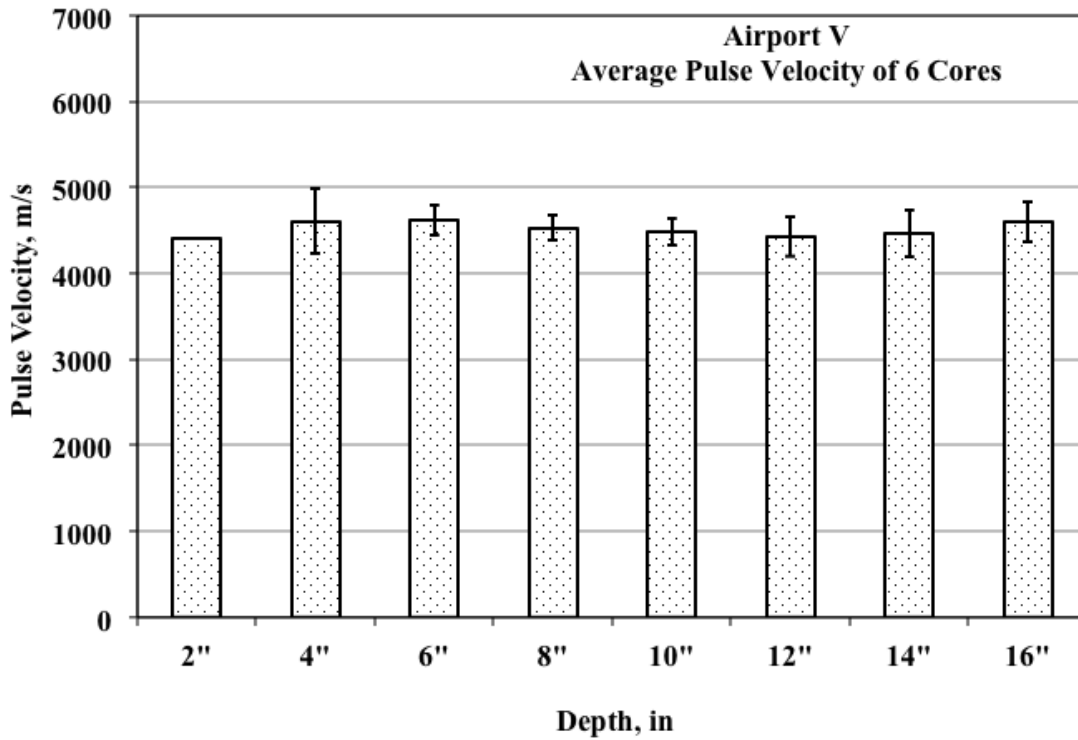


Figure 5: Pulse Velocity Results for Airport V

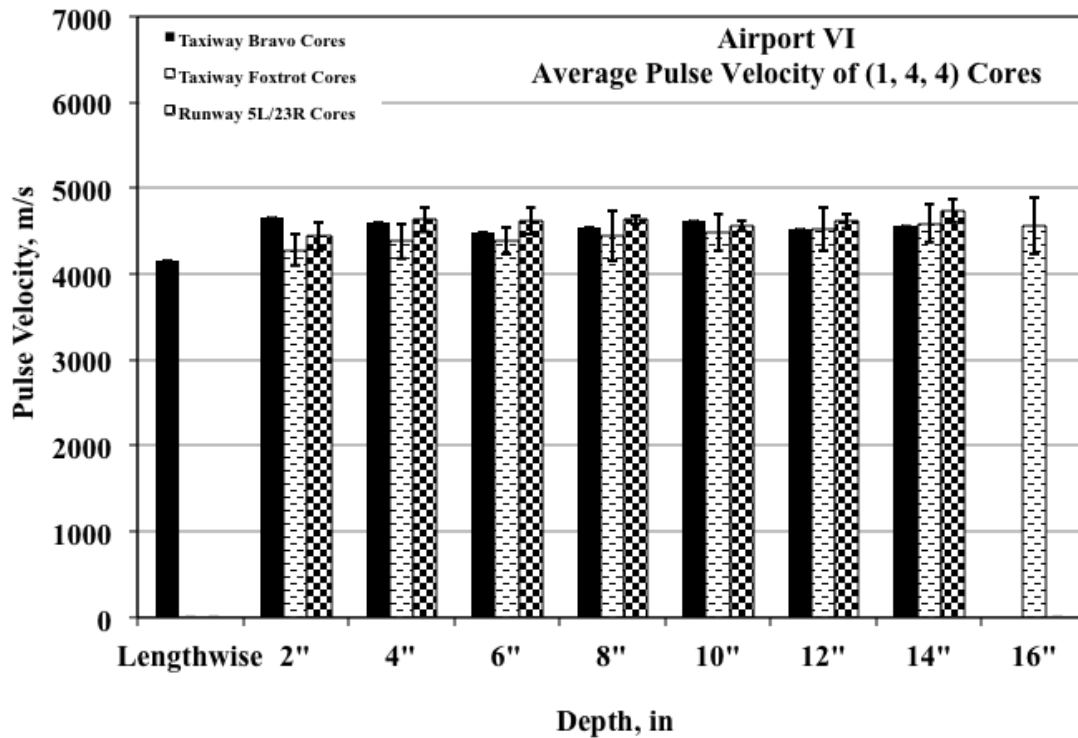


Figure 6: Pulse Velocity Results for Airport VI

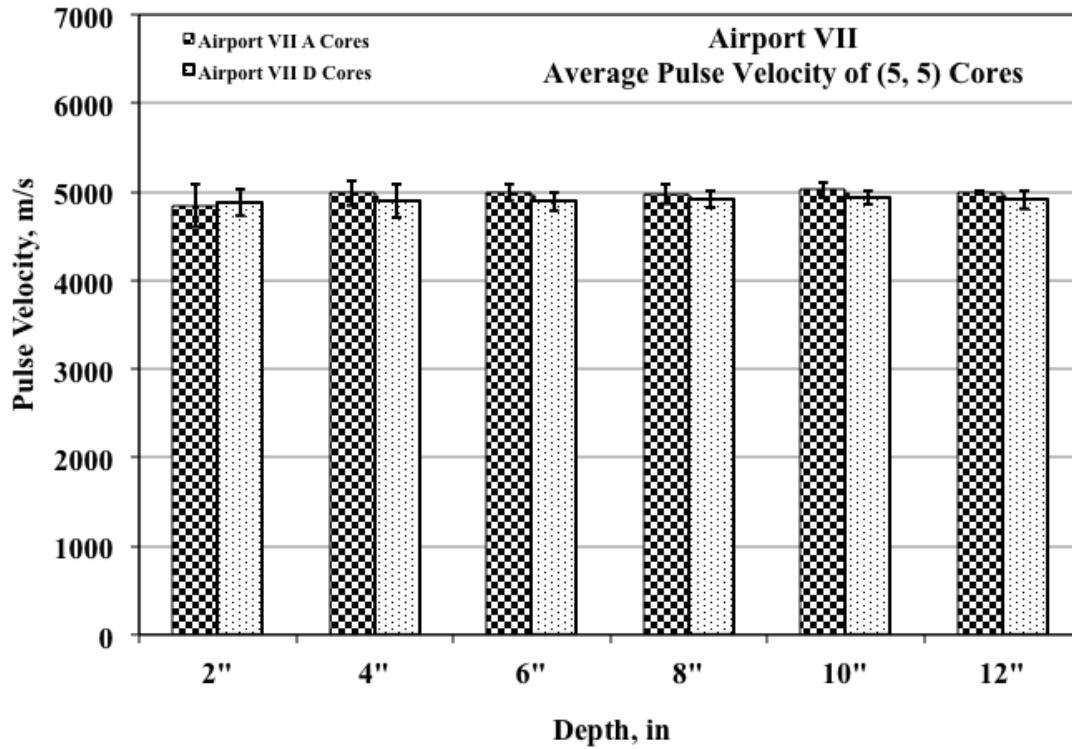


Figure 7: Pulse Velocity Results for Airport VII

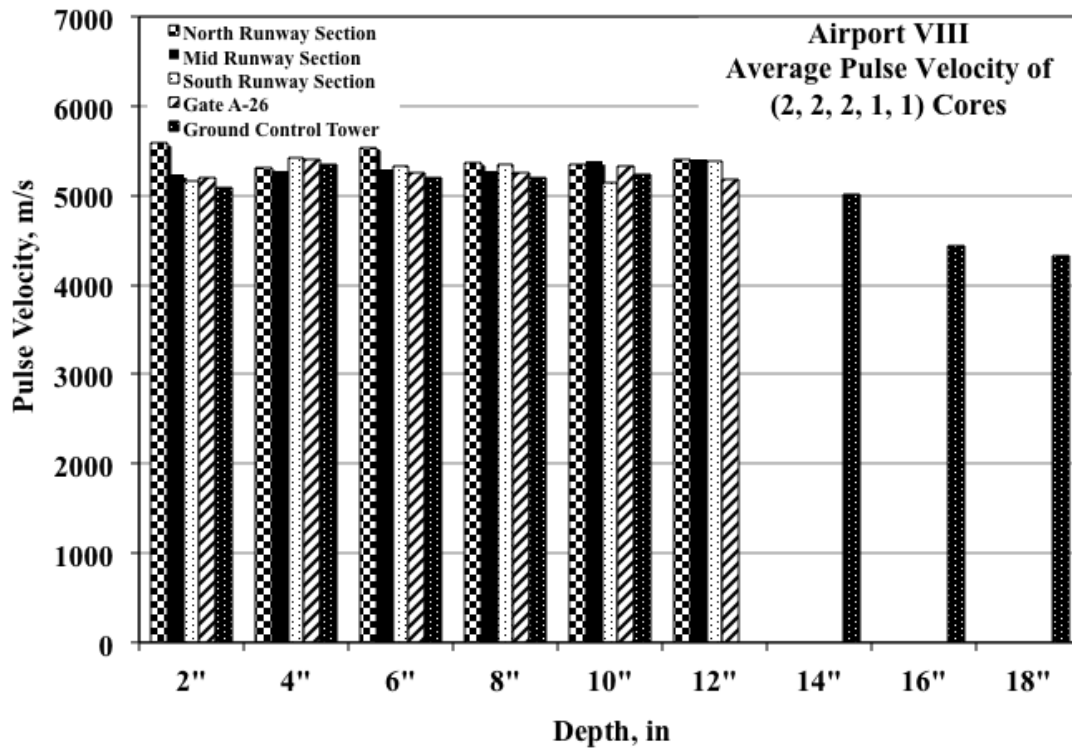


Figure 8: Pulse Velocity Results for Airport VIII

Table 1: Modulus of Elasticity Values for All Airport Cores

Label	Longitudinal Modulus of Elasticity (psi)	Transverse Avg. Modulus of Elasticity (psi)
Airport I-Echo	5.76E+06	6.25E+06
Airport I-Tango	6.53E+06	6.38E+06
Airport I-Victor	6.82E+06	6.62E+06
Airport II	7.60E+06	7.42E+06
Airport III	5.35E+06	6.08E+06
Airport IV-Golf	NA	6.39E+06
Airport IV-Charlie 7	NA	7.05E+06
Airport IV-Echo 5	NA	6.79E+06
Airport IV-Echo 4	NA	6.54E+06
Airport IV-Deicing Pad	NA	5.44E+06
Airport V	NA	6.20E+06
Airport VI-Bravo	5.13E+06	6.19E+06
Airport VI-Foxtrot	NA	6.31E+06
Airport VI-Runway 5L/23R	NA	6.44E+06
Airport VII-A Cores	NA	7.62E+06
Airport VII-B Cores	NA	7.90E+06
Airport VIII-North Section	NA	9.94E+06
Airport VIII-Mid Section	NA	9.45E+06
Airport VIII-South Section	NA	8.76E+06
Airport VIII-Gate	NA	9.28E+06
Airport-Ground Control	NA	9.05E+06

Discussion

From the data it is evident that the variability in pulse velocity in concrete cores from each of the airports was very minimal. In general, the pulse velocities for all the cores ranged between 4000 m/sec and 5500 m/sec. Also, no significant differences in pulse velocity between longitudinal and transverse direction were observed in cores from any of the airports that could be tested in both directions. No clear trend in pulse velocities could be established as a function of depth from the top surface of the pavement in any of the cores. The dynamic modulus of elasticity of cores based on the length-wise and diameter-wise measurements of pulse velocity are given in Table 1. The values were calculated using Equation 1 and converted to units of psi.

Equation 1: Modulus of Elasticity Calculation

$$E = \frac{V^2 r(1 + m)(1 - 2m)}{(1 - m)}$$

Where: E = Modulus of Elasticity

V = Pulse Velocity

ρ = Density

μ = Poisson's Ratio (assumed to be 0.18 for all samples)

Conclusion

Pulse velocity results were pretty much consistent throughout all of the airfield cores. In general, the pulse velocities for all the cores ranged between 4000 m/sec and 5000 m/sec. The Modulus of Elasticity values calculated from the pulse velocity testing were consistent with the magnitude of a typical strength concrete.

Part 2: Air Content Analysis

Introduction

The hardened air content was determined for representative samples from each airfield pavement. This was done to assess what the condition of the air void system currently is for all of the airfields, which is important to know in order to determine if the concrete system is freeze-thaw durable.

Method

The air void systems of the concrete cores were determined by using *ASTM C 457: The Standard Practice for Microscopical Determination of Air-Void Content and Parameters of the Air-Void System in Hardened Concrete*. For each airfield core sample tested two samples were taken from each. The samples were taken from zero to four inches and four to eight inches. The airfield cores were cut longitudinally in half and then cut perpendicularly at four and eight inches. Once the interior of the core was exposed the observed maximum size of aggregate was determined. Having this information, the minimum test area for the ASTM C 457 method could be found by using table 1 located in the standard along with the minimum length of traverse and the minimum number of stops found in tables 2 and 3 respectively. Samples were then polished according to the standard using a silicon carbide abrasive material. A Nikon SMZ 1000 Stereomicroscope was used at 50X magnification for the procedure. The air-void system was looked at on an as it basis, that is to say that if an air-void was filled it was not included in the air content calculation.

Results

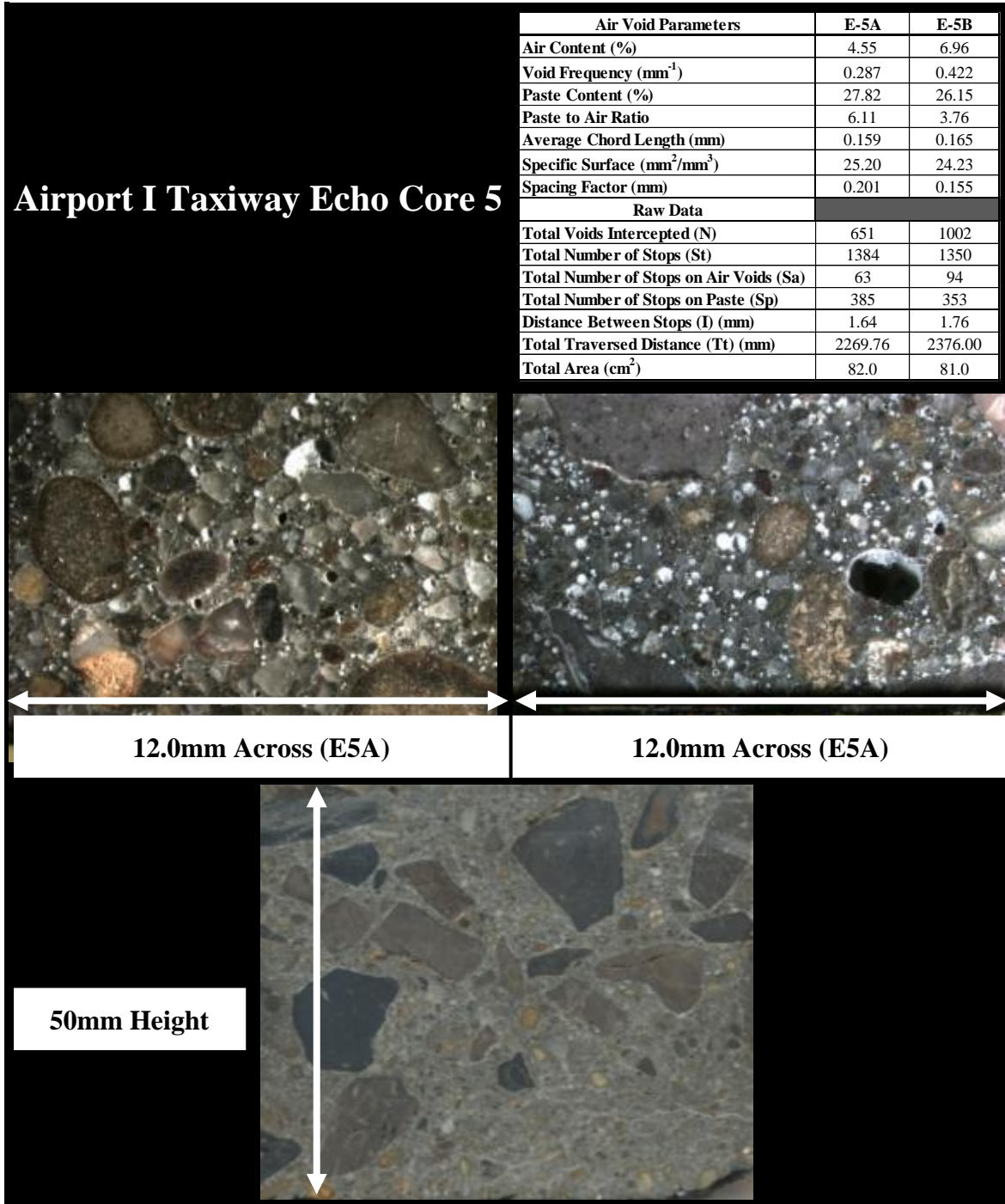


Figure 9: Airport I Echo 5 Core Air Content Results and Raw Data

Airport I Taxiway Tango Core 4

Air Void Parameters	T-4A	T-4B
Air Content (%)	5.72	4.83
Void Frequency (mm^{-1})	0.367	0.327
Paste Content (%)	24.28	21.68
Paste to Air Ratio	4.25	4.49
Average Chord Length (mm)	0.156	0.148
Specific Surface (mm^2/mm^3)	25.66	27.04
Spacing Factor (mm)	0.165	0.163
Raw Data		
Total Voids Intercepted (N)	768	836
Total Number of Stops (St)	1277	1490
Total Number of Stops on Air Voids (Sa)	73	72
Total Number of Stops on Paste (Sp)	310	323
Distance Between Stops (I) (mm)	1.64	1.72
Total Traversed Distance (Tt) (mm)	2094.28	2559.08
Total Area (cm^2)	82.0	76.6

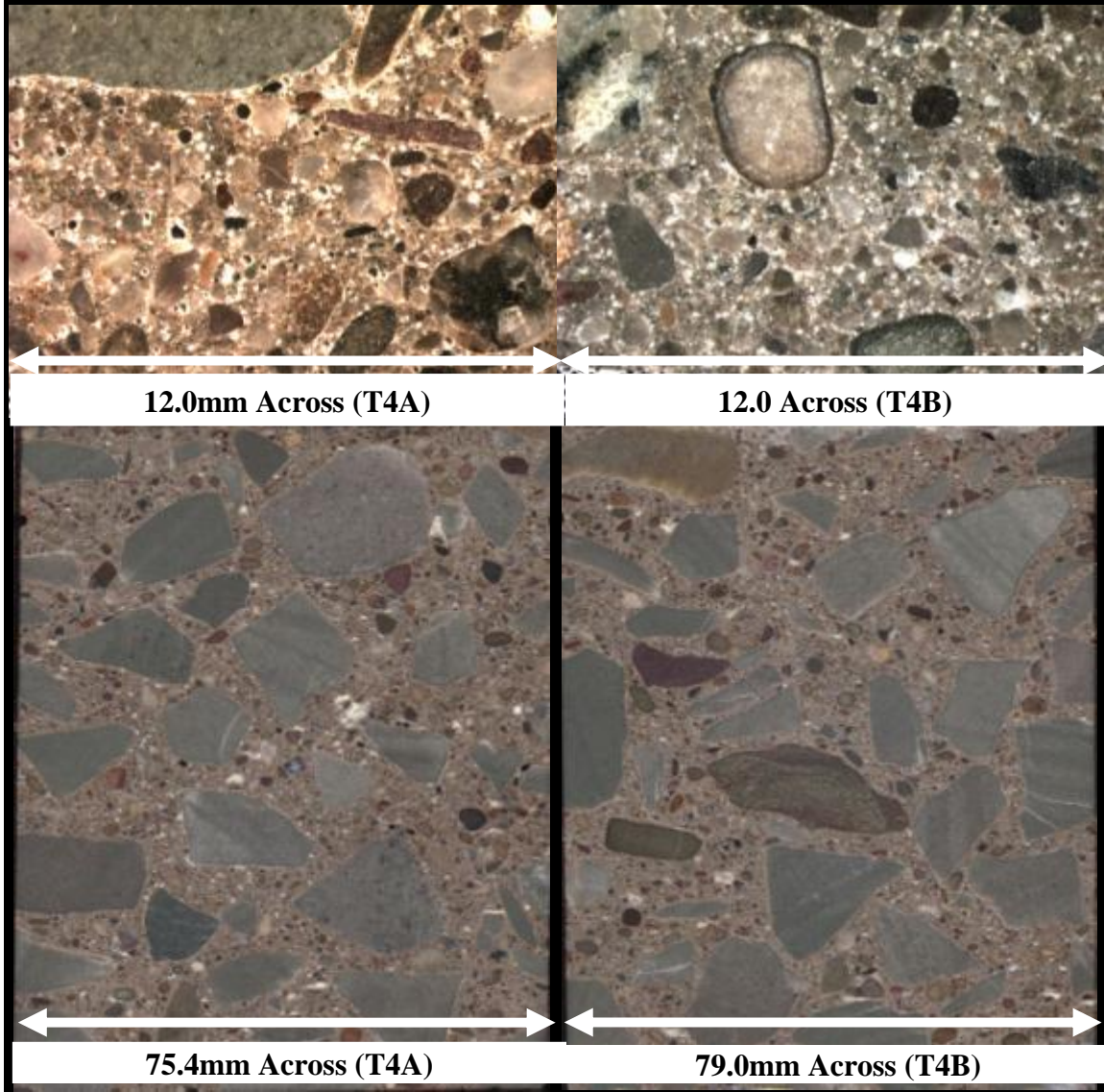


Figure 10: Airport I Tango 4 Core Air Content Results and Raw Data

Airport I Taxiway Victor Core 3

Air Void Parameters	V-3A	V-3B
Air Content (%)	4.31	5.48
Void Frequency (mm^{-1})	0.229	0.362
Paste Content (%)	30.41	25.48
Paste to Air Ratio	7.05	4.65
Average Chord Length (mm)	0.188	0.152
Specific Surface (mm^2/mm^3)	21.26	26.40
Spacing Factor (mm)	0.255	0.170
Raw Data		
Total Voids Intercepted (N)	510	801
Total Number of Stops (St)	1322	1350
Total Number of Stops on Air Voids (Sa)	57	74
Total Number of Stops on Paste (Sp)	402	344
Distance Between Stops (I) (mm)	1.68	1.64
Total Traversed Distance (Tt) (mm)	2225.92	2214.00
Total Area (cm^2)	78.4	86.0

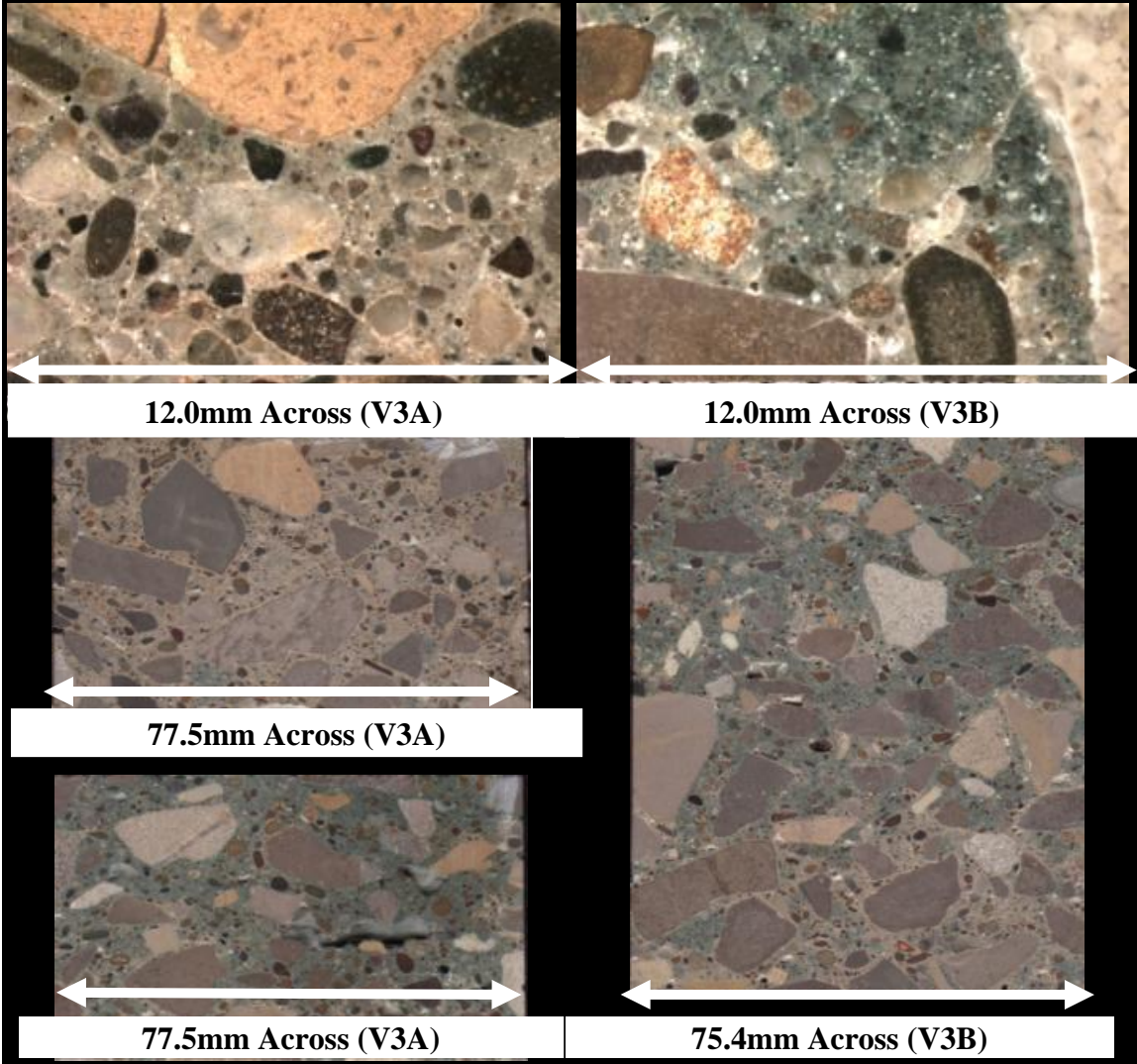


Figure 11: Airport I Victor 3 Core Air Content Results and Raw Data

Airport II Runway Core 4

Air Void Parameters	4A	4B
Air Content (%)	6.07	6.88
Void Frequency (mm^{-1})	0.427	0.519
Paste Content (%)	24.43	23.48
Paste to Air Ratio	4.02	3.41
Average Chord Length (mm)	0.142	0.133
Specific Surface (mm^2/mm^3)	28.10	30.18
Spacing Factor (mm)	0.143	0.113
Raw Data		
Total Voids Intercepted (N)	1086	1257
Total Number of Stops (St)	1482	1410
Total Number of Stops on Air Voids (Sa)	90	97
Total Number of Stops on Paste (Sp)	362	331
Distance Between Stops (I) (mm)	1.72	1.72
Total Traversed Distance (Tt) (mm)	2545.34	2421.68
Total Area (cm^2)	82.6	79.2

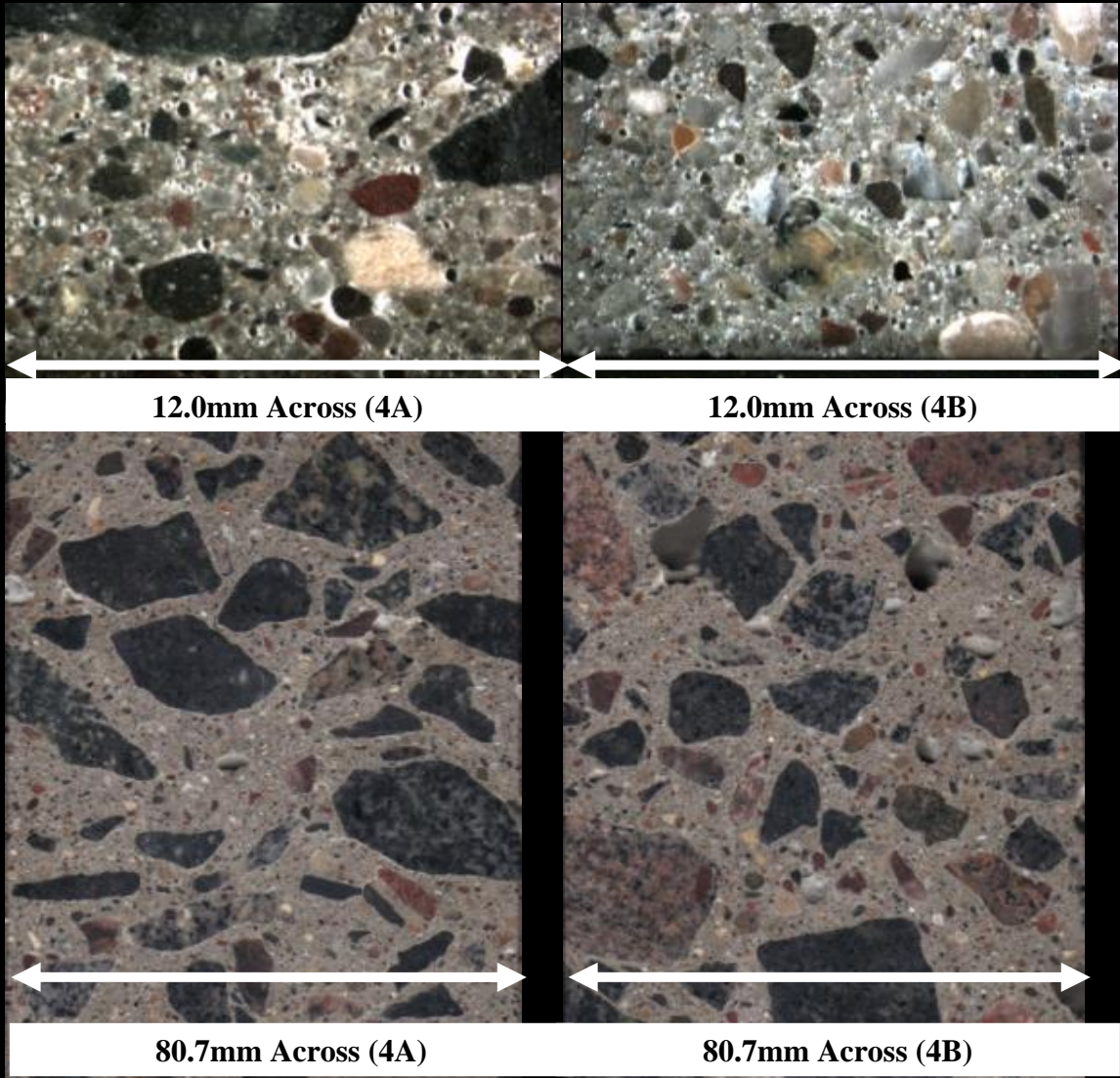


Figure 12: Airport II Runway Core 4 Air Content Results and Raw Data

Airport II Runway Core 10

Air Void Parameters	10A	10B
Air Content (%)	6.15	6.98
Void Frequency (mm^{-1})	0.438	0.531
Paste Content (%)	24.74	25.50
Paste to Air Ratio	4.02	3.65
Average Chord Length (mm)	0.140	0.132
Specific Surface (mm^2/mm^3)	28.50	30.41
Spacing Factor (mm)	0.141	0.120
Raw Data		
Total Voids Intercepted (N)	970	1222
Total Number of Stops (St)	1350	1404
Total Number of Stops on Air Voids (Sa)	83	98
Total Number of Stops on Paste (Sp)	334	358
Distance Between Stops (I) (mm)	1.64	1.64
Total Traversed Distance (Tt) (mm)	2214.00	2302.56
Total Area (cm^2)	80.4	82.0

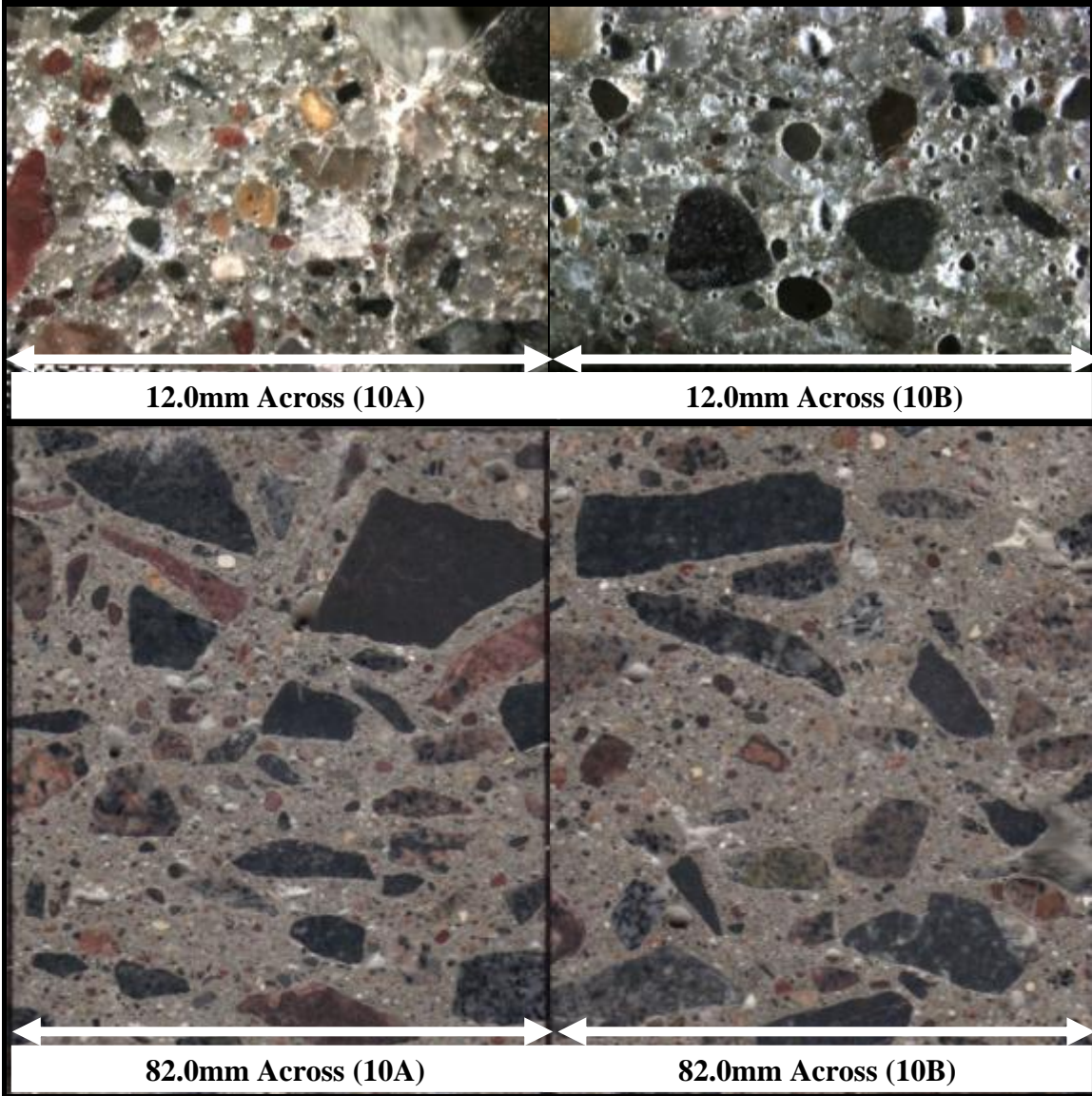


Figure 13: Airport II Runway Core 10 Air Content Results and Raw Data

Airport III Runway Core 104

Air Void Parameters	104A	104B
Air Content (%)	5.62	7.36
Void Frequency (mm^{-1})	0.353	0.511
Paste Content (%)	29.15	27.88
Paste to Air Ratio	5.18	3.79
Average Chord Length (mm)	0.159	0.144
Specific Surface (mm^2/mm^3)	25.11	27.77
Spacing Factor (mm)	0.188	0.136
Raw Data		
Total Voids Intercepted (N)	884	1177
Total Number of Stops (St)	1458	1345
Total Number of Stops on Air Voids (Sa)	82	99
Total Number of Stops on Paste (Sp)	425	375
Distance Between Stops (I) (mm)	1.72	1.71
Total Traversed Distance (Tt) (mm)	2504.12	2303.31
Total Area (cm^2)	81.0	81.0

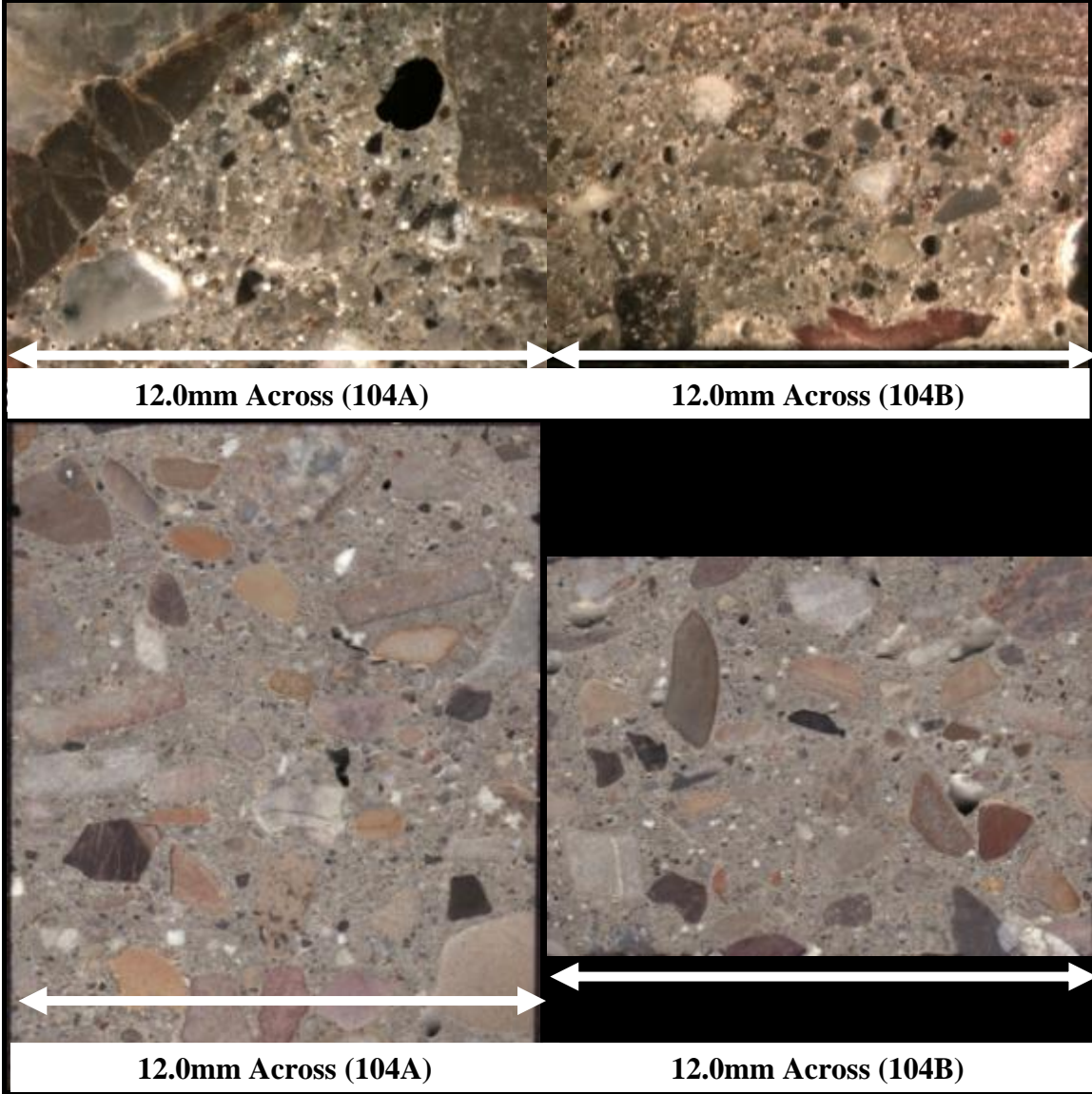


Figure 14: Airport III Runway Core 104 Air Content Results and Raw Data

Airport III Runway Core 108

Air Void Parameters	108A	108B
Air Content (%)	6.00	6.85
Void Frequency (mm^{-1})	0.388	0.409
Paste Content (%)	23.43	22.08
Paste to Air Ratio	3.90	3.22
Average Chord Length (mm)	0.155	0.168
Specific Surface (mm^2/mm^3)	25.84	23.85
Spacing Factor (mm)	0.151	0.135
Raw Data		
Total Voids Intercepted (N)	890	960
Total Number of Stops (St)	1400	1372
Total Number of Stops on Air Voids (Sa)	84	94
Total Number of Stops on Paste (Sp)	328	303
Distance Between Stops (I) (mm)	1.64	1.71
Total Traversed Distance (Tt) (mm)	2296.00	2349.55
Total Area (cm^2)	86.1	81.0

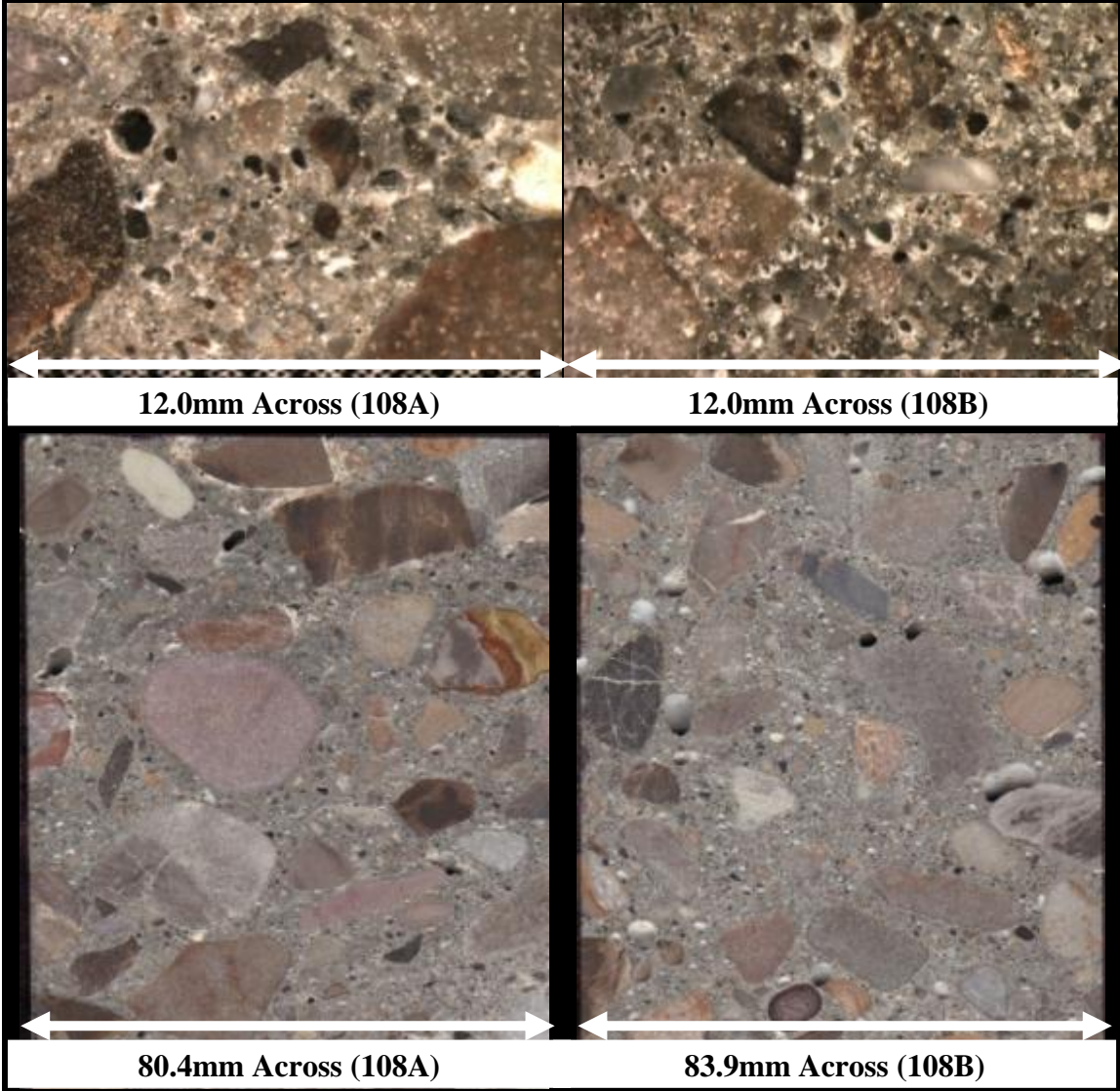


Figure 15: Airport III Runway Core 108 Air Content Results and Raw Data

Airport III Runway Core 111

Air Void Parameters	111A	111B
Air Content (%)	5.13	6.82
Void Frequency (mm^{-1})	0.361	0.502
Paste Content (%)	23.80	22.41
Paste to Air Ratio	4.64	3.29
Average Chord Length (mm)	0.142	0.136
Specific Surface (mm^2/mm^3)	28.16	29.41
Spacing Factor (mm)	0.159	0.112
Raw Data		
Total Voids Intercepted (N)	1076	1099
Total Number of Stops (St)	1735	1334
Total Number of Stops on Air Voids (Sa)	89	91
Total Number of Stops on Paste (Sp)	413	299
Distance Between Stops (I) (mm)	1.72	1.64
Total Traversed Distance (Tt) (mm)	2979.86	2191.10
Total Area (cm^2)	80.0	75.6

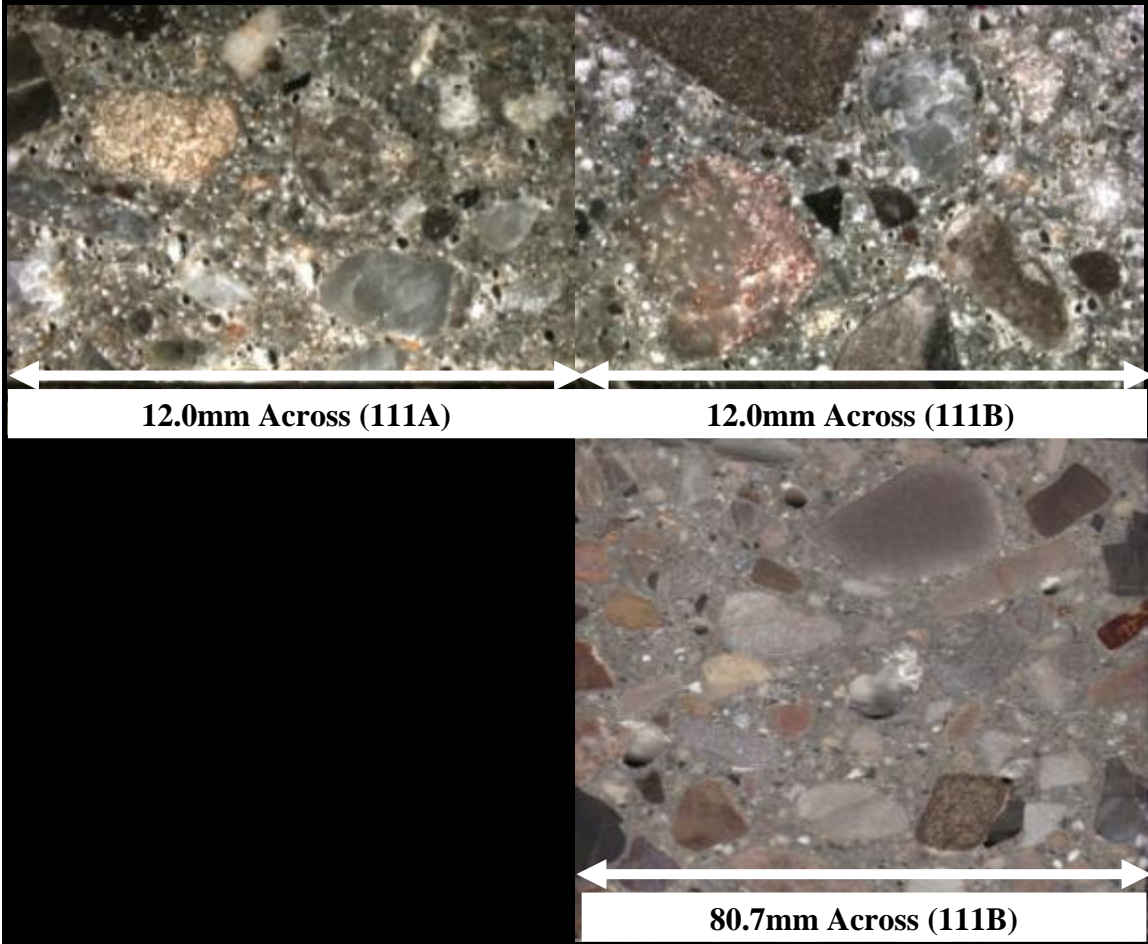


Figure 16: Airport III Runway Core 111 Air Content Results and Raw Data

**Airport IV Taxiway
Charlie 7 Core 3**

Air Void Parameters	C7C3A	C7C3B
Air Content (%)	5.29	7.18
Void Frequency (mm^{-1})	0.445	0.532
Paste Content (%)	24.24	23.85
Paste to Air Ratio	4.58	3.32
Average Chord Length (mm)	0.119	0.135
Specific Surface (mm^2/mm^3)	33.63	29.65
Spacing Factor (mm)	0.132	0.112
Raw Data		
Total Voids Intercepted (N)	1120	1296
Total Number of Stops (St)	1456	1434
Total Number of Stops on Air Voids (Sa)	77	103
Total Number of Stops on Paste (Sp)	353	342
Distance Between Stops (I) (mm)	1.73	1.70
Total Traversed Distance (Tt) (mm)	2518.88	2434.22
Total Area (cm^2)	81.0	81.0

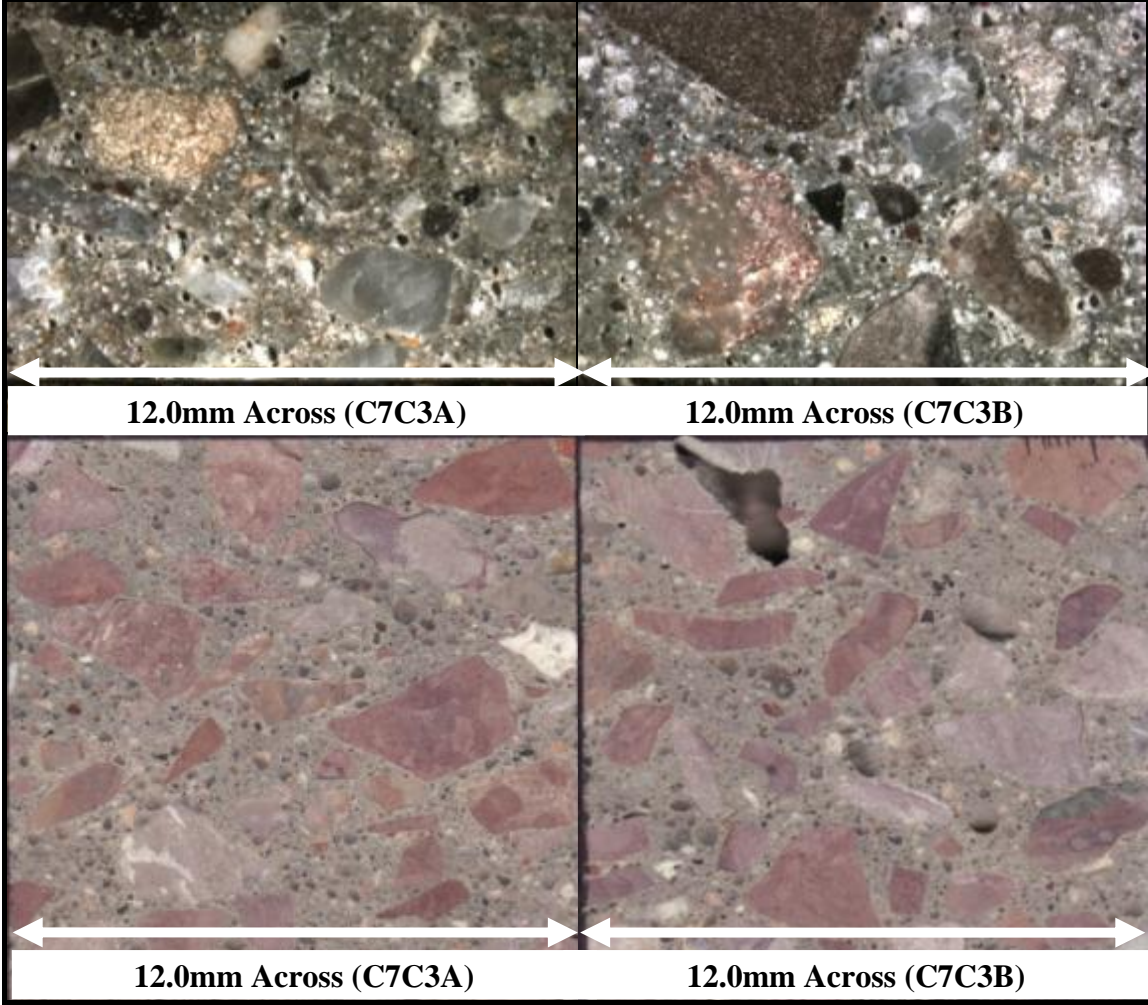


Figure 17: Airport IV Taxiway Charlie 7 Core 3 Air Content Results and Raw Data

**Airport IV Taxiway
Echo Core 5B**

Air Void Parameters	E5C3B
Air Content (%)	3.84
Void Frequency (mm^{-1})	0.202
Paste Content (%)	20.55
Paste to Air Ratio	5.35
Average Chord Length (mm)	0.190
Specific Surface (mm^2/mm^3)	21.02
Spacing Factor (mm)	0.227
Raw Data	
Total Voids Intercepted (N)	500
Total Number of Stops (St)	1431
Total Number of Stops on Air Voids (Sa)	55
Total Number of Stops on Paste (Sp)	294
Distance Between Stops (I) (mm)	1.73
Total Traversed Distance (Tt) (mm)	2475.63
Total Area (cm^2)	81.0

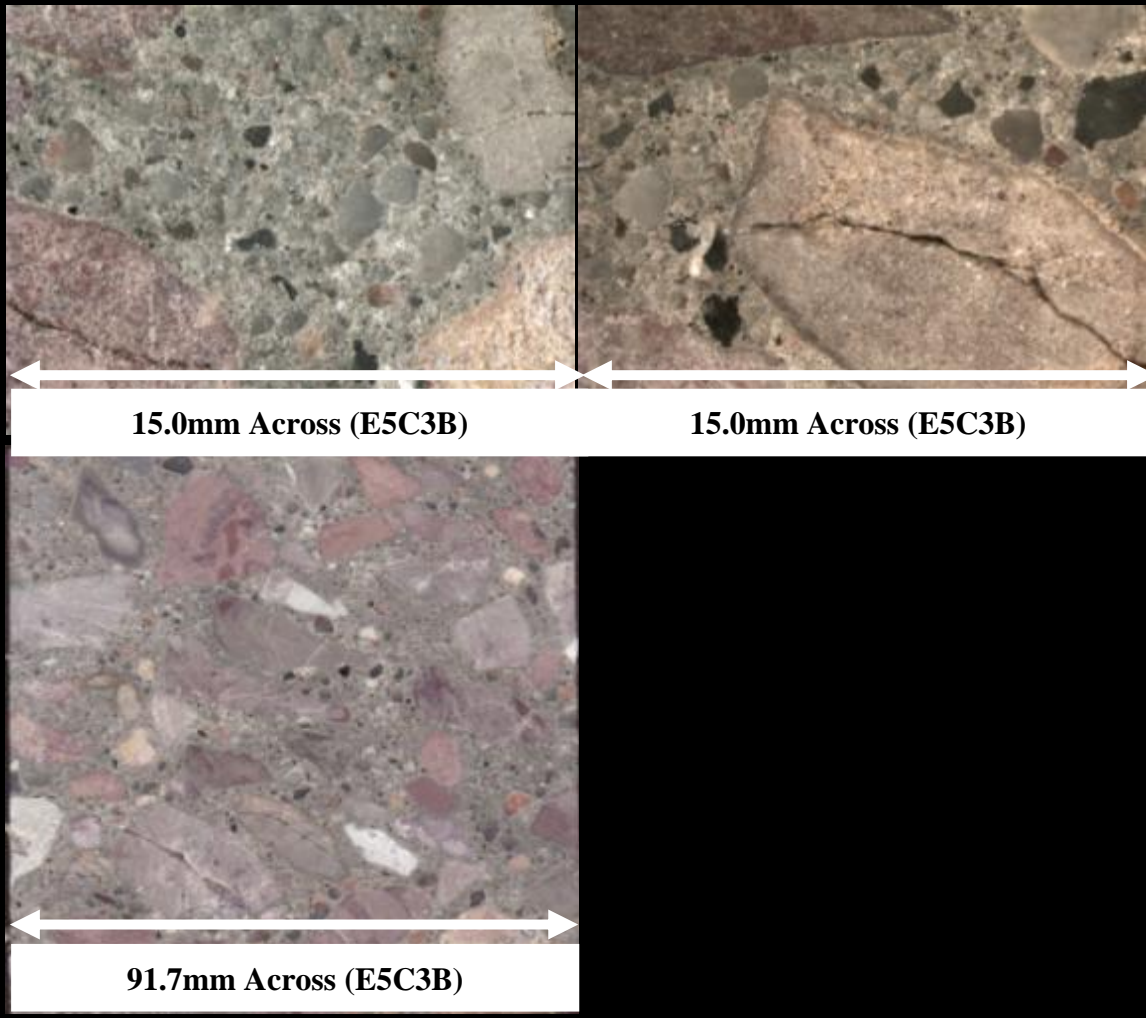


Figure 18: Airport IV Taxiway Echo 5 Core 5B Air Content Results and Raw Data

Airport IV Taxiway Golf Core 3

Air Void Parameters	G3A	G3B
Air Content (%)	6.25	4.81
Void Frequency (mm^{-1})	0.431	0.406
Paste Content (%)	21.28	21.09
Paste to Air Ratio	3.40	4.39
Average Chord Length (mm)	0.145	0.118
Specific Surface (mm^2/mm^3)	27.59	33.76
Spacing Factor (mm)	0.123	0.129
Raw Data		
Total Voids Intercepted (N)	1002	1034
Total Number of Stops (St)	1424	1456
Total Number of Stops on Air Voids (Sa)	89	70
Total Number of Stops on Paste (Sp)	303	307
Distance Between Stops (I) (mm)	1.63	1.75
Total Traversed Distance (Tt) (mm)	2324.68	2548.00
Total Area (cm^2)	89.2	82.8

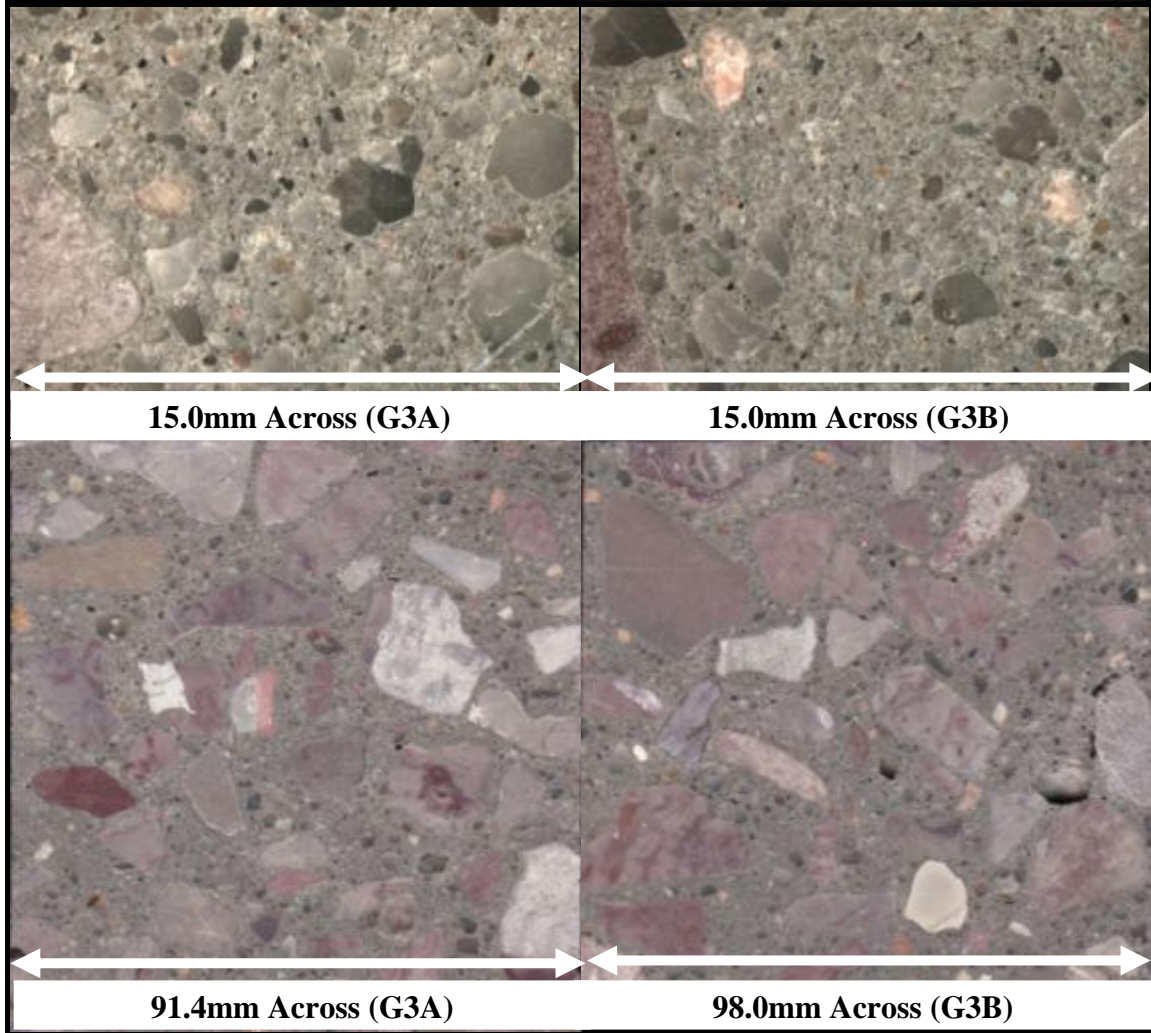


Figure 19: Airport IV Taxiway Golf Core 1 Air Content Results and Raw Data

Airport V Runway Core 1

Air Void Parameters	C1A	C1B
Air Content (%)	5.17	7.17
Void Frequency (mm^{-1})	0.432	0.541
Paste Content (%)	25.93	28.53
Paste to Air Ratio	5.01	3.98
Average Chord Length (mm)	0.120	0.132
Specific Surface (mm^2/mm^3)	33.44	30.21
Spacing Factor (mm)	0.139	0.132
Raw Data		
Total Voids Intercepted (N)	1050	1372
Total Number of Stops (St)	1431	1493
Total Number of Stops on Air Voids (Sa)	74	107
Total Number of Stops on Paste (Sp)	371	426
Distance Between Stops (I) (mm)	1.70	1.70
Total Traversed Distance (Tt) (mm)	2429.12	2534.37
Total Area (cm^2)	81.0	81.0

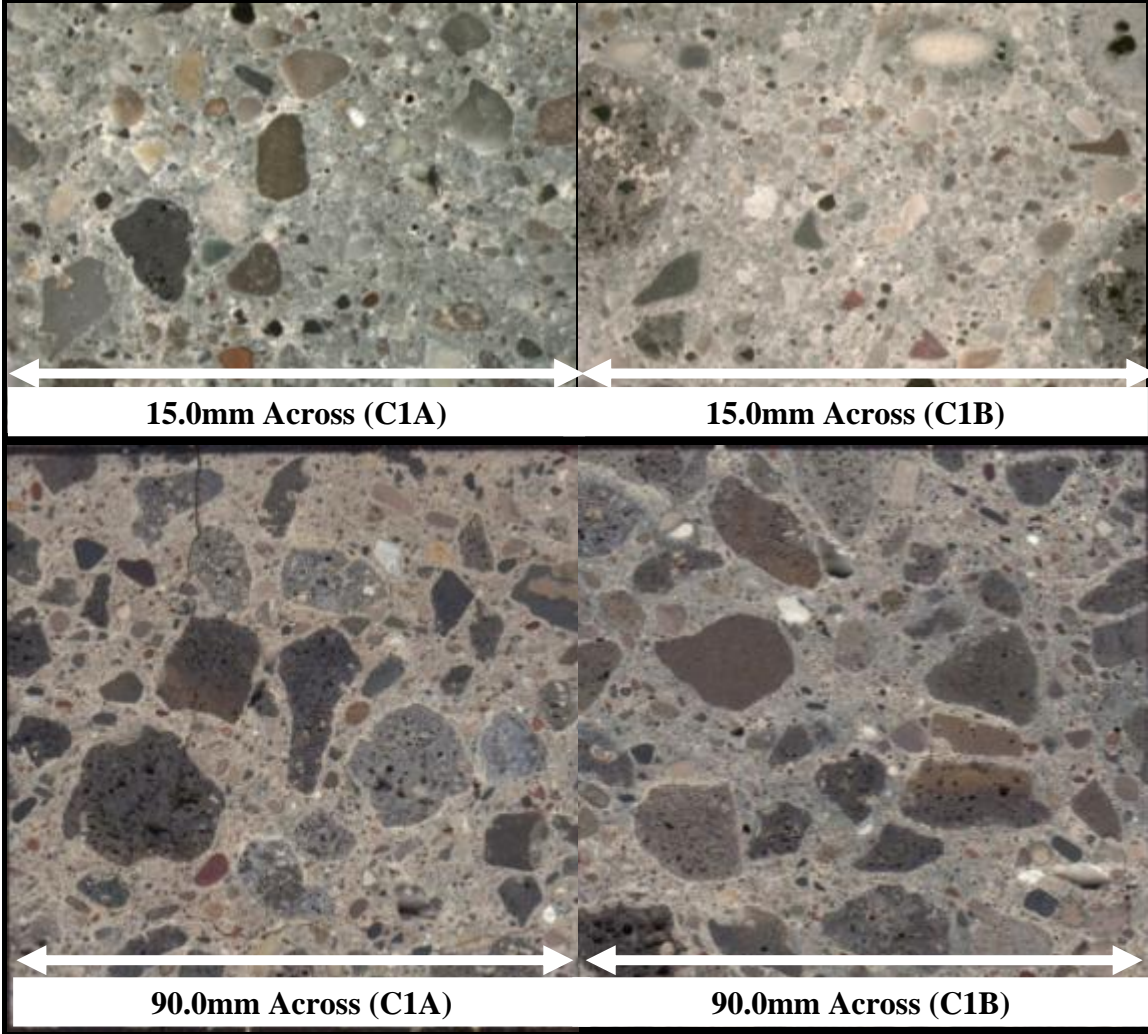


Figure 20: Airport V Runway Core 1 Air Content Results and Raw Data

Airport V Runway Core 6

Air Void Parameters	C6A	C6B
Air Content (%)	6.85	7.68
Void Frequency (mm^{-1})	0.432	0.433
Paste Content (%)	23.13	22.82
Paste to Air Ratio	3.38	2.97
Average Chord Length (mm)	0.158	0.177
Specific Surface (mm^2/mm^3)	25.25	22.58
Spacing Factor (mm)	0.134	0.132
Raw Data		
Total Voids Intercepted (N)	1050	1054
Total Number of Stops (St)	1431	1433
Total Number of Stops on Air Voids (Sa)	98	110
Total Number of Stops on Paste (Sp)	331	327
Distance Between Stops (I) (mm)	1.70	1.70
Total Traversed Distance (Tt) (mm)	2429.12	2432.52
Total Area (cm^2)	81.0	81.0

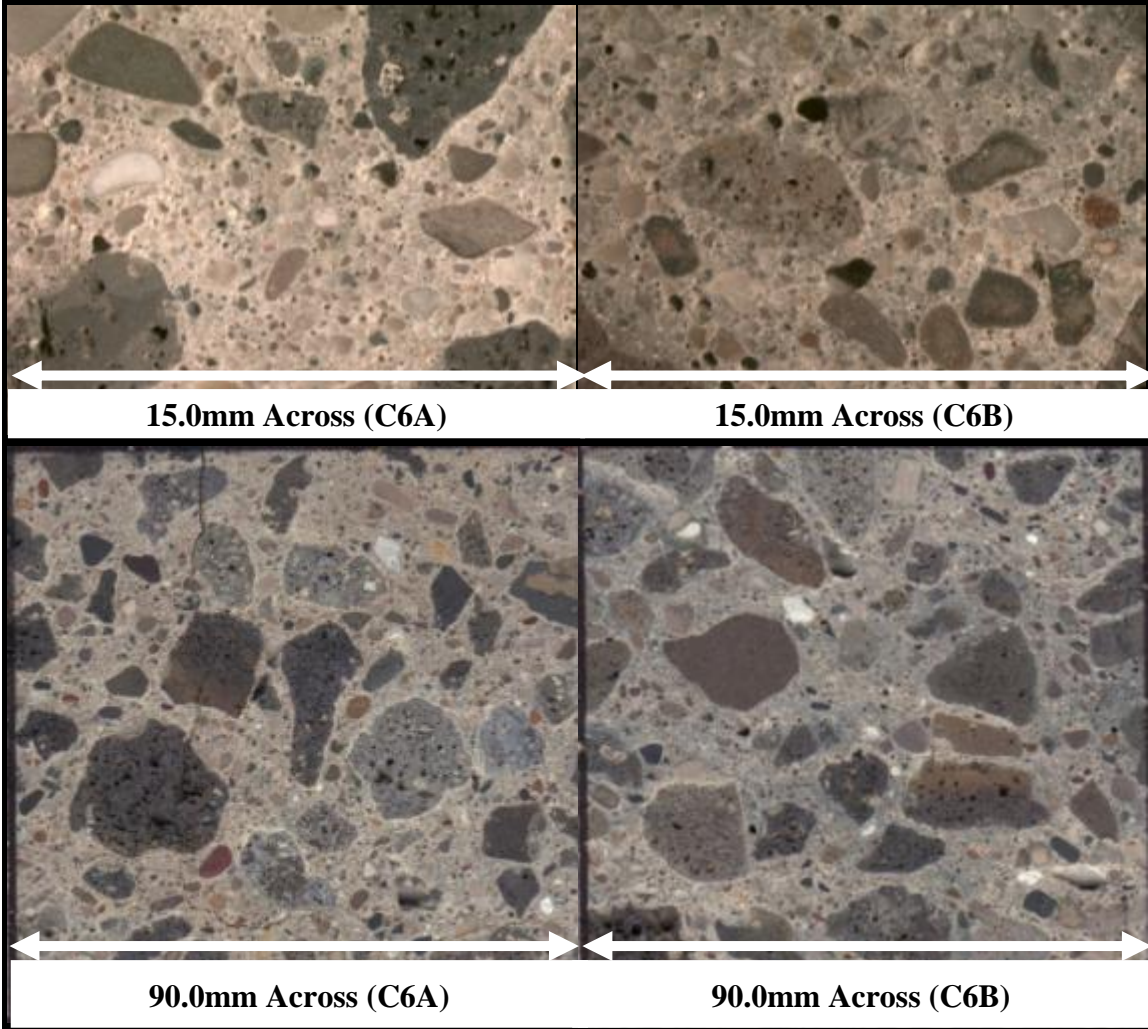


Figure 21: Airport V Runway Core 1 Air Content Results and Raw Data

Airport VI Taxiway Foxtrot Core 5

Air Void Parameters	F5A	F5B
Air Content (%)	5.95	5.88
Void Frequency (mm^{-1})	0.289	0.257
Paste Content (%)	22.67	25.49
Paste to Air Ratio	3.81	4.33
Average Chord Length (mm)	0.206	0.229
Specific Surface (mm^2/mm^3)	19.45	17.48
Spacing Factor (mm)	0.196	0.248
Raw Data		
Total Voids Intercepted (N)	754	650
Total Number of Stops (St)	1478	1479
Total Number of Stops on Air Voids (Sa)	88	87
Total Number of Stops on Paste (Sp)	335	377
Distance Between Stops (I) (mm)	1.76	1.71
Total Traversed Distance (Tt) (mm)	2604.98	2529.09
Total Area (cm^2)	90.5	91.9

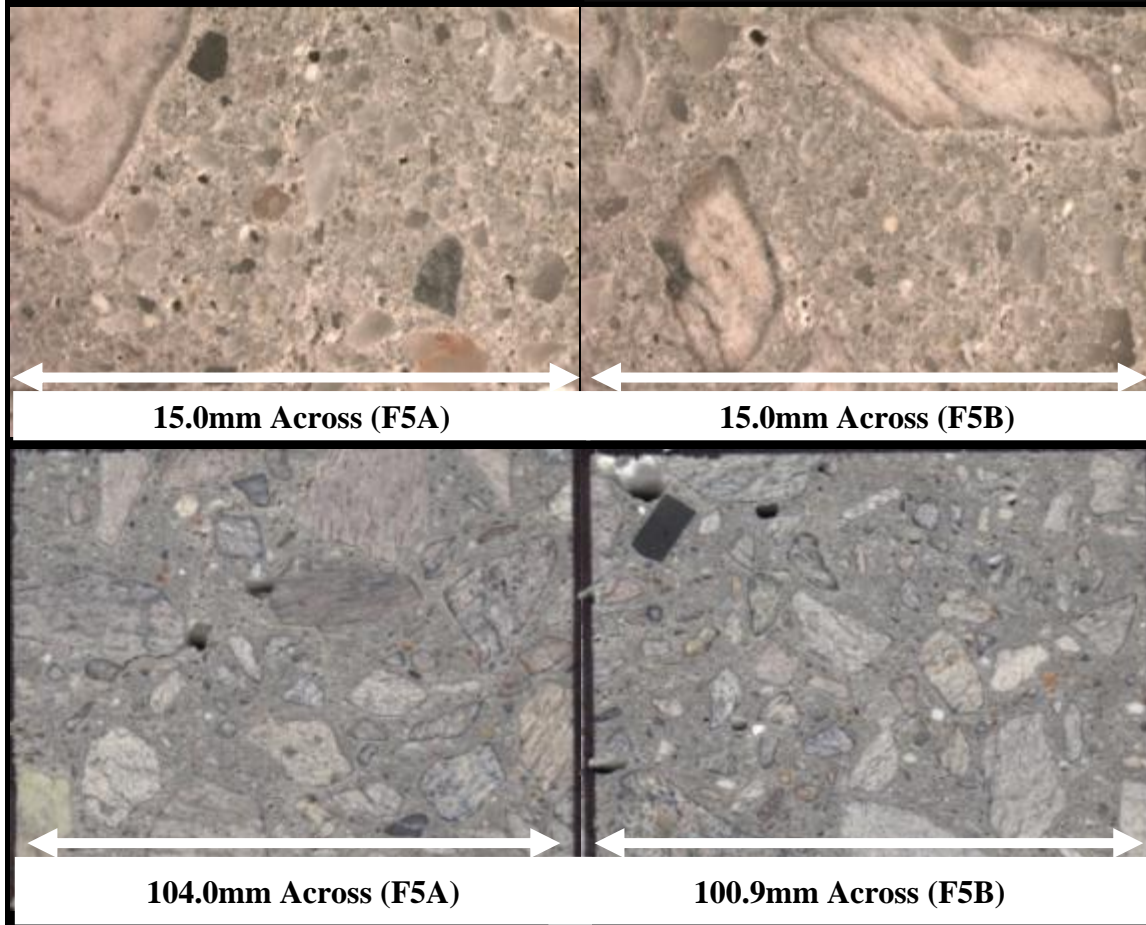


Figure 22: Airport VI Taxiway Foxtrot Core 5 Air Content Results and Raw Data

Airport VI Taxiway Foxtrot Core 6

Air Void Parameters	F6A	F6B
Air Content (%)	5.24	4.24
Void Frequency (mm^{-1})	0.296	0.303
Paste Content (%)	22.52	22.29
Paste to Air Ratio	4.30	5.26
Average Chord Length (mm)	0.177	0.140
Specific Surface (mm^2/mm^3)	22.57	28.57
Spacing Factor (mm)	0.190	0.166
Raw Data		
Total Voids Intercepted (N)	755	757
Total Number of Stops (St)	1470	1440
Total Number of Stops on Air Voids (Sa)	77	61
Total Number of Stops on Paste (Sp)	331	321
Distance Between Stops (I) (mm)	1.74	1.74
Total Traversed Distance (Tt) (mm)	2554.13	2502.00
Total Area (cm^2)	91.2	91.2

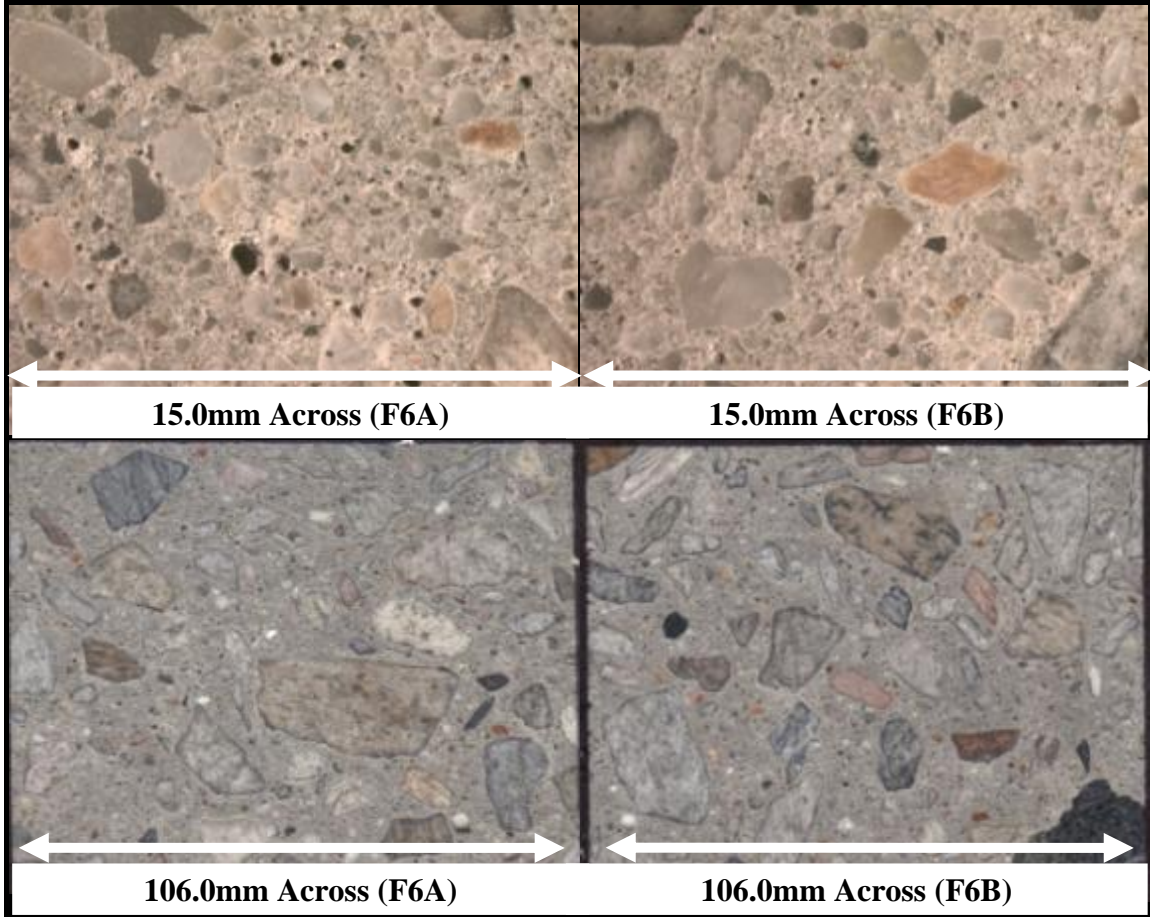


Figure 23: Airport VI Taxiway Foxtrot Core 6 Air Content Results and Raw Data

Airport VI Runway Core 2

Air Void Parameters	R2A	R2B
Air Content (%)	5.41	4.20
Void Frequency (mm^{-1})	0.455	0.336
Paste Content (%)	30.90	21.97
Paste to Air Ratio	5.71	5.23
Average Chord Length (mm)	0.119	0.125
Specific Surface (mm^2/mm^3)	33.61	31.94
Spacing Factor (mm)	0.146	0.148
Raw Data		
Total Voids Intercepted (N)	1163	864
Total Number of Stops (St)	1479	1475
Total Number of Stops on Air Voids (Sa)	80	62
Total Number of Stops on Paste (Sp)	457	324
Distance Between Stops (I) (mm)	1.73	1.75
Total Traversed Distance (Tt) (mm)	2558.67	2573.88
Total Area (cm^2)	86.7	88.6

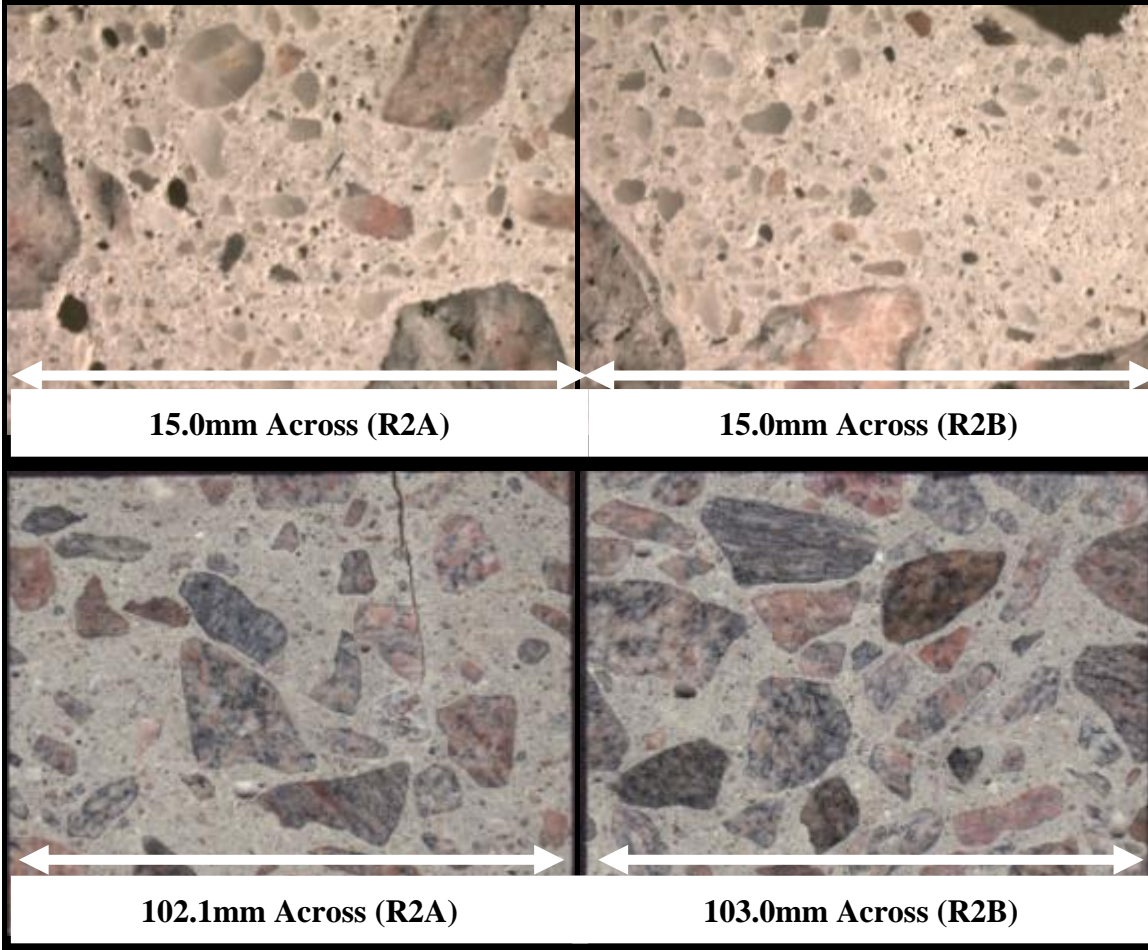


Figure 24: Airport VI Runway Core 2 Air Content Results and Raw Data

Airport VI Runway Core 6

Air Void Parameters	R6A	R6B
Air Content (%)	6.32	5.64
Void Frequency (mm^{-1})	0.421	0.336
Paste Content (%)	22.64	18.52
Paste to Air Ratio	3.58	3.29
Average Chord Length (mm)	0.150	0.168
Specific Surface (mm^2/mm^3)	26.65	23.84
Spacing Factor (mm)	0.134	0.138
Raw Data		
Total Voids Intercepted (N)	1058	855
Total Number of Stops (St)	1440	1490
Total Number of Stops on Air Voids (Sa)	91	84
Total Number of Stops on Paste (Sp)	326	276
Distance Between Stops (I) (mm)	1.75	1.71
Total Traversed Distance (Tt) (mm)	2512.80	2544.18
Total Area (cm^2)	87.6	91.2

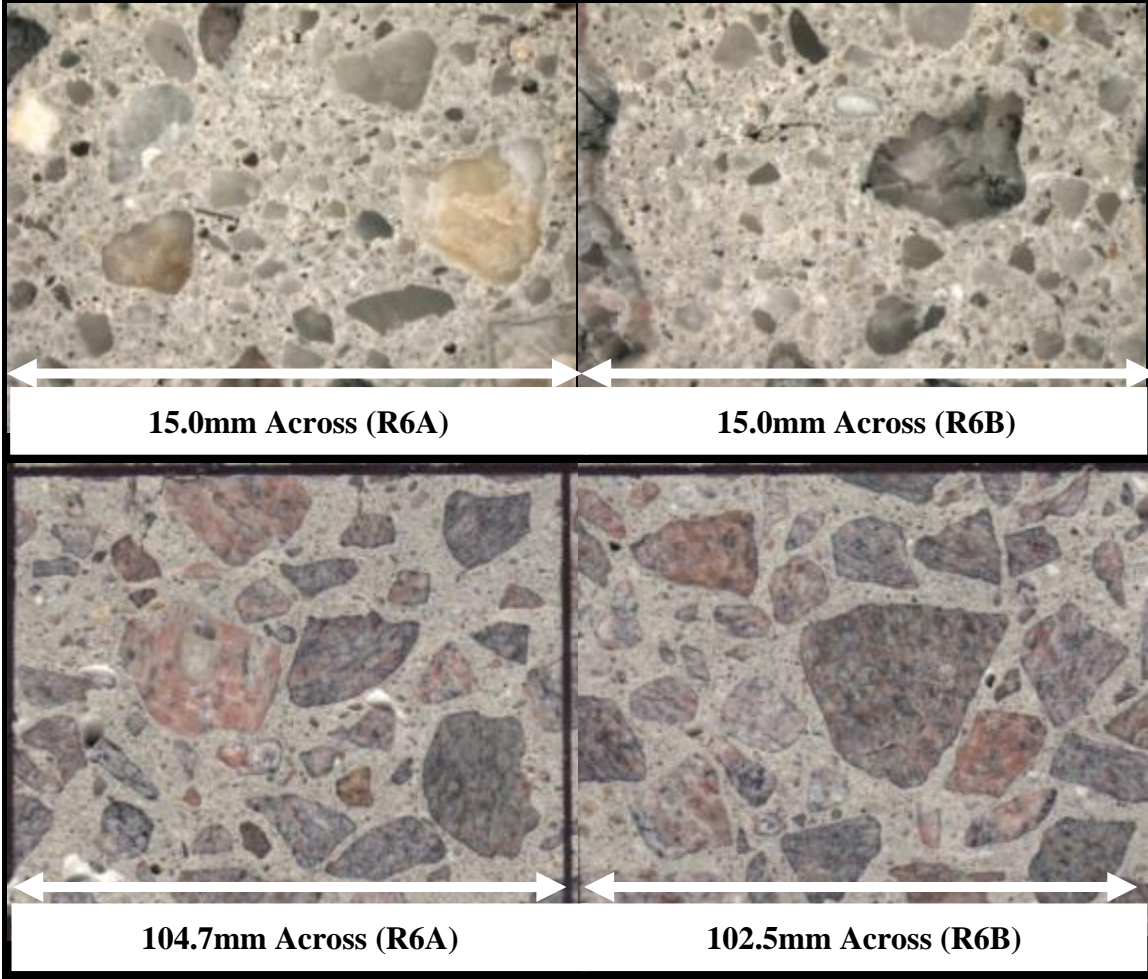


Figure 25: Airport VI Runway Core 6 Air Content Results and Raw Data

Airport VII Core A5

Air Void Parameters	A5A	A5B
Air Content (%)	6.70	6.07
Void Frequency (mm^{-1})	0.444	0.406
Paste Content (%)	23.01	22.13
Paste to Air Ratio	3.44	3.65
Average Chord Length (mm)	0.151	0.150
Specific Surface (mm^2/mm^3)	26.52	26.75
Spacing Factor (mm)	0.130	0.136
Raw Data		
Total Voids Intercepted (N)	1135	1056
Total Number of Stops (St)	1508	1500
Total Number of Stops on Air Voids (Sa)	101	91
Total Number of Stops on Paste (Sp)	347	332
Distance Between Stops (I) (mm)	1.70	1.74
Total Traversed Distance (Tt) (mm)	2556.06	2602.50
Total Area (cm^2)	72.5	79.1

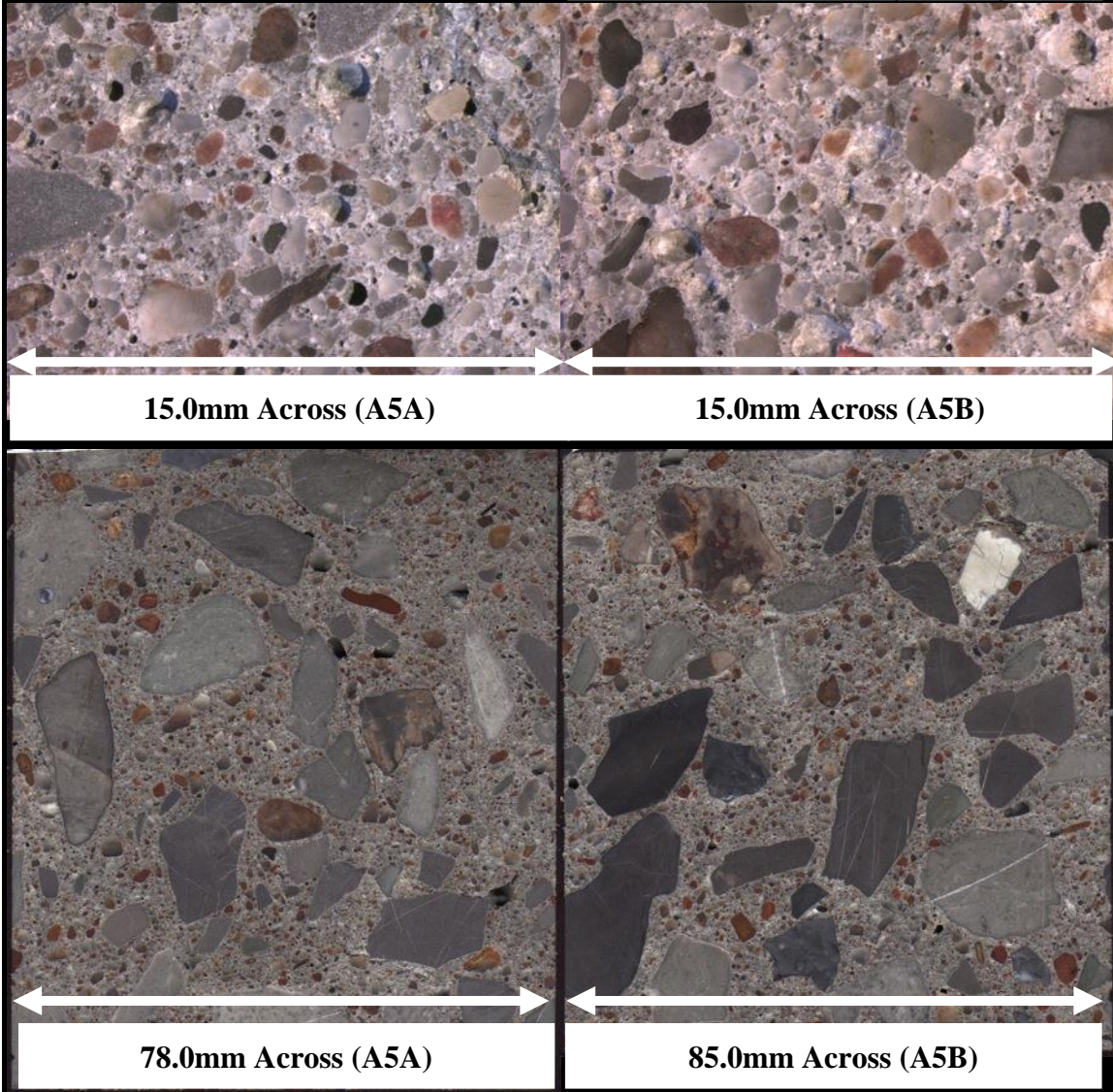


Figure 26: Airport VII Core A5 Air Content Results and Raw Data

Airport VII Core D10

Air Void Parameters	D10A	D10B
Air Content (%)	5.15	4.90
Void Frequency (mm ⁻¹)	0.398	0.389
Paste Content (%)	21.77	24.01
Paste to Air Ratio	4.23	4.90
Average Chord Length (mm)	0.129	0.126
Specific Surface (mm ² /mm ³)	30.93	31.79
Spacing Factor (mm)	0.137	0.144
Raw Data		
Total Voids Intercepted (N)	1036	979
Total Number of Stops (St)	1516	1491
Total Number of Stops on Air Voids (Sa)	78	73
Total Number of Stops on Paste (Sp)	330	358
Distance Between Stops (I) (mm)	1.72	1.69
Total Traversed Distance (Tt) (mm)	2603.73	2516.06
Total Area (cm ²)	73.5	74.5

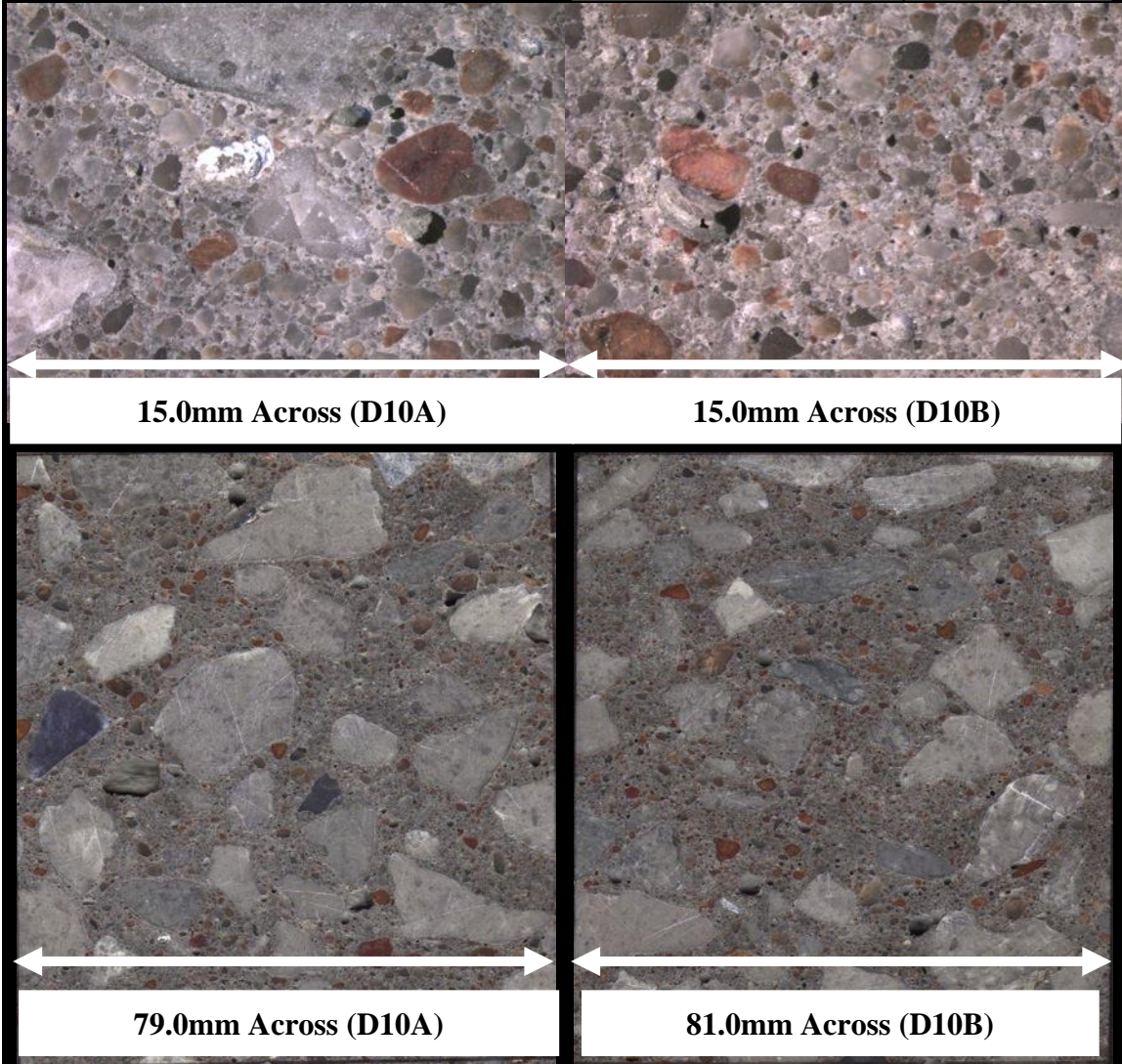


Figure 27: Airport VII Core D10 Air Content Results and Raw Data

Airport VIII Core 2

Air Void Parameters	Core 2
Air Content (%)	3.74
Void Frequency (mm^{-1})	0.294
Paste Content (%)	24.41
Paste to Air Ratio	6.53
Average Chord Length (mm)	0.127
Specific Surface (mm^2/mm^3)	31.47
Spacing Factor (mm)	0.166
Raw Data	
Total Voids Intercepted (N)	839
Total Number of Stops (St)	1659
Total Number of Stops on Air Voids (Sa)	62
Total Number of Stops on Paste (Sp)	405
Distance Between Stops (I) (mm)	1.72
Total Traversed Distance (Tt) (mm)	2853.48
Total Area (cm^2)	168.6

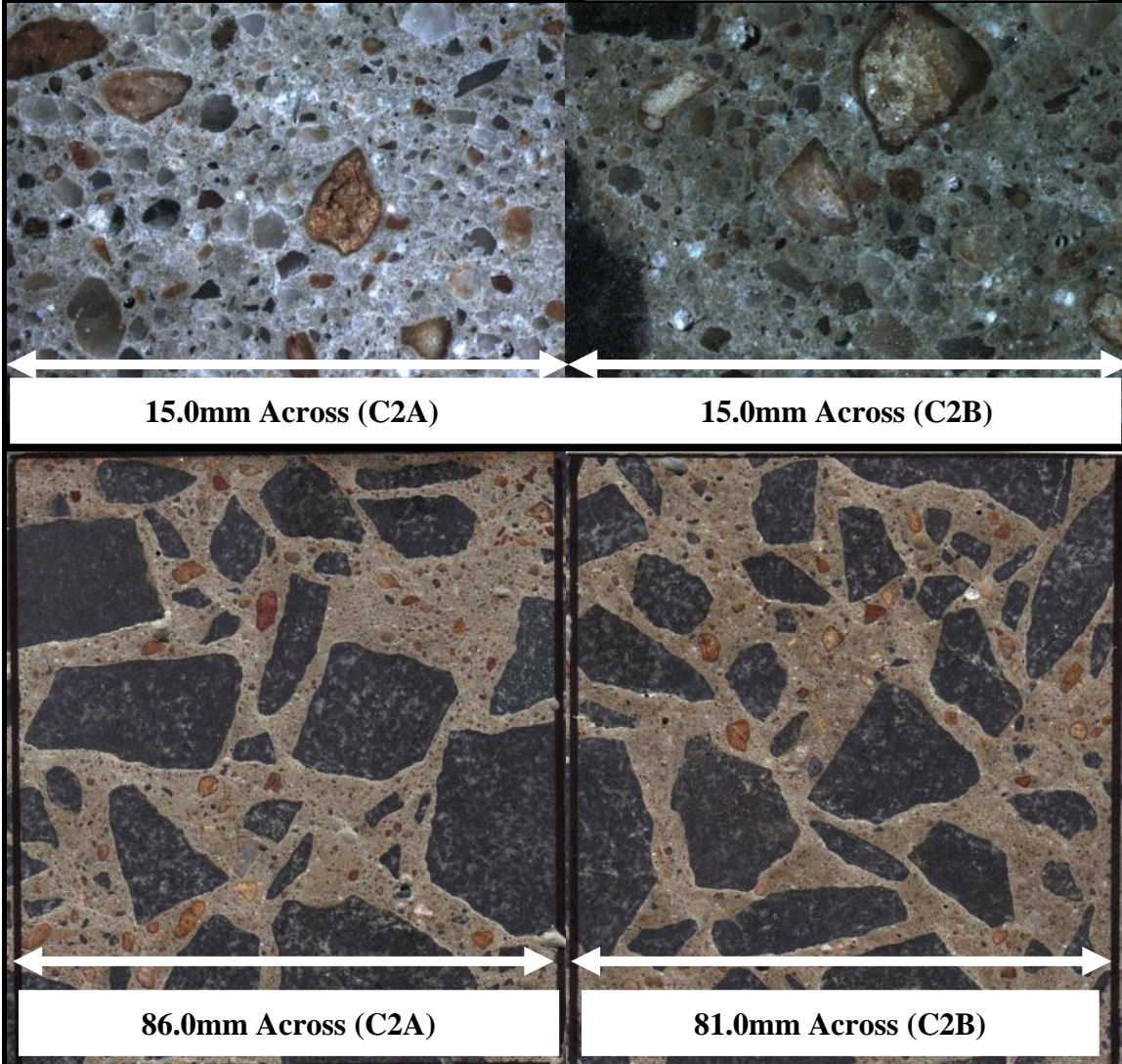


Figure 28: Airport VIII Core 2 Air Content Results and Raw Data

Airport VIII Core 5

Air Void Parameters	Core 5
Air Content (%)	4.94
Void Frequency (mm ⁻¹)	0.415
Paste Content (%)	27.19
Paste to Air Ratio	5.51
Average Chord Length (mm)	0.119
Specific Surface (mm ² /mm ³)	33.59
Spacing Factor (mm)	0.144
Raw Data	
Total Voids Intercepted (N)	1161
Total Number of Stops (St)	1600
Total Number of Stops on Air Voids (Sa)	79
Total Number of Stops on Paste (Sp)	435
Distance Between Stops (I) (mm)	1.75
Total Traversed Distance (Tt) (mm)	2800.00
Total Area (cm ²)	170.6

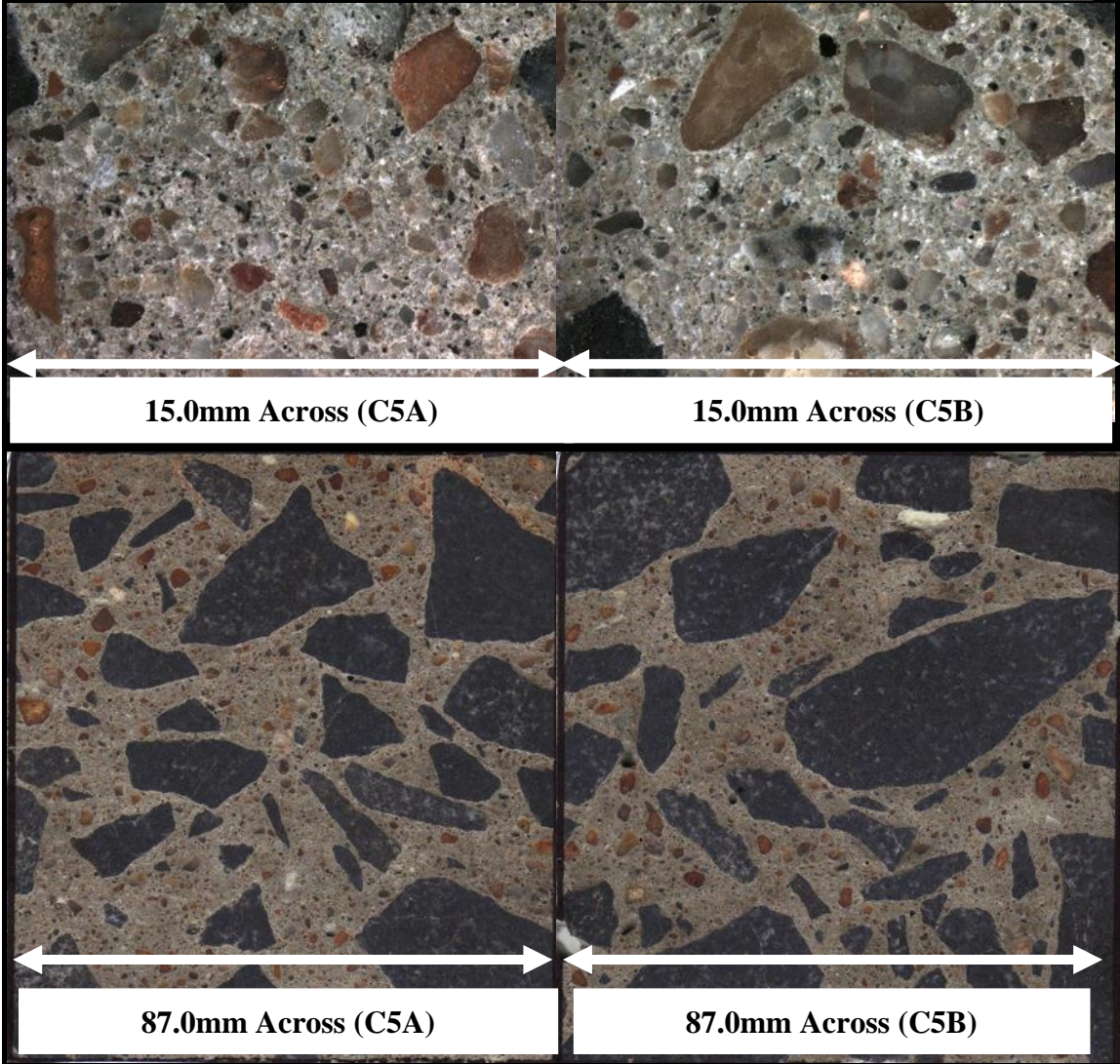


Figure 29: Airport VIII Core 5 Air Content Results and Raw Data

Discussion

Based on these results, it appears that all the cores investigated have acceptable air contents (3.7% - 7.7%), with spacing factors ranging from 0.112 mm to 0.255 mm. The spacing factors in some of these cores are somewhat considered marginal in nature, but do not necessarily reflect poor concrete. Concrete with an air-void spacing factor of 0.200 mm or less is considered to possess a good air-void system that is capable of resisting the effects of freeze-thaw cycling. Overall 90% of the samples had spacing factors less than 0.200 mm and 87% had air contents greater than 4.5% showing that overall for the study the Airfield pavements had decent air void systems with respect to freeze-thaw mitigation.

Conclusion

The hardened air content analysis showed that the majority of field cores had sufficient air entraining and also sufficient air void systems. Based on the results, it appears that all the cores investigated have acceptable air contents (3.7% - 7.7%), with spacing factors ranging from 0.112 mm to 0.255 mm. The spacing factors in some of these cores are somewhat considered marginal in nature, but do not necessarily reflect poor concrete. These pavements were therefore considered to have sufficient air void parameters to resist deterioration from freeze thaw cycles alone.

Part 3: Depth of Deicer Penetration

Introduction

This analysis was performed to determine what the typical penetration depth of the deicer was and how different conditions affect the rate of penetration. This study was performed in two stages; the first stage was to determine the effectiveness of the new method in determining the depth of penetration and what affect different conditions played in the rate of penetration. The second stage was to determine the penetration depths in Airports I – VII, Airport VIII was left off due to time restrictions. A trip was made to Airport I to take samples directly from the pavement to be compared to the results of the core analysis from the same Airport.

Method

Calibration Study

The Calibration Study was completed to determine the feasibility of using ICP analysis on powdered concrete samples to determine the depth of the penetration of potassium ions. This study was done by first creating Portland cement concrete samples in two ways: the first type of sample created by casting 4" diameter cylinders with heights varying between 4 and 5 inches and cured for 1 month at 100%RH at 23°C, the second type of sample was created by first casting a 1'x1'x5" square, curing the sample for 1 day at 38C to ensure that micro-cracking on the surface was present, and then coring the sample after 1 month of curing at 100%RH at 23°C using a 4" diameter bit. The result was 6-cast samples and 4-cored samples. Cores 1-6 are the cast samples and cores 7-10 are the cored samples. The concrete had an air content of 6.5% and a plastic unit weight of 139.5 lb/ft³. These samples were then exposed to following conditions: Cores 1 and 4 were the control samples which were not exposed to the potassium acetate deicer, cores 2 and 7 were constantly exposed to the deicer and subjected to a 24hr period of -20°C followed by a 24hr period of 25°C, cores 3 and 8 were constantly exposed to the deicer, cores 6 and 10 were subjected to a 24hr period of deicer application followed by a 24hr period of no deicer application at 25°C, and finally cores 5 and 9 were subjected to the same regiment as cores 6 and 10 with the exception of the drying period temperature which was changed from 25°C to 80°C. Collars were attached to the cylinders with silicone leaving a basin area above the cylinders for the Potassium Acetate to be applied. The different conditioning regiments were continued for 3 months. All of the cores had their collars removed and then were left in the 80°C oven to completely dry out all of the samples. Once the calibration study samples were dried, samples were taken in the following two ways and then processed for ICP testing to determine the potassium ion concentration:

Drill Dust Samples

Drill Dust Samples were taken in increments of ½” using a percussion drill with depth gage and a hand vacuum. The hand vacuum had a hose attachment that could focus the suction to only the area of the drilling. The vacuum was bag less and had an exhaust filter. After the sample was collected in the vacuum, the sample was taken out of the collection section of the vacuum and placed in a sealable plastic bag. After each ½” increment the entire vacuum and filter was cleaned using a compressed air tank. This method of sample taking was used primarily for field applications and was compared to the disc sample method whenever possible to check consistency. The drill dust samples were then processed for ICP testing to determine the potassium ion concentration.

Disc Samples

All airfield pavements had selected cores that were sectioned in ½” increments starting from the top surface to four inches in depth creating discs. These discs were then crushed using a hammer and then placed in a ball mill for five minutes at 350 rpm with 88.2 grams of stainless steel balls used as an abrasive charge. The powder was then sieved over a #70 sieve. Once the sample was in powder form it was then processed for ICP testing to determine potassium ion concentration.

Determining Potassium Ion Concentration

Once the samples were in the powdered form they were then taken and diluted at a rate of one gram to fifty milliliters of deionized water. These diluted samples were then mixed for twenty-four hours with a rock tumbler. Once these samples were taken out of the tumbler they were then vacuum filtrated to remove the remaining solids and the remaining liquid was then tested using the ICP apparatus located at the Agriculture Service Lab at Clemson University. The result of the ICP testing on the powders was the potassium ion concentration for the given depth of sample.

Results

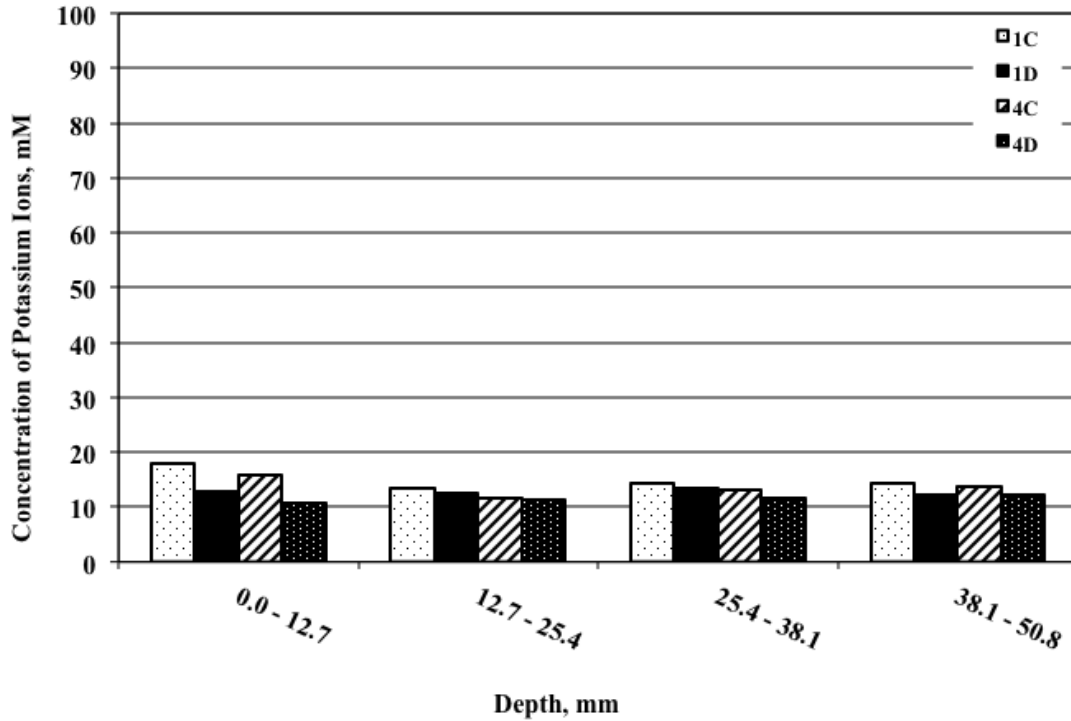


Figure 30: Depth of Penetration Calibration Results for the Control Condition

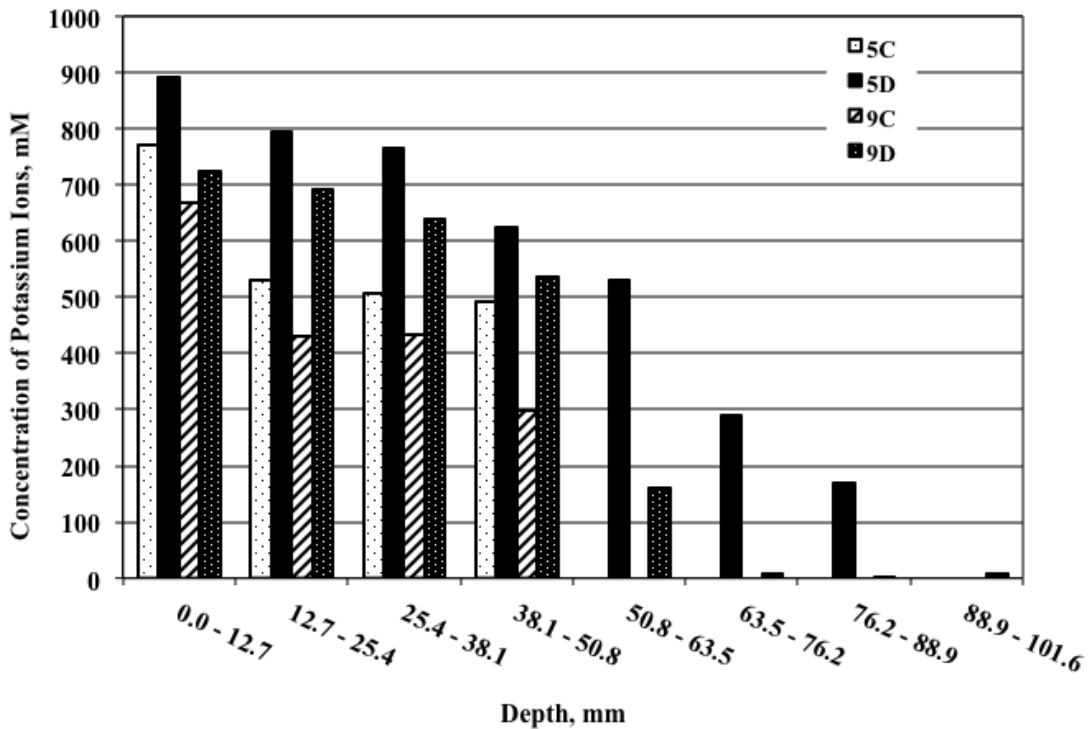


Figure 31: Depth of Penetration Calibration Results for the Wetting-Drying Condition @ 80C

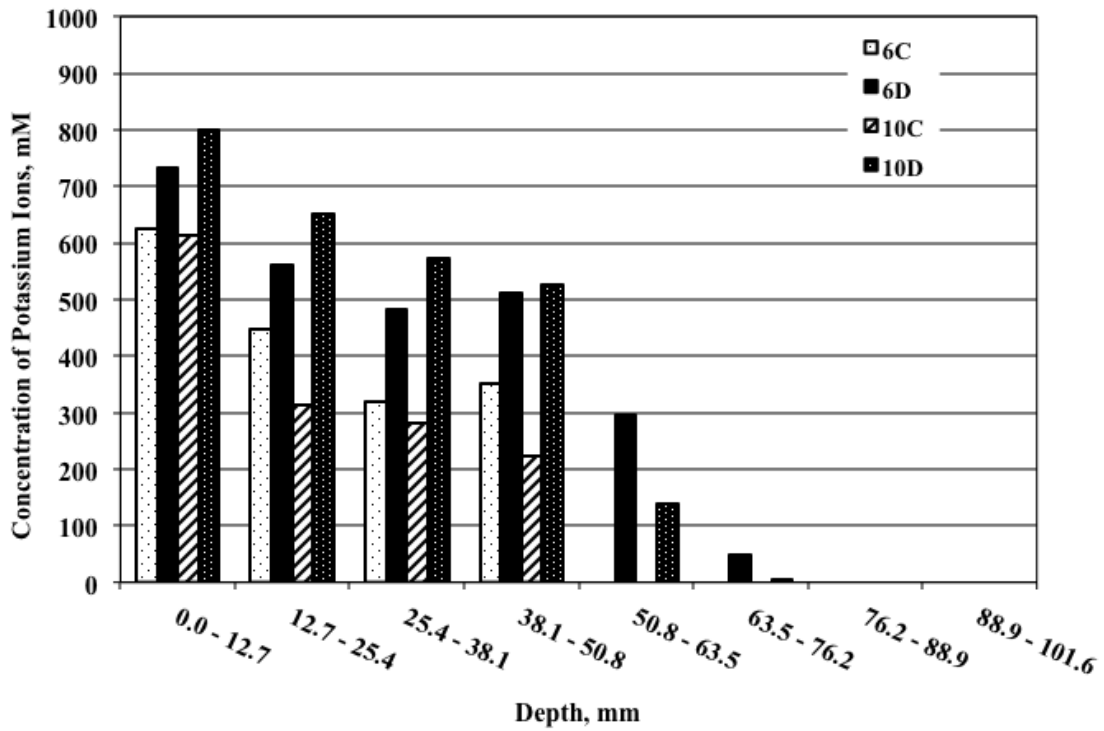


Figure 32: Depth of Penetration Calibration Results for Wetting-Drying Condition @ 23C

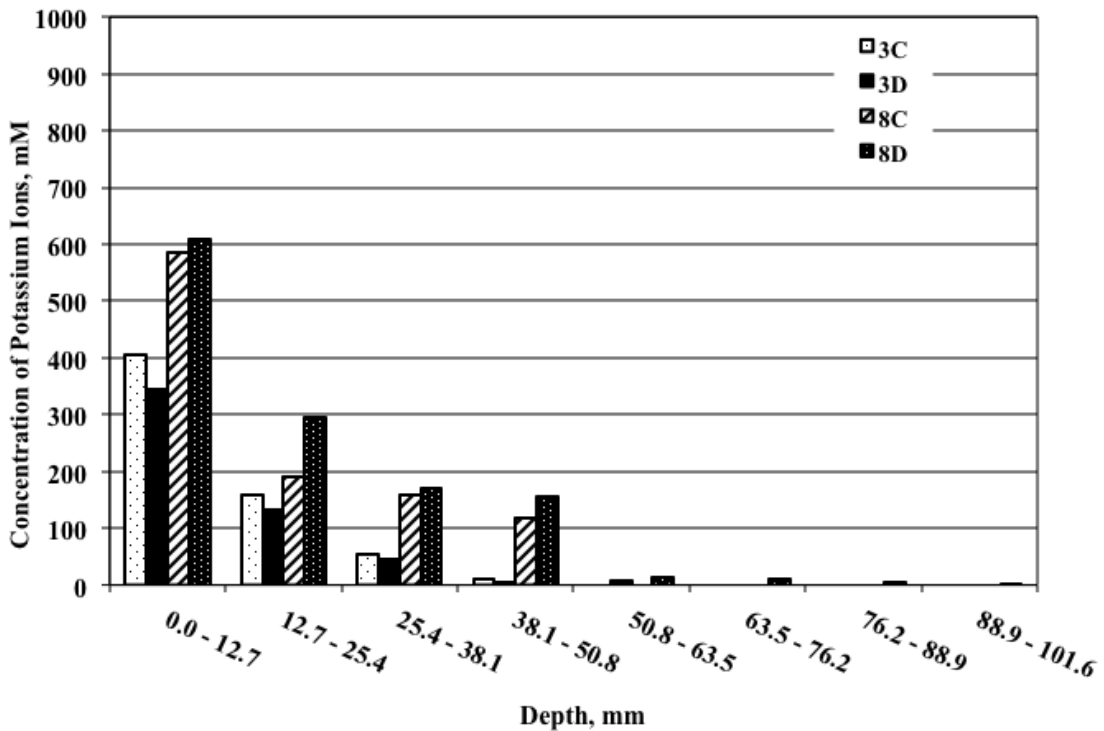


Figure 33: Depth of Penetration Calibration Results for Constant Application Condition @ 23C

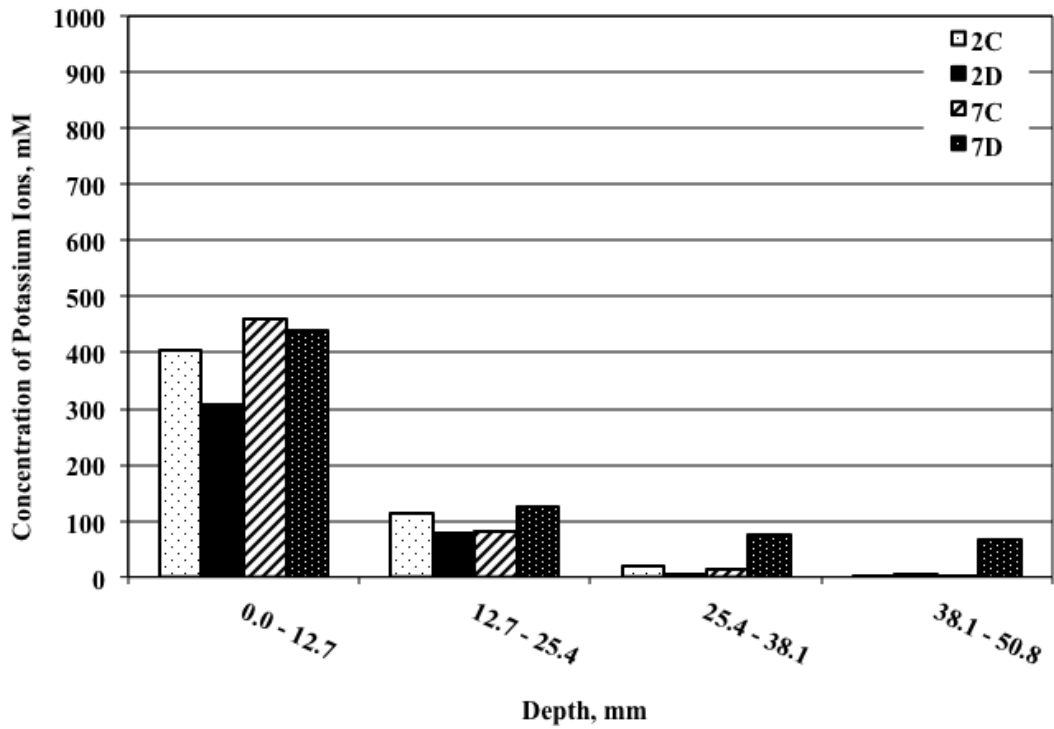


Figure 34: Depth of Penetration Calibration Results for the Freeze-Thaw Condition

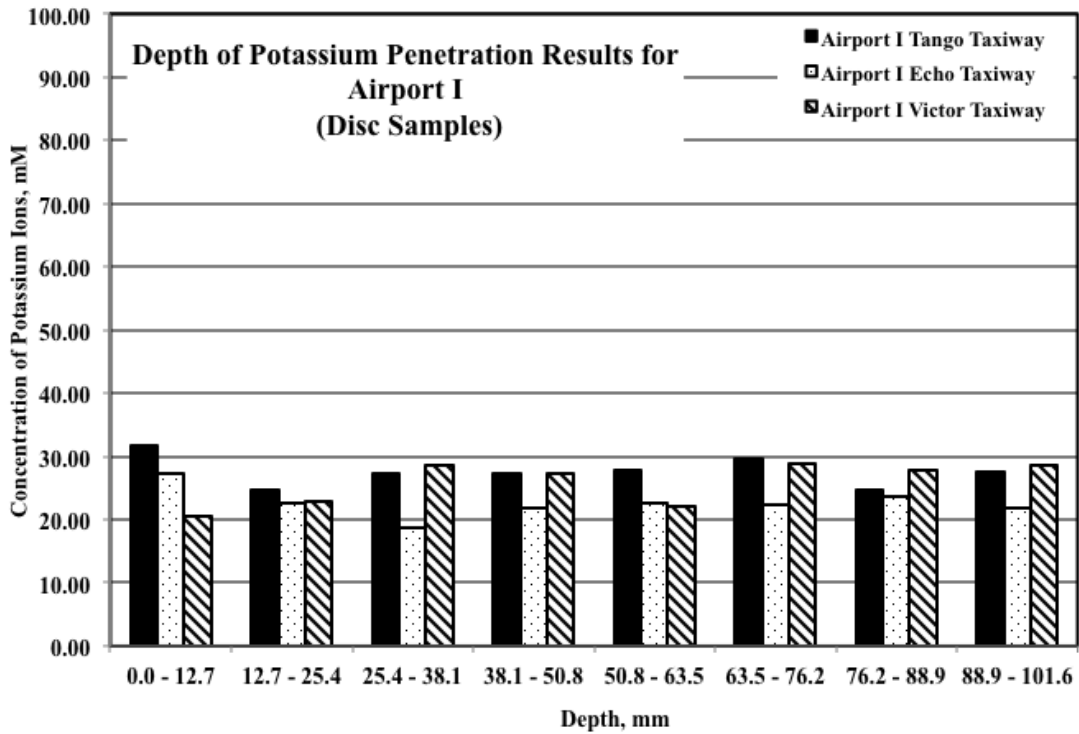


Figure 35: Depth of Penetration Results for Airport I (Core Analysis)

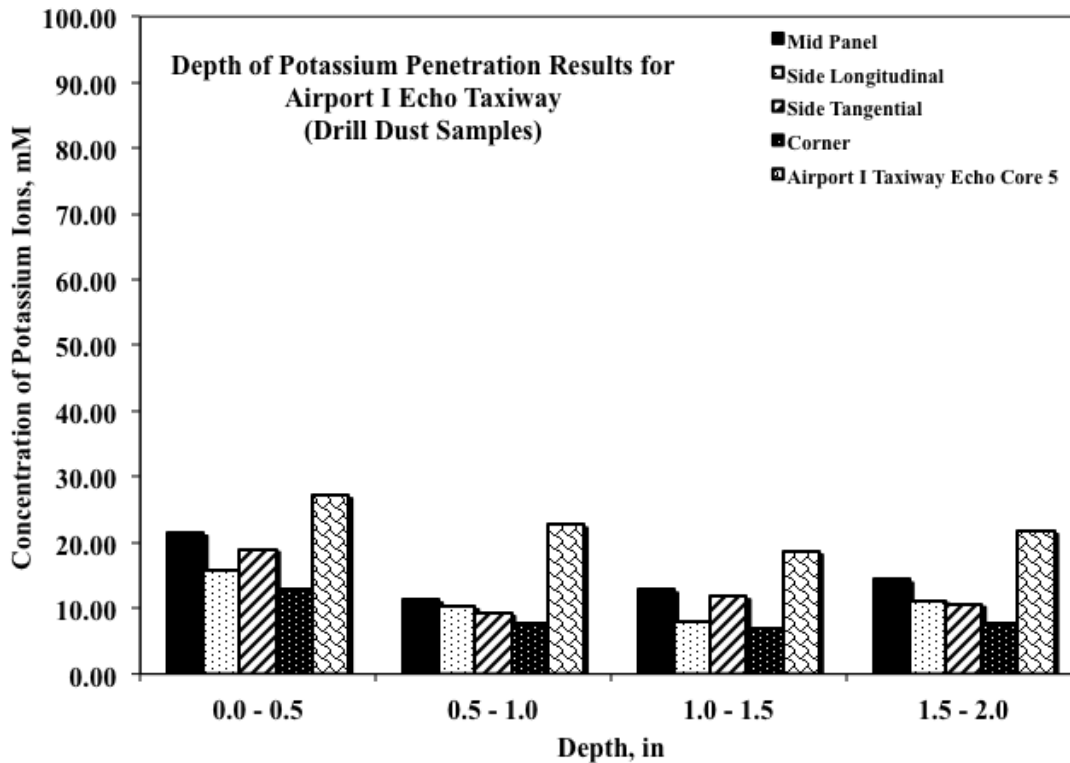


Figure 36: Depth of Ion Penetration Results for Airport I Taxiway Echo (Field Analysis)

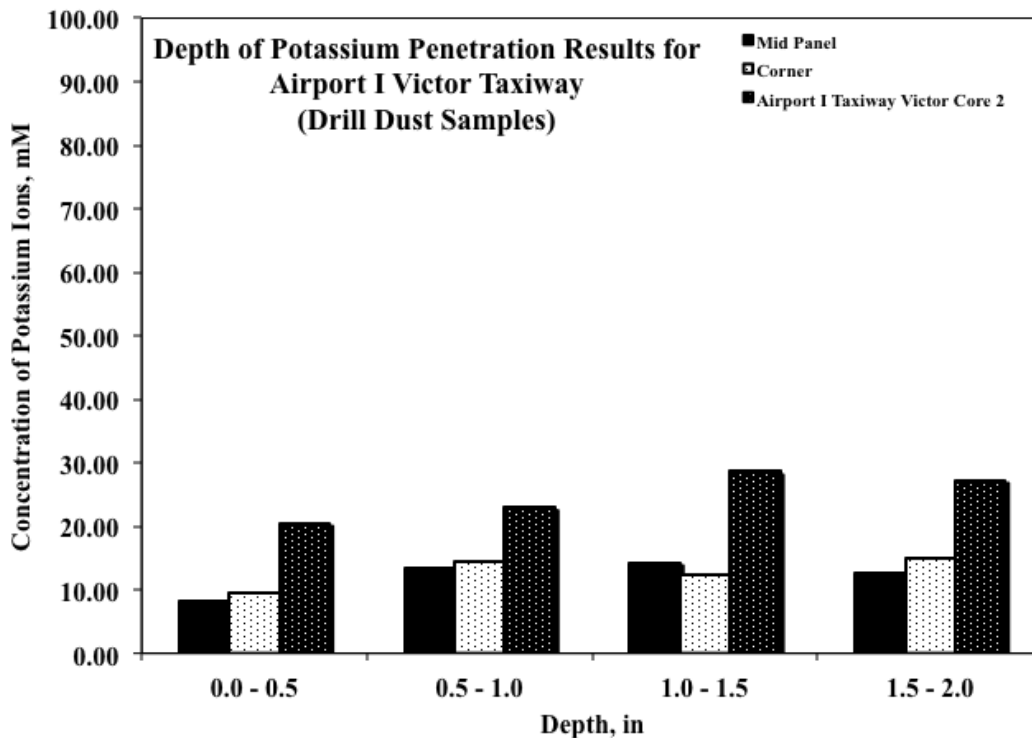


Figure 37: Depth of Ion Penetration Results for Airport I Taxiway Victor (Field Analysis)

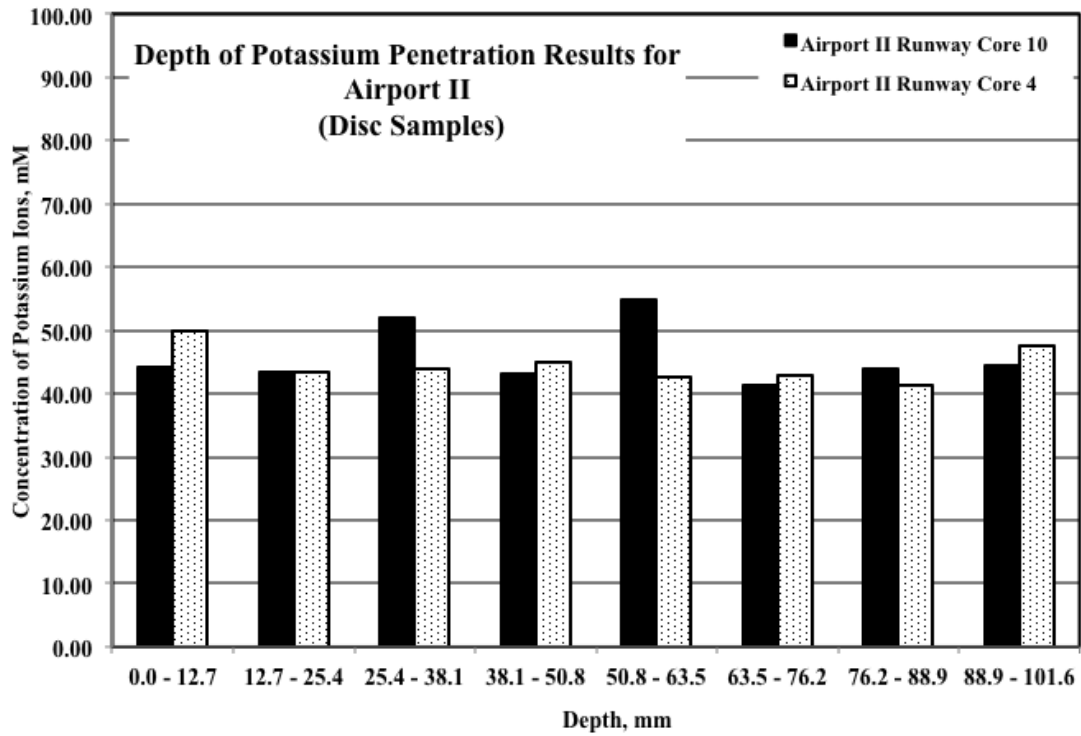


Figure 38: Depth of Penetration Results for Airport II (Core Analysis)

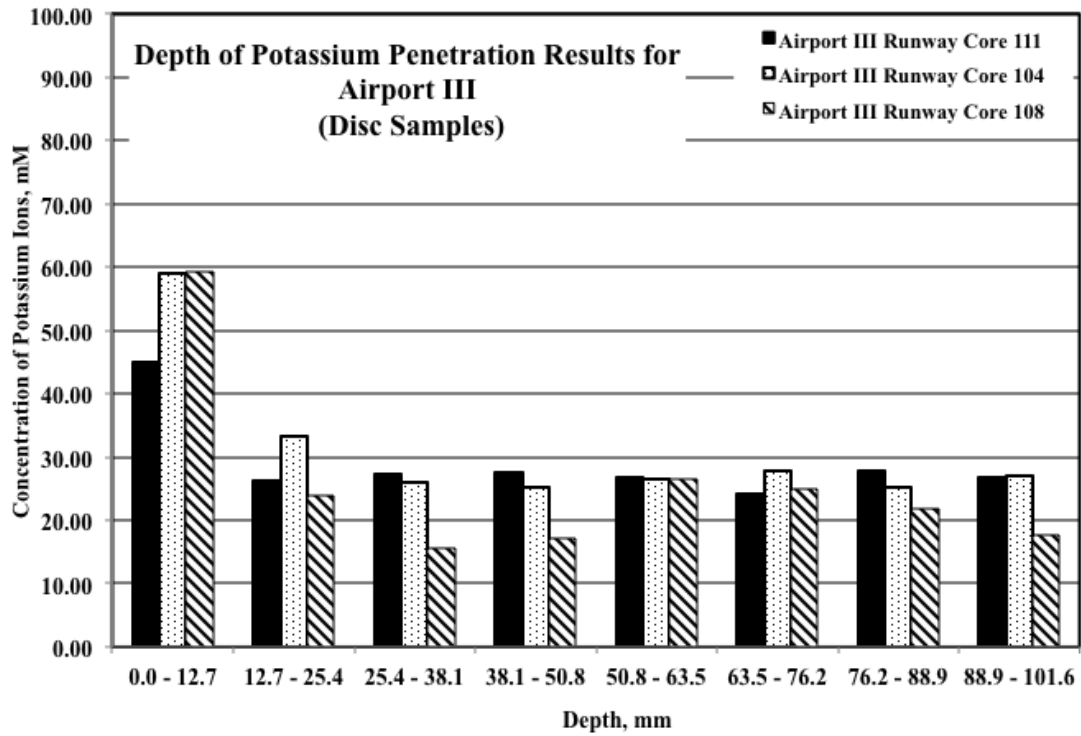


Figure 39: Depth of Penetration Results for Airport III (Core Analysis)

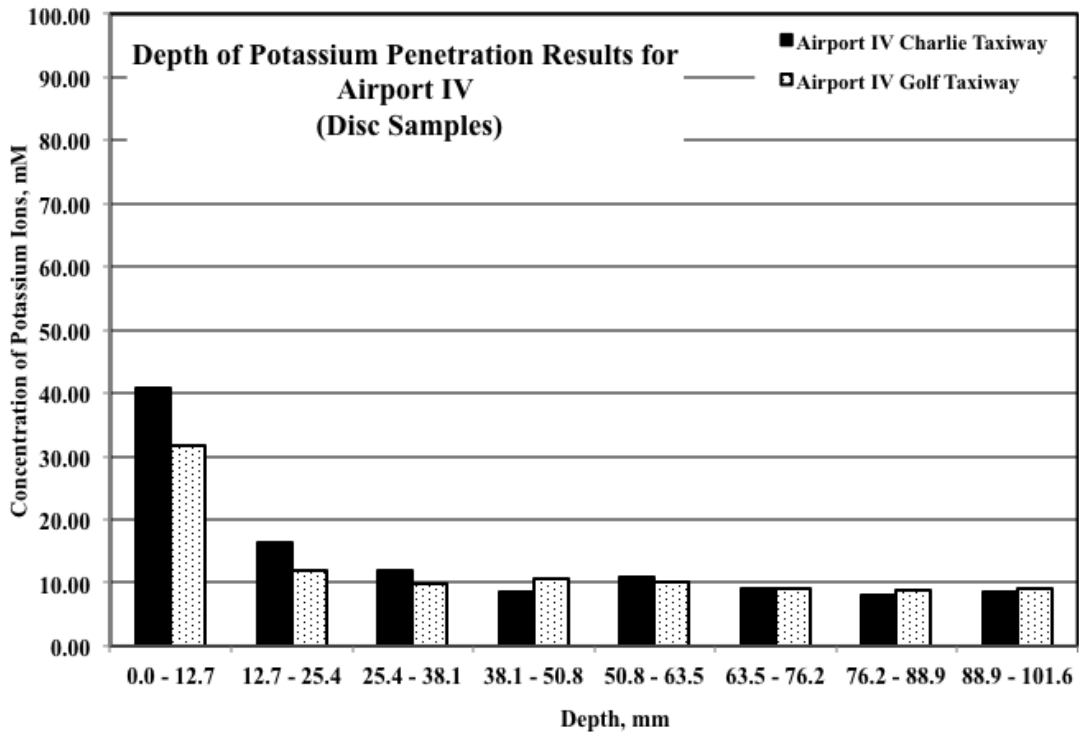


Figure 40: Depth of Penetration Results for Airport IV (Core Analysis)

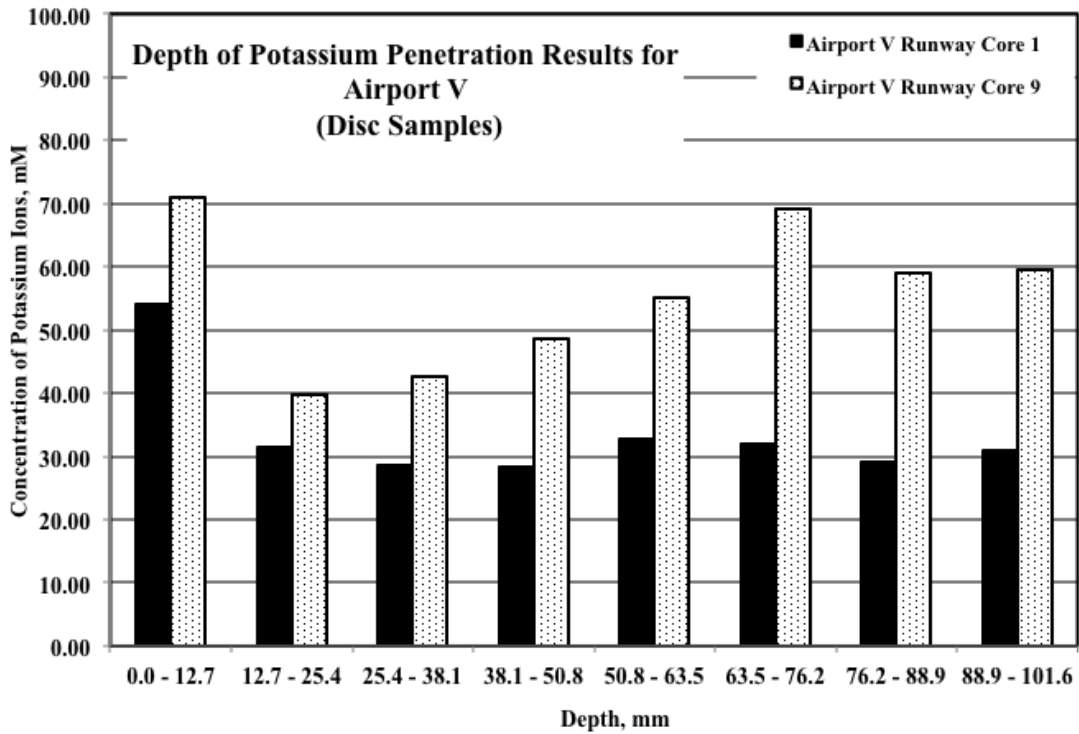


Figure 41: Depth of Penetration Results for Airport V (Core Analysis)

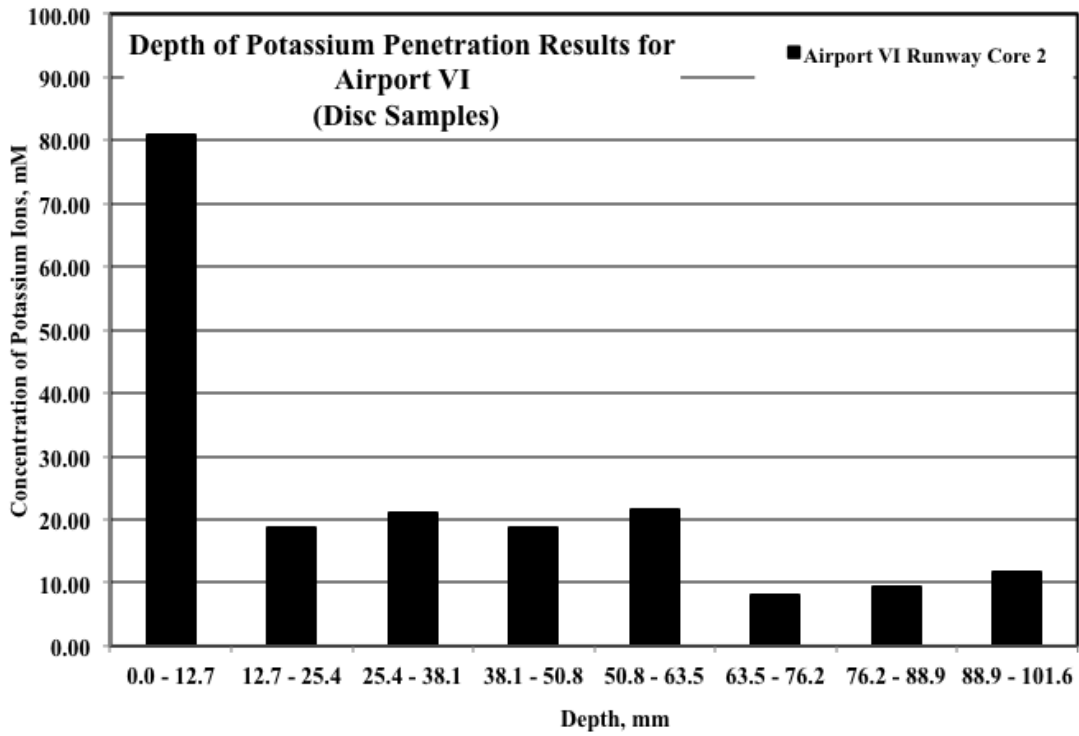


Figure 42: Depth of Penetration Results for Airport VI (Core Analysis)

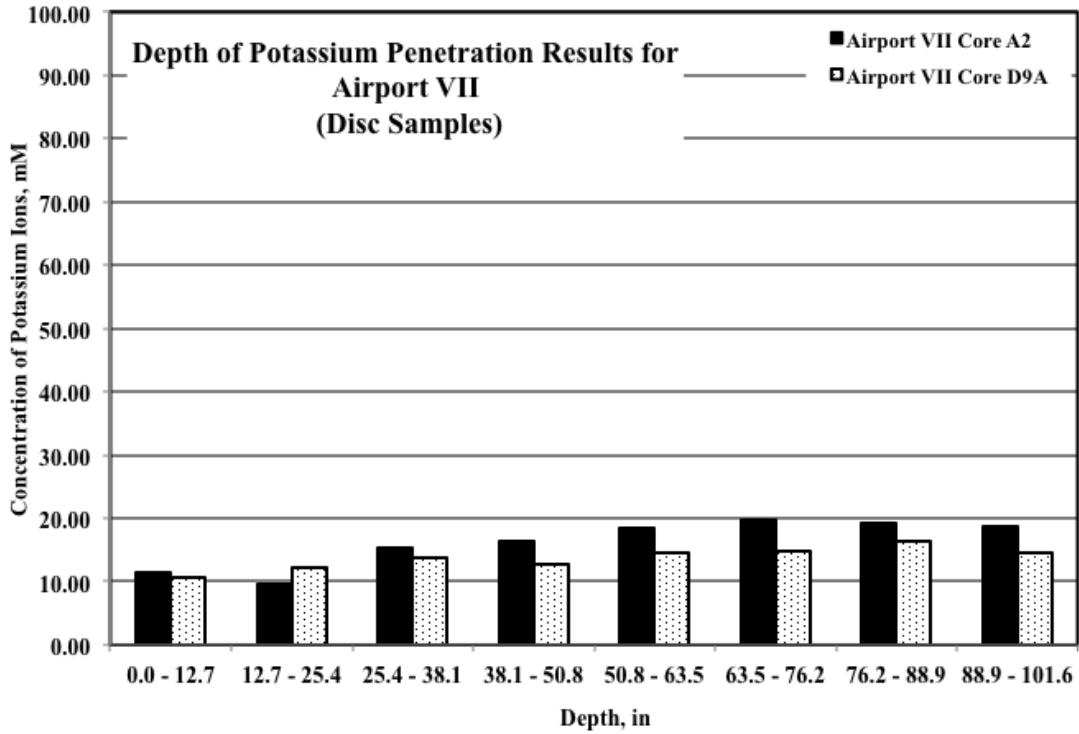


Figure 43: Depth of Penetration Results for Airport VII (Core Analysis)

Discussion

Calibration Study

The results from the calibration study showed that the disc sampling method produced equivalent or higher concentrations of potassium ions when compared with the powder sampling method. This is probably due to the increased surface area of the sampling area, which helps to create a more representative sample.

The baseline potassium ion reading was calculated from the control samples and subtracted out of the values for the other types of conditioning. The baseline potassium ion value for the materials used in this study was determined to be 12.55 millimoles. The conditioning that produced the highest depth of penetration of the potassium ion was the wetting and drying condition at 80C followed by the wetting and drying condition at 23C (ambient). This was due to the capillary suction action of the concrete created during the drying conditioning. These two conditions would not reflect field conditions due to the fact that anti icers would not be applied at 23C and also the temperature after application would not be 23C or higher (80C). Although these two conditions would not reflect field conditions, the physical action of wetting and drying at lower temperatures would follow the same trend producing higher depths of potassium ion penetration when compared to the freezing and thawing condition and the constant application condition.

The wetting and drying condition produced penetration depths beyond two inches for both temperatures, while the constant application condition produced between one and two inches of penetration and the freeze thaw condition produced only about a half inch of penetration. The freeze thaw condition was considered the most reflective of the field conditions and this was confirmed in the field samples. No clear trend was established between the cored and cast sample that was consistent through all of the conditions.

Airport Field and Core Study

The results of the airfield samples had similar trend to that of the freezing and thawing conditioning in the Calibration Study, that is that the penetration was only about a half of an inch. This trend held true through all of the airfield samples. The background levels could not be subtracted out due to the fact that we did not have samples that were not exposed to potassium acetate deicer.

Only one airport could be sampled in this method due to access issues. Airport I Echo taxiway and limited taxiway Victor were sampled using the powder sampling method to determine in place depth of potassium ion penetration. Samples were obtained by drilling holes in the pavement and collecting the drill dust or powder. Samples were only tested to a depth of two inches due to time and equipment restrictions. No clear trend can be made except to say that the concentration was less for the powder samples when compared to the core samples (disc sampling method) and that the depth of penetration

must be very low due to the concentration being somewhat consistent throughout the two-inch depth.

Conclusion

From the fundamental studies (calibration study) conducted to understand the migration of potassium acetate into concrete, it was found that the wetting and drying of concrete was most aggressive and resulted in penetration of potassium to over two inches, regardless of the storage temperature. The continuous exposure of concrete to potassium acetate deicer yielded potassium penetration between one and two inches from the surface. Exposure of concrete to deicer under freeze-thaw conditions resulted in a penetration of potassium to only about a one half of an inch from the surface. The freeze thaw condition was considered the most reflective of the field conditions and this was confirmed in the field samples having similar exposure.

The results of the determination of potassium ion penetration in airfield samples had similar trend to that of the freezing and thawing conditioning in the Calibration Study, that is that the penetration was only about one half of an inch or 12.7mm. This trend held true through all of the airfield samples.

Part 4: Freeze-Thaw Analysis

Introduction

In order to evaluate what affect the potassium acetate based deicers have on field samples during freeze-thaw cycling a new test method was developed. This test method incorporated field samples that were exposed to the deicer prior to and periodically during the test. The depth of deicer penetration study found that the deicer only penetrated to a maximum depth of half an inch into the pavement. These samples were exposed to deicers in an exaggerate way, along with extreme freezing and thawing cycles in order to simulate long-term exposure. The best method of testing the samples durability was through the use of pulse velocity testing at set intervals, along with visual observations of the samples. Due to time restrictions testing was only completed on Airports I-VI

Method

The cores used for this test were cut to a thickness of about 2.9” and a height of four inches and then holes were drilled in the top and bottom to install studs for length measurements. The reason for the modification of the minimum thickness (Less than 3”) was due to size restraints of the sample holders in the freeze-thaw apparatus. A diagram of the freeze-thaw regime can be seen in Figure 44. Readings were taken every sixty cycles, which is also a modification from the standard, which is 36 cycles. The biggest modification to the test was the storage of samples prior to the test and after every 60 cycles. Samples were kept in protective wrapping prior to the test to ensure that the moisture content remained the same as when first arrived to Clemson. Once the test was ready to begin (i.e. samples were saw cut to size and studs embedded) the samples were placed in an environmental chamber at 23C for 24hrs. Once this was completed the samples were placed in storage solutions (Deionized H₂O for Control test and 6.4M KAc for modified test) and kept at 38C for 48 hrs. After this was completed the samples were again kept at 23C for 24hrs in the environmental chamber. The initial readings were then taken and all following readings were compared to these. The readings consisted of weight readings, pulse velocity readings, and length measurements. The samples were then put in the freeze-thaw chamber to begin the testing and after every 60 cycles this conditioning process was completed and readings taken. This test was continued until the failure of the samples (i.e. the samples completely fell apart). Example photographs of a prepared sample and the freeze-thaw testing machine can be seen in Figure 45.

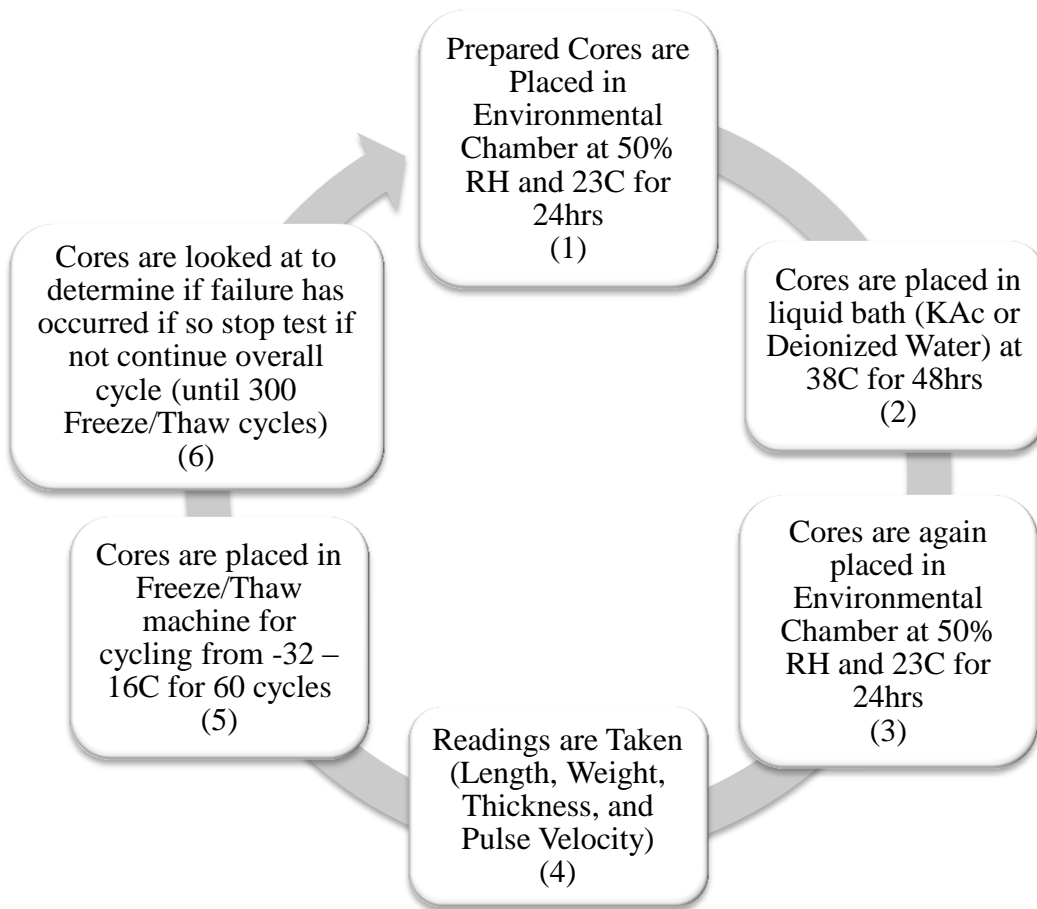


Figure 44: Modified Freeze-Thaw Testing Regime

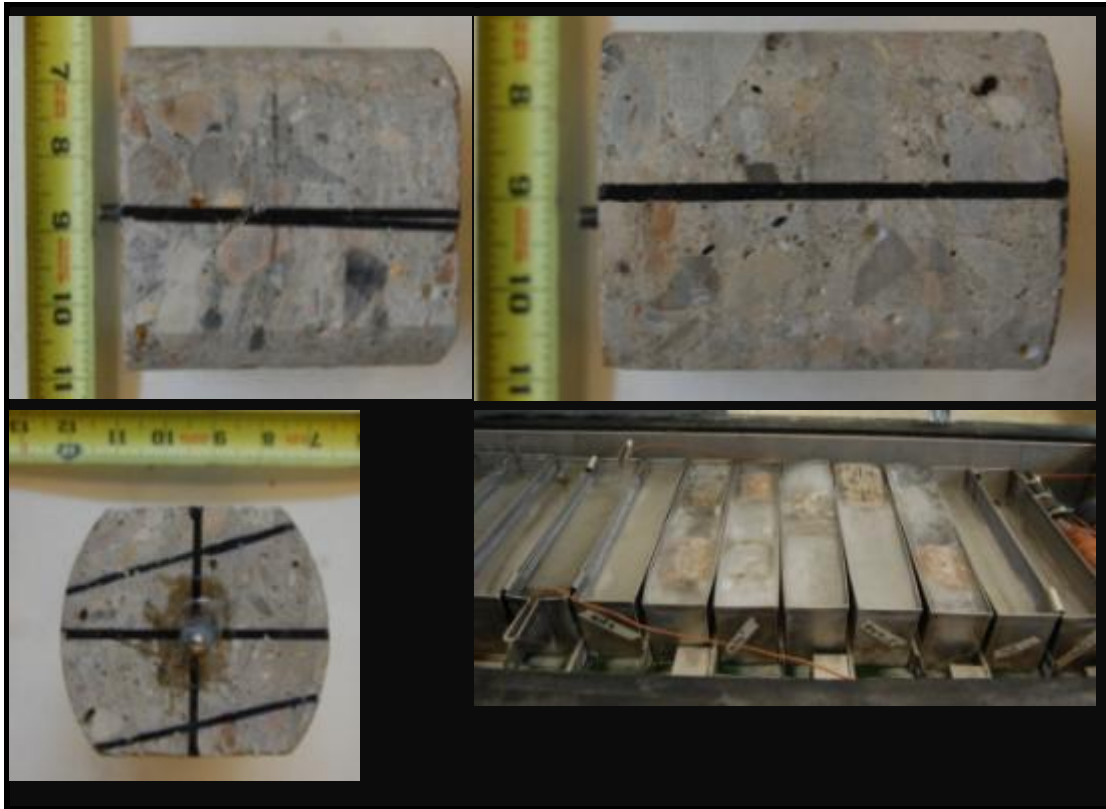


Figure 45: Example Photos of Prepared Freeze-Thaw Samples and Test Setup

Results

The freeze thaw testing of modified field cores showed a general trend with respect to increased deterioration when exposed to potassium acetate. The percentage difference in pulse velocity readings throughout the test compared to the initial readings can be seen in Figure 46, Figure 47, Figure 48, and Figure 49. The visual and pulse velocity results both support the hypothesis that the potassium acetate deicer reduces the freeze thaw durability of the concrete system. The visual results show a failure of the mortar fraction of the concrete surface surrounding the coarse aggregates. During the test the samples exposed to KAc typically failed once the pulse velocity values went below 80% of the original value. This trend did not hold true for the control samples, which had some samples last to the end of the regime with pulse velocity values below 80% of the original. The results of the first set of samples (Airports I – III) showed that the control samples had pulse velocity values greater than or equal to 90% of their original values, while the samples exposed to KAc had values less than or equal to 85% of the original value with two of the samples failing before the end of the test. The results of the second set of samples (Airports VI – VI) had a slightly different trend with control samples having pulse velocity values greater than or equal to 75% of their original values. The second set of samples exposed to KAc had only one sample that was able to last till the

end of the test with the majority of the rest failing before the start of the 4th cycle. It should be noted that the exposure cycle of this modified test method to KAc was an intense short-term exposure. A recommendation as a result of this study is to try and determine how the cycling of this test can be correlated to actual field conditions, and be used to predict at what age these defects should start appearing.

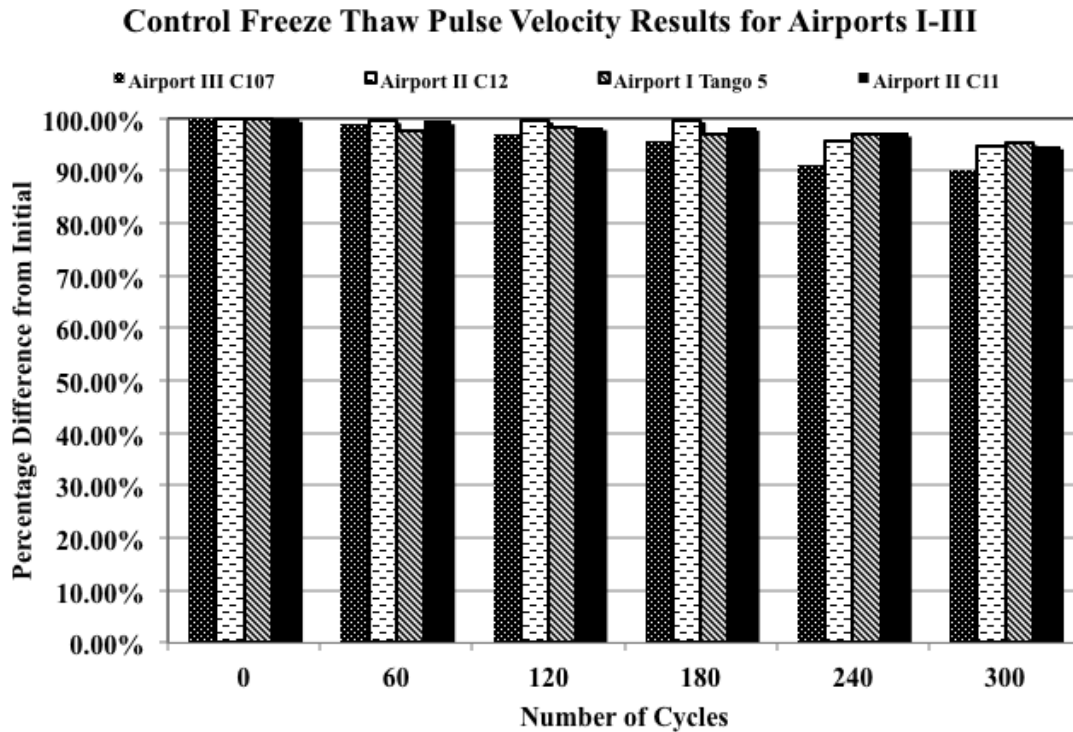


Figure 46: Control Freeze-Thaw Pulse Velocity Results for Airports I - III

KAc Freeze Thaw Pulse Velocity Results for Airports I-III

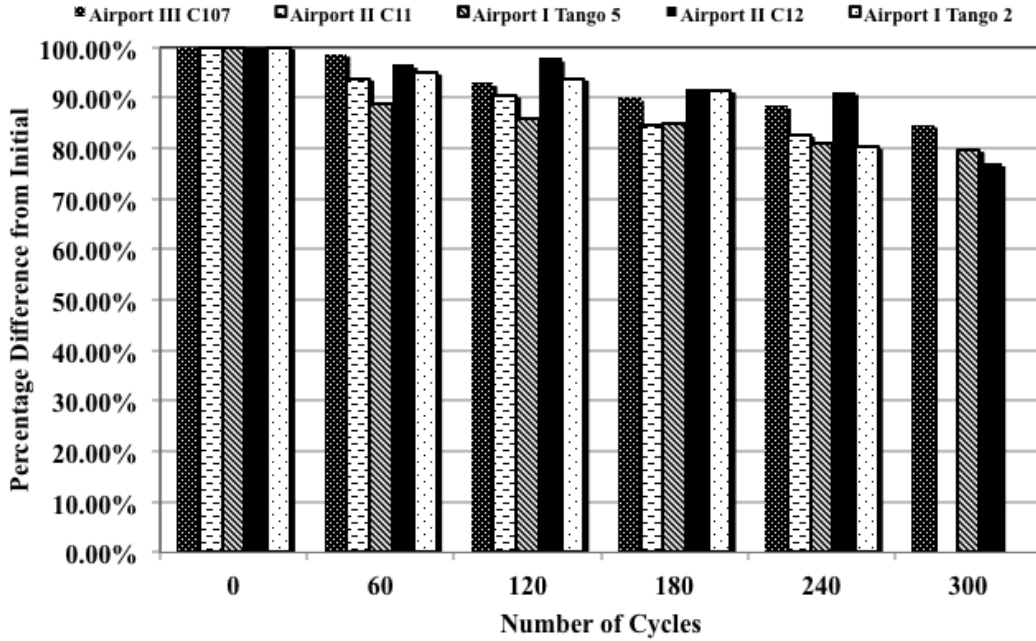


Figure 47: KAc Freeze-Thaw Pulse Velocity Results for Airports I - III

Control Freeze Thaw Pulse Velocity Results for Airports IV-VI

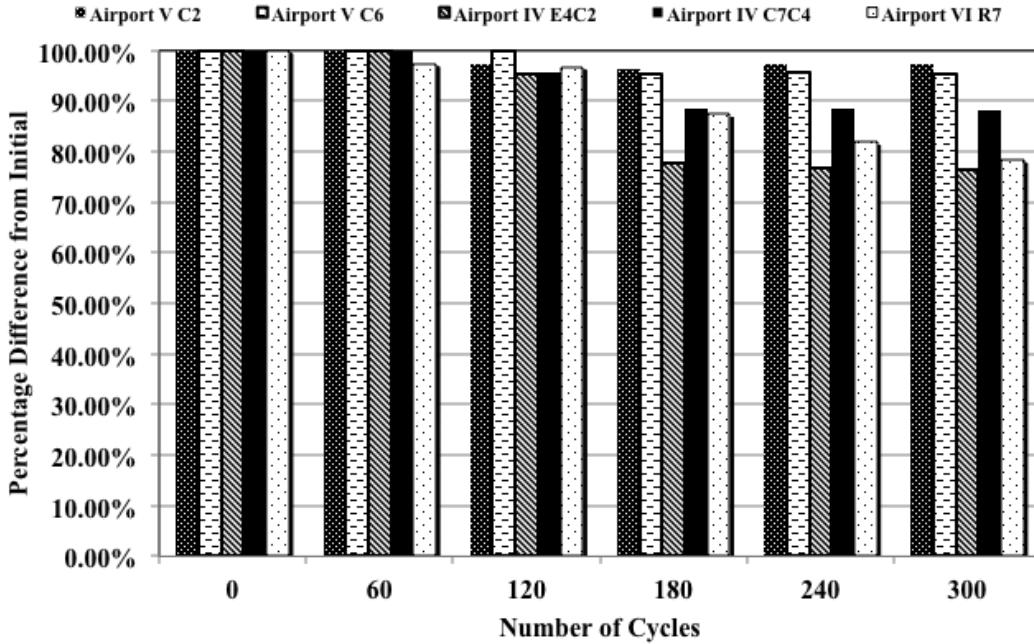


Figure 48: Control Freeze-Thaw Pulse Velocity Results for Airports IV - VI

KAc Freeze Thaw Pulse Velocity Results for Airports IV-VI

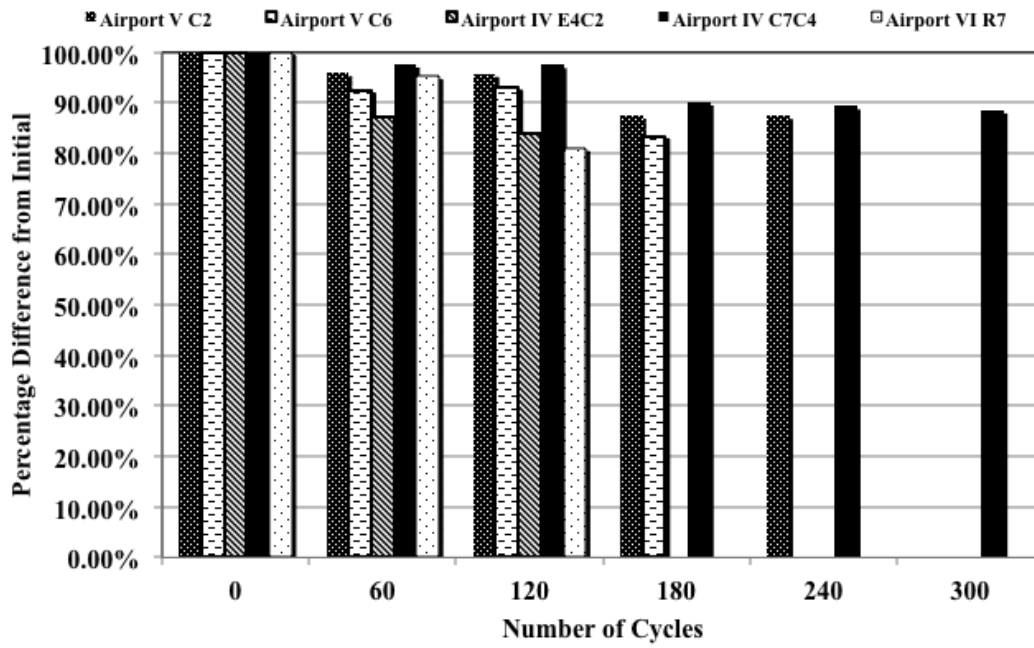


Figure 49: KAc Freeze-Thaw Pulse Velocity Results for Airports IV – VI



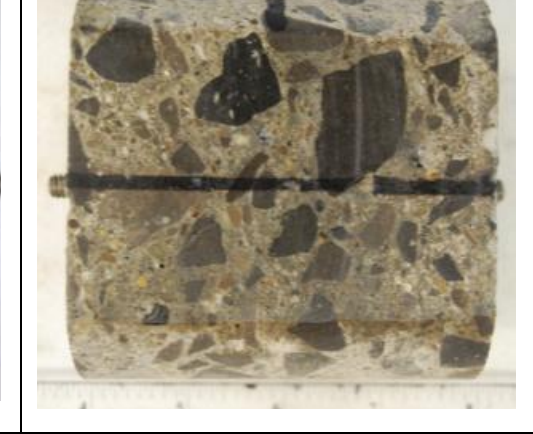


		
Initial Picture	After 1 st Cycle	After 2 nd Cycle
Picture Not Available		
After 3 rd Cycle	After 4 th Cycle	End of Test Picture

Figure 50: Visual Record of Airport I Taxiway Tango Core 5 (Control) During Freeze-Thaw Testing

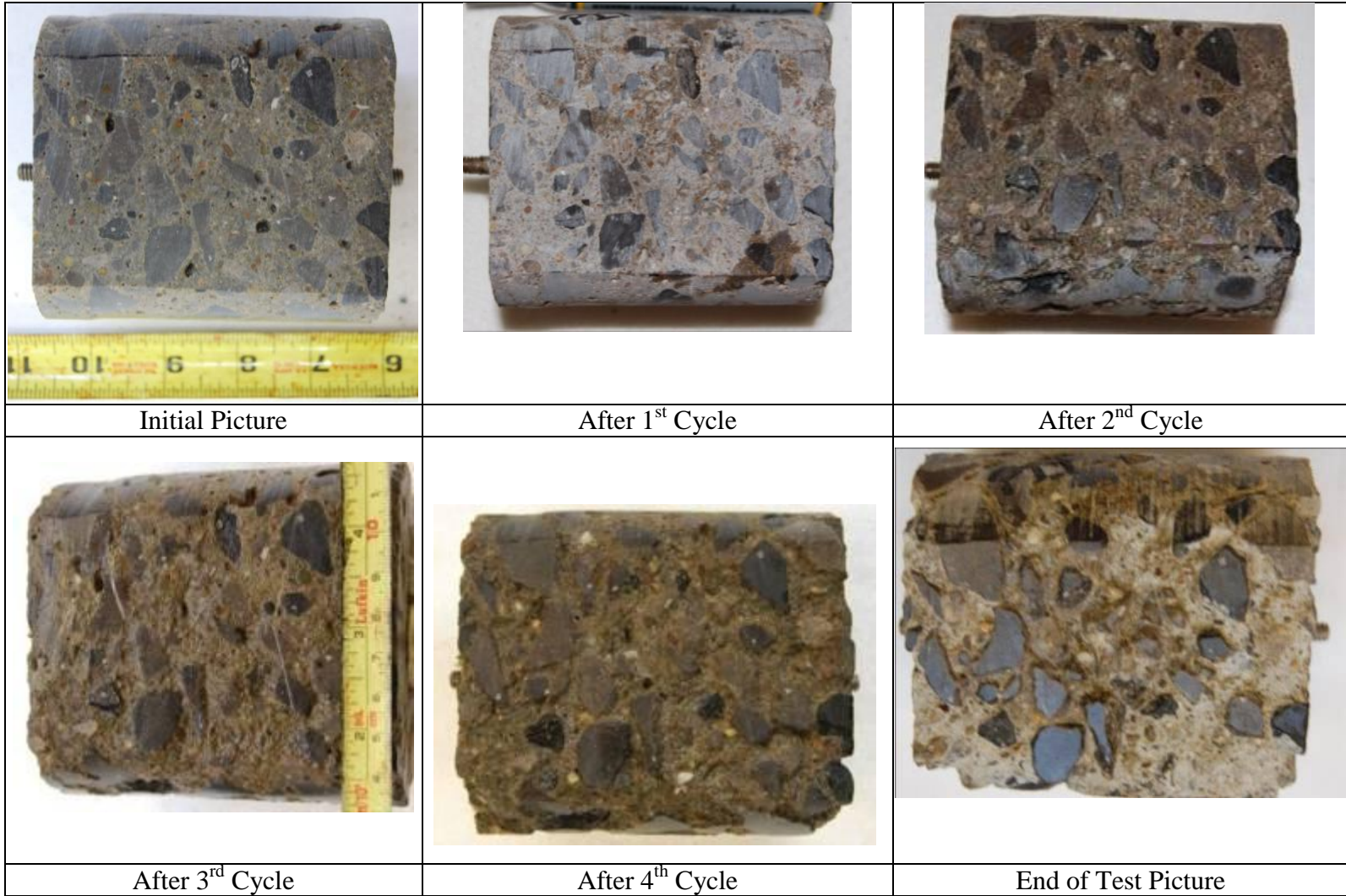


Figure 51: Visual Record of Airport I Taxiway Tango Core 5 (6.4M KAc) During Freeze-Thaw Testing

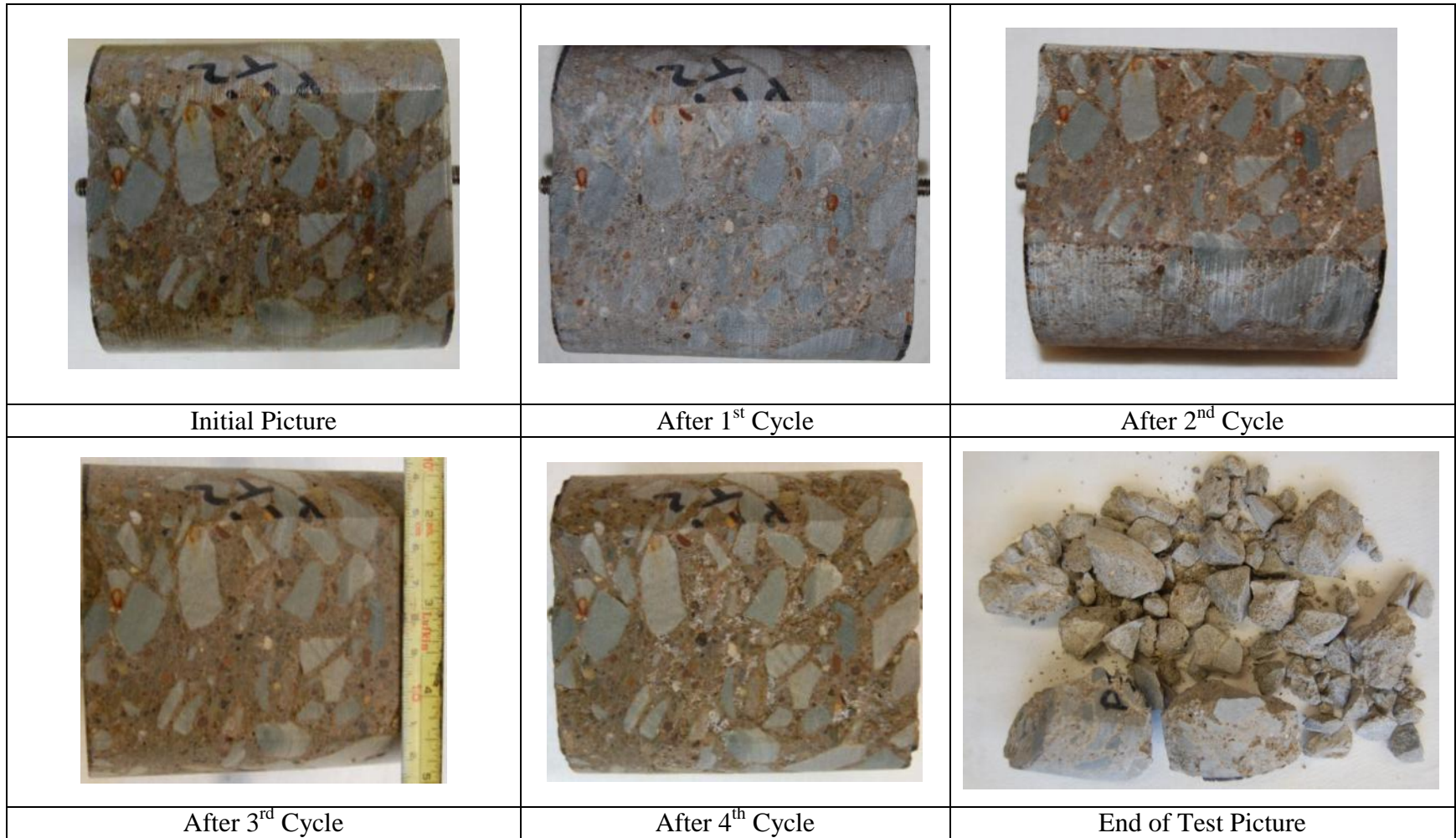


Figure 52: Visual Record of Airport I Taxiway Tango Core 2 (6.4M KAc) During the Freeze Thaw Testing


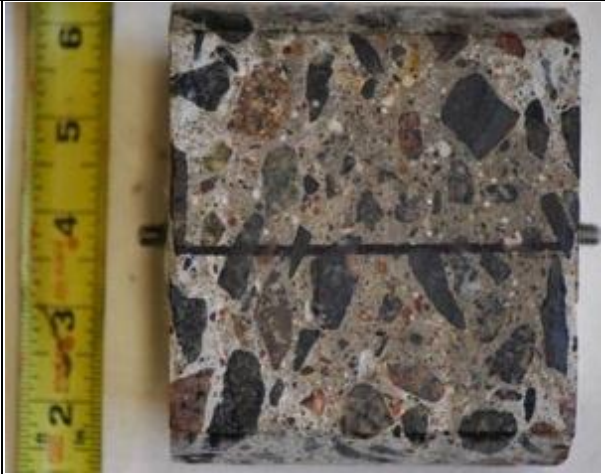
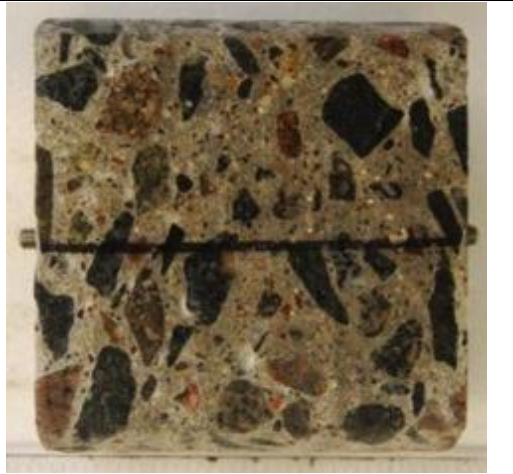
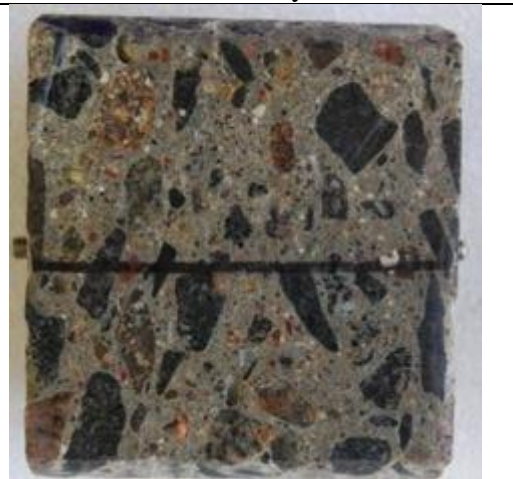
		
Initial Picture	After 1 st Cycle	After 2 nd Cycle
<p style="text-align: center;">Picture Not Available</p>		
After 3 rd Cycle	After 4 th Cycle	End of Test Picture

Figure 53: Visual Record of Airport II Runway Core 11 (Control) During the Freeze Thaw Testing

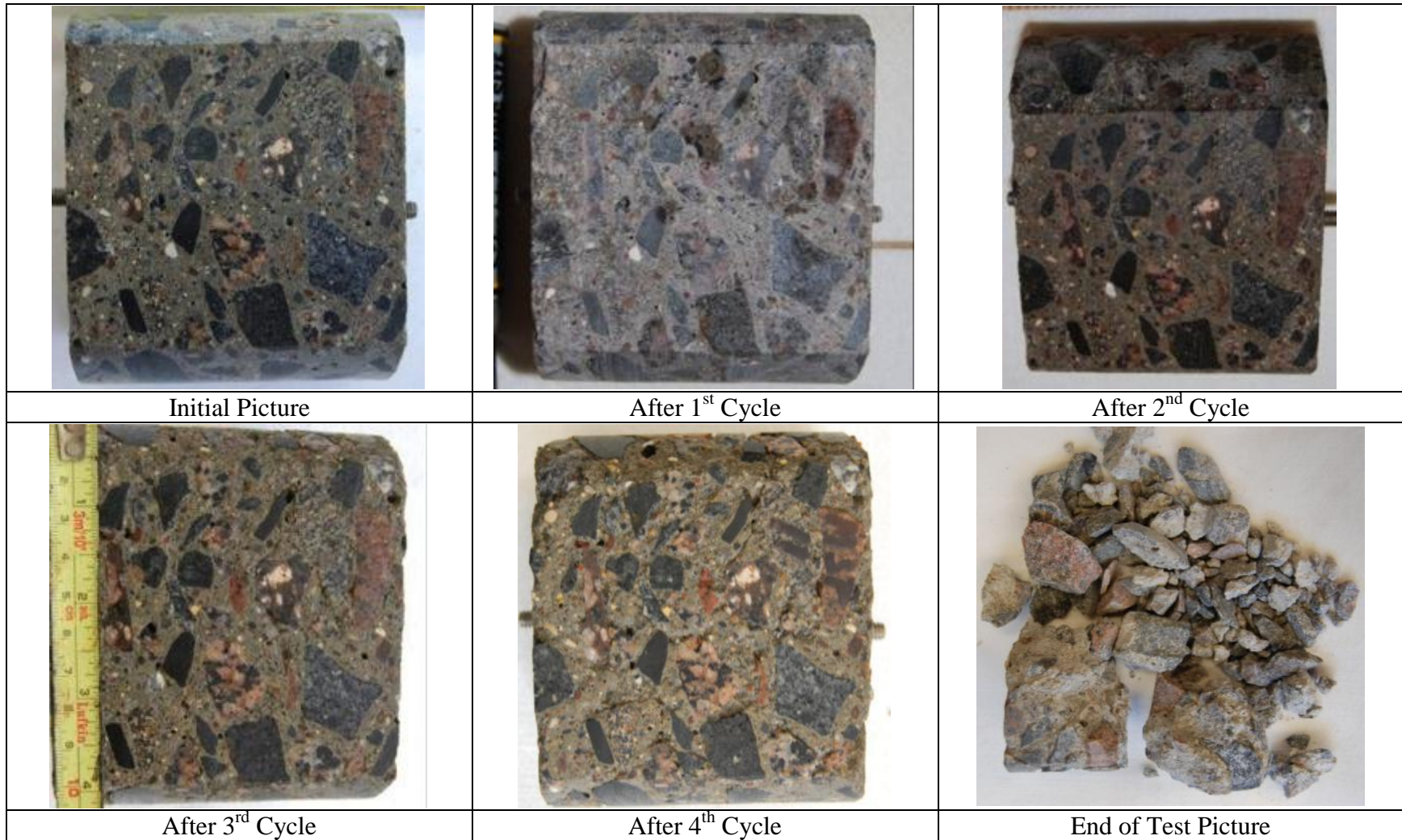


Figure 54: Visual Record of Airport II Runway Core 11 (6.4M KAc) During the Freeze Thaw Testing

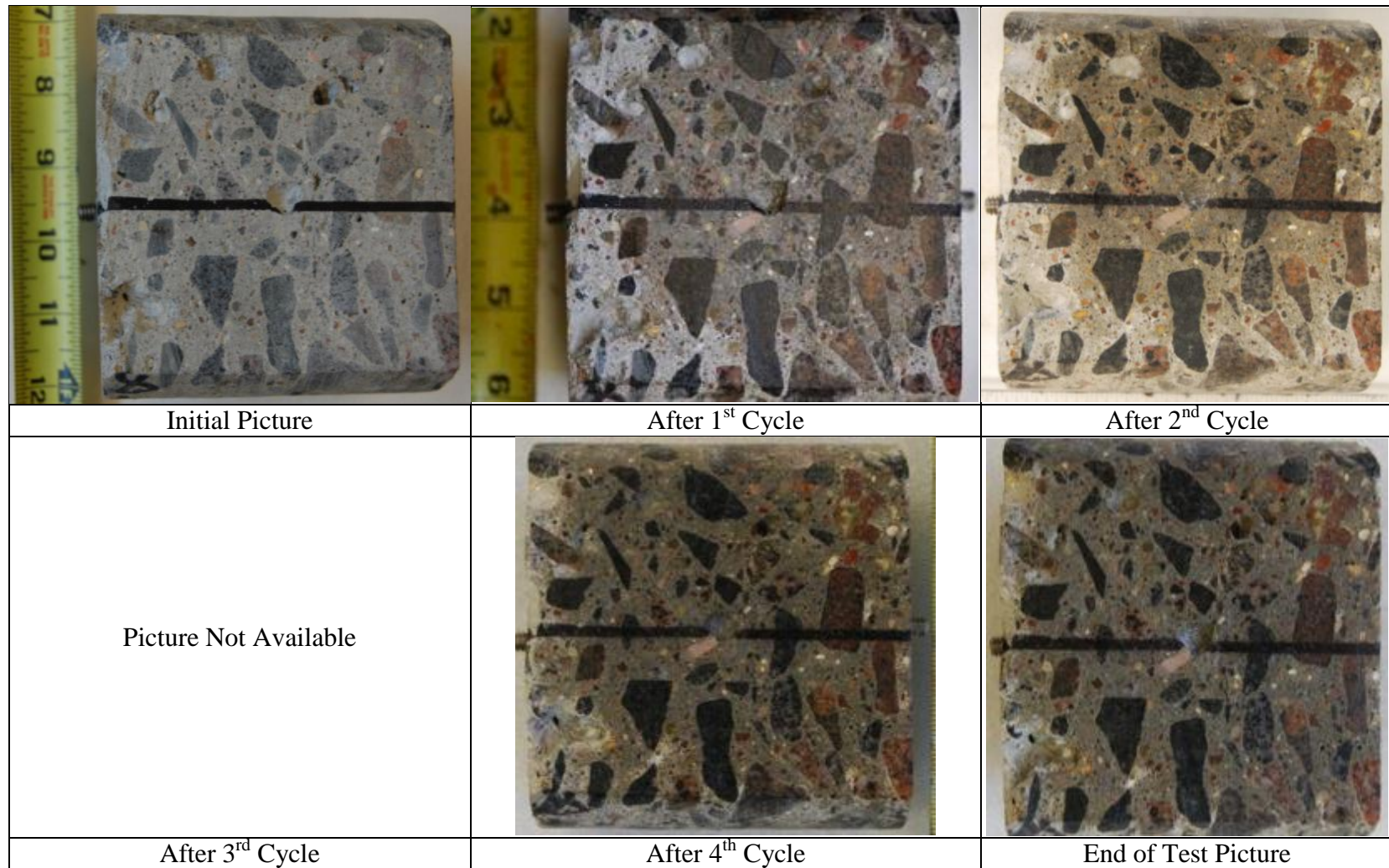


Figure 55: Visual Record of Airport II Runway Core 12 (Control) During the Freeze Thaw Testing

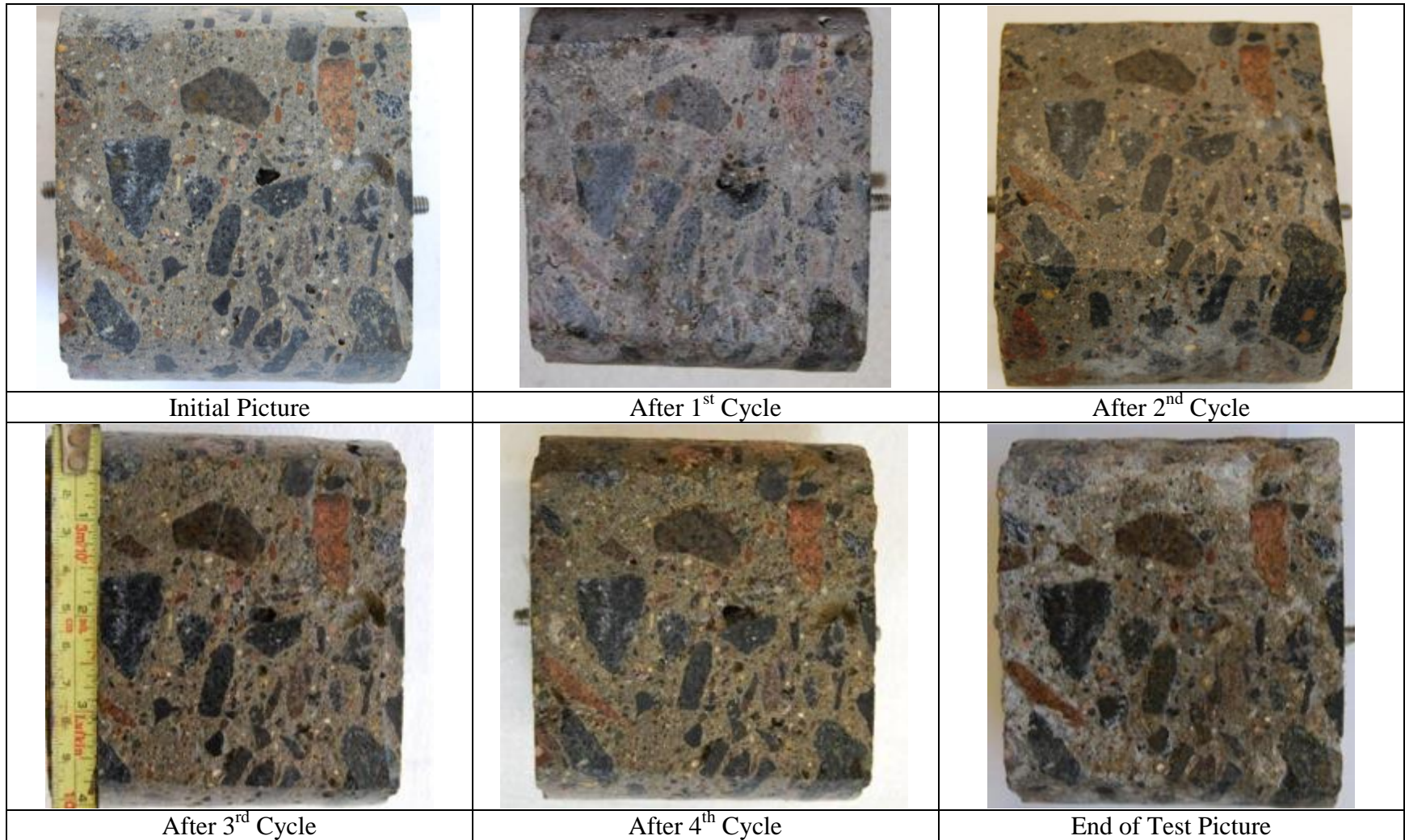


Figure 56: Visual Record of Airport II Runway Core 12 (6.4M KAc) During the Freeze Thaw Testing

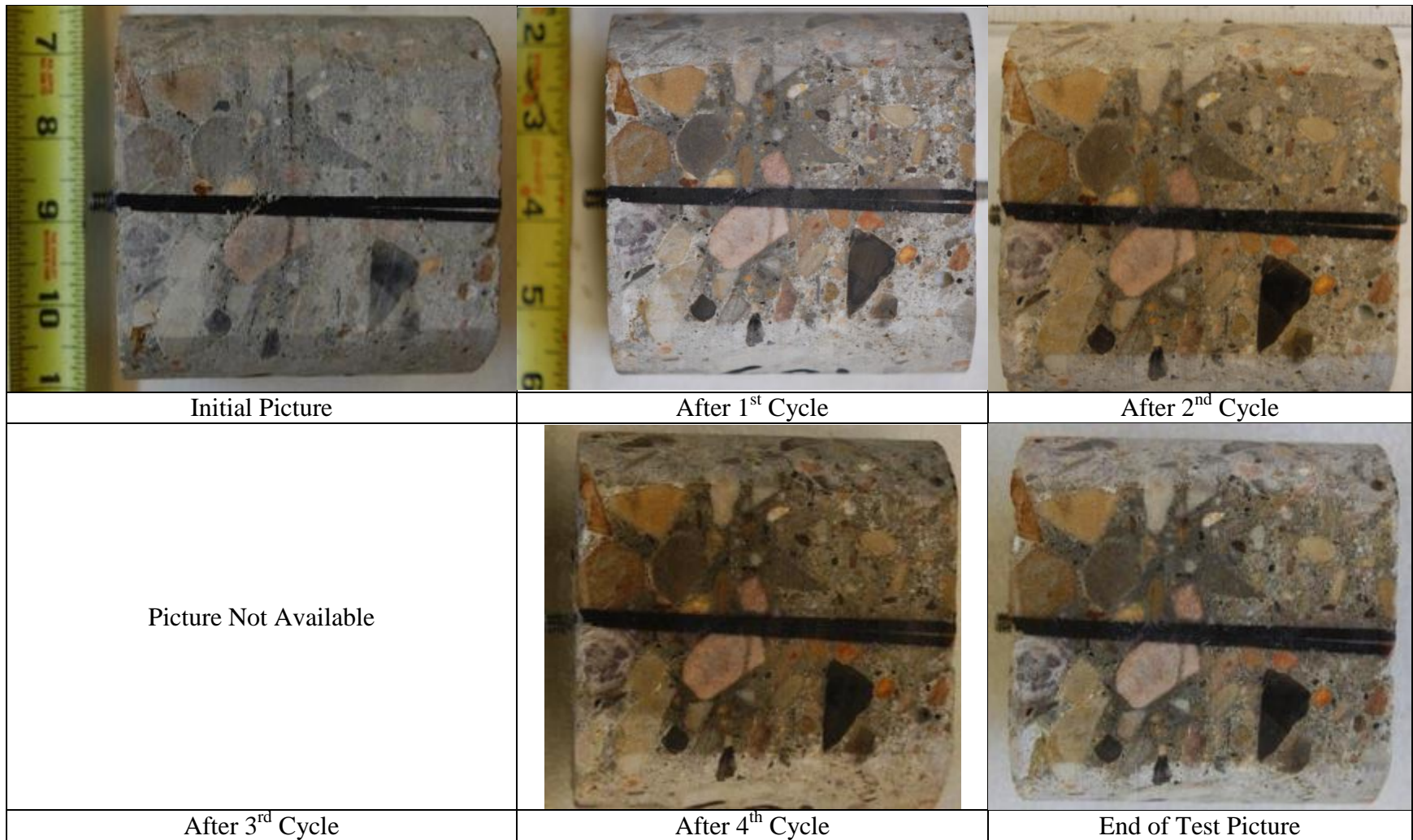


Figure 57: Visual Record of Airport III Runway Core 107 (Control) During the Freeze Thaw Testing

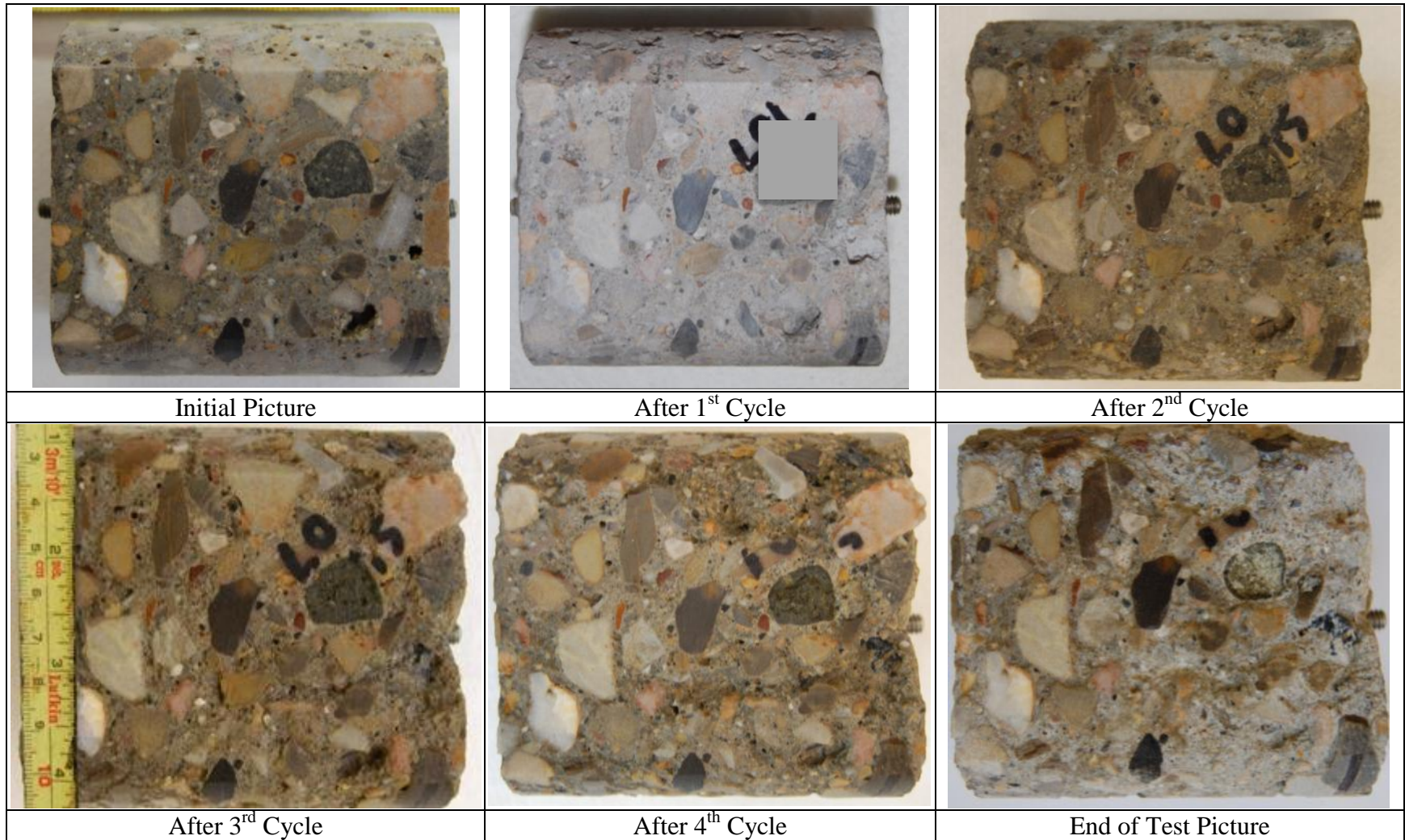


Figure 58: Visual Record of Airport III Runway Core 107 (6.4M KAc) During the Freeze Thaw Testing

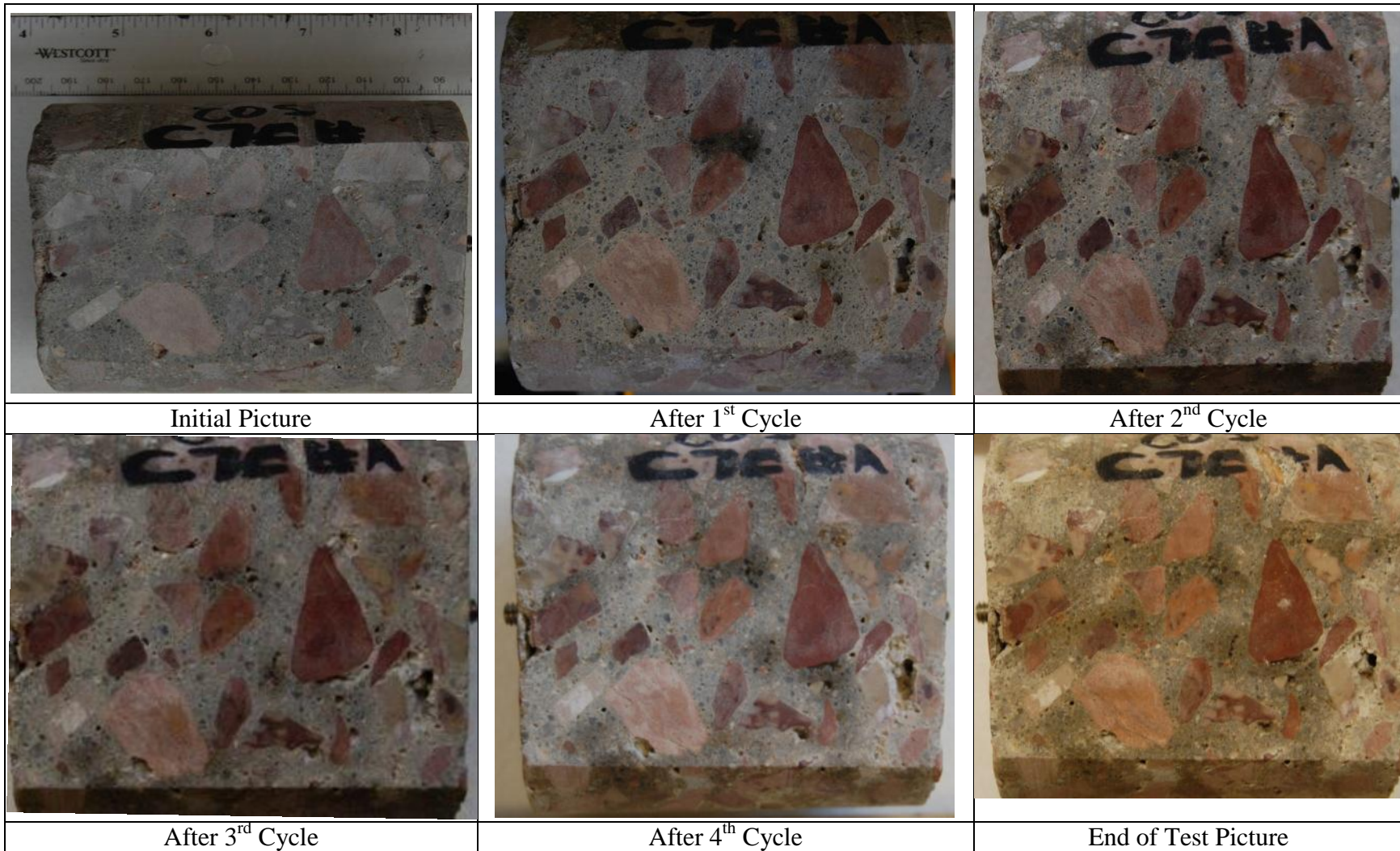


Figure 59: Visual Record of Airport IV Taxiway Charlie 7 Core 4 (Control) During the Freeze Thaw Testing

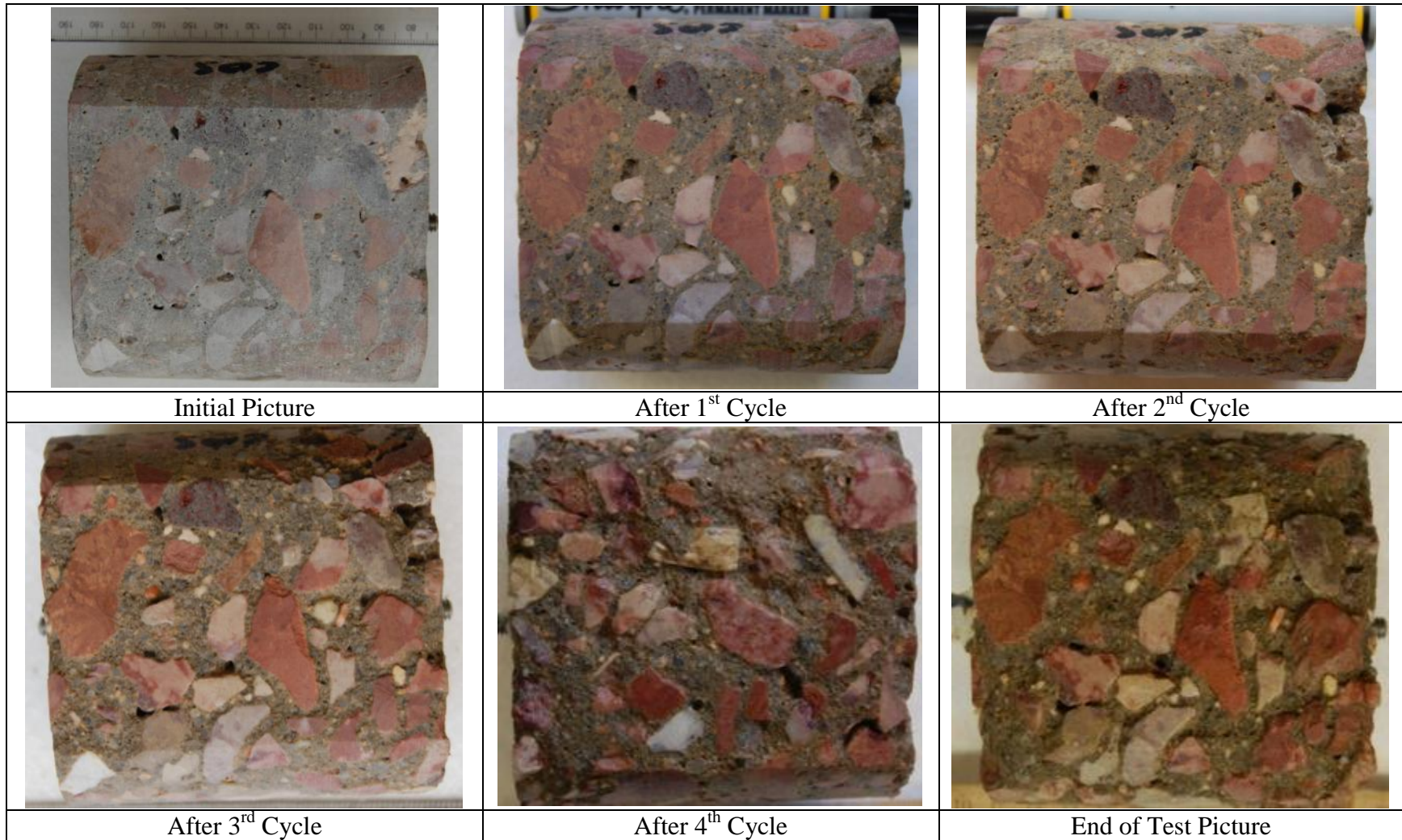


Figure 60: Visual Record of Airport IV Taxiway Charlie 7 Core 4 (6.4M KAc) During the Freeze Thaw Testing

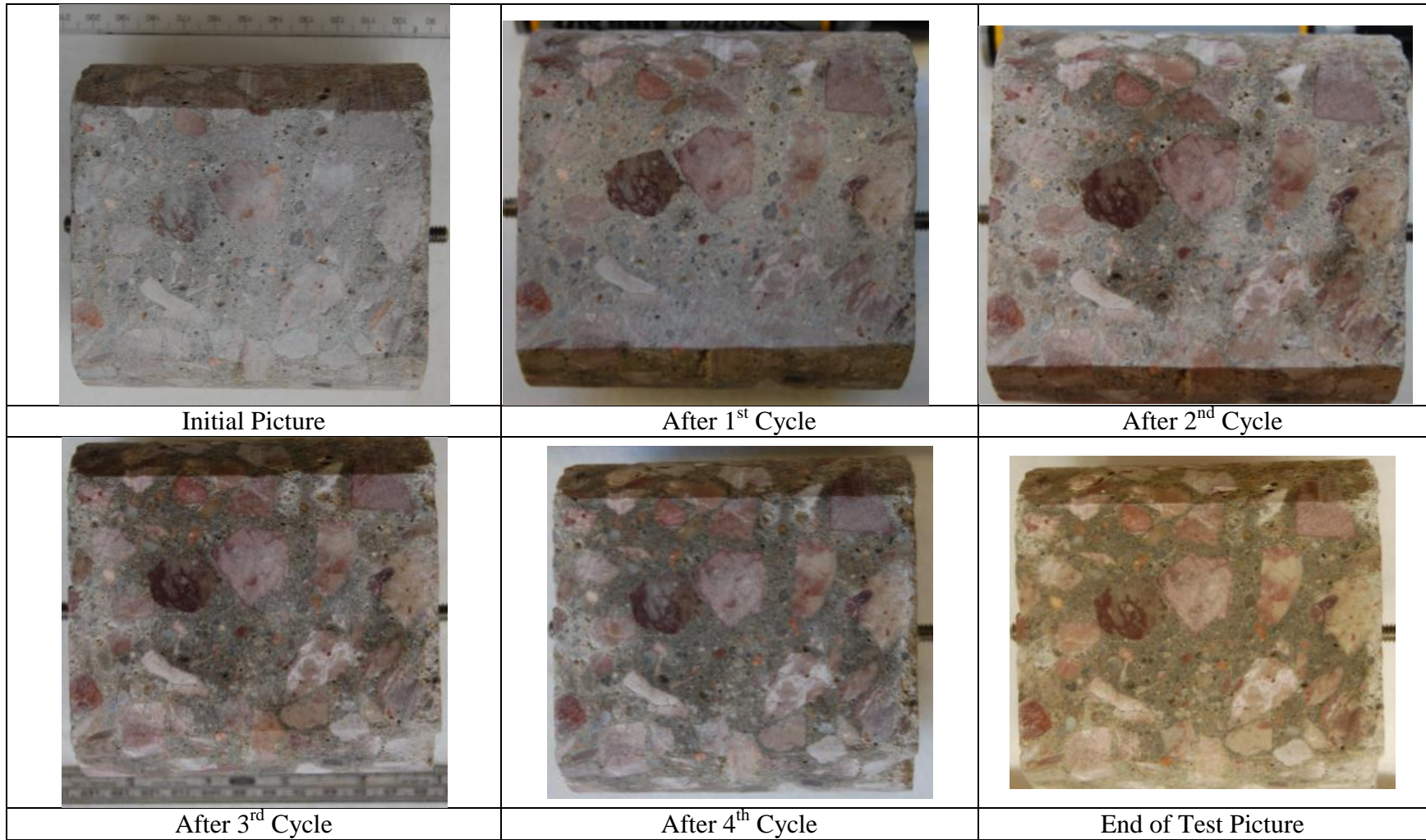


Figure 61: Visual Record of Airport IV Taxiway Echo 4 Core 2 (Control) During the Freeze Thaw Testing





		
Initial Picture	After 1 st Cycle	After 2 nd Cycle
	<p data-bbox="961 979 1136 1008">Sample Failed</p>	<p data-bbox="1535 979 1709 1008">Sample Failed</p>
After 3 rd Cycle	After 4 th Cycle	End of Test Picture

Figure 62: Visual Record of Airport IV Taxiway Echo 4 Core 2 (6.4M KAc) During the Freeze Thaw Testing

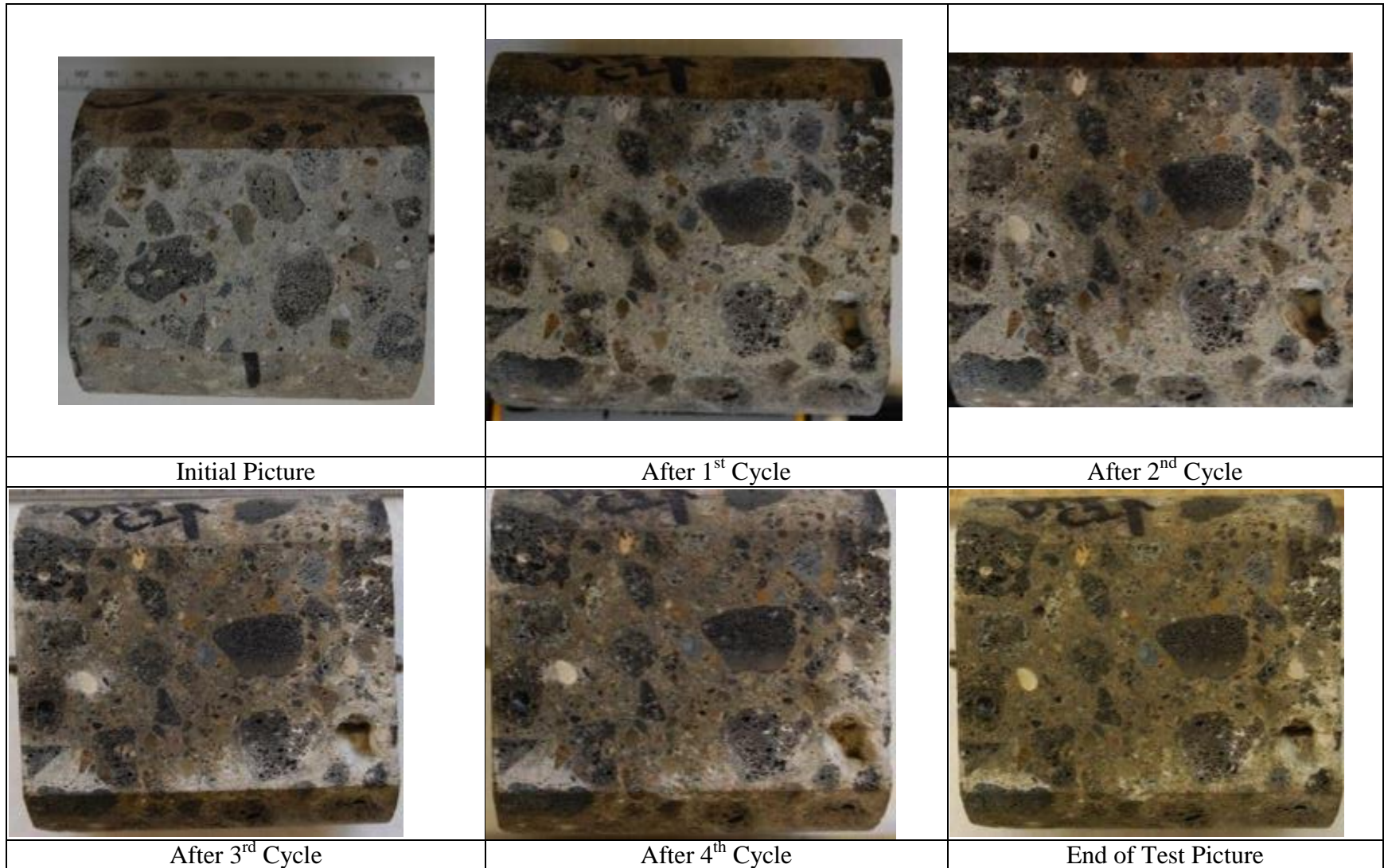


Figure 63: Visual Record of Airport V Runway Core 2 (Control) During the Freeze Thaw Testing

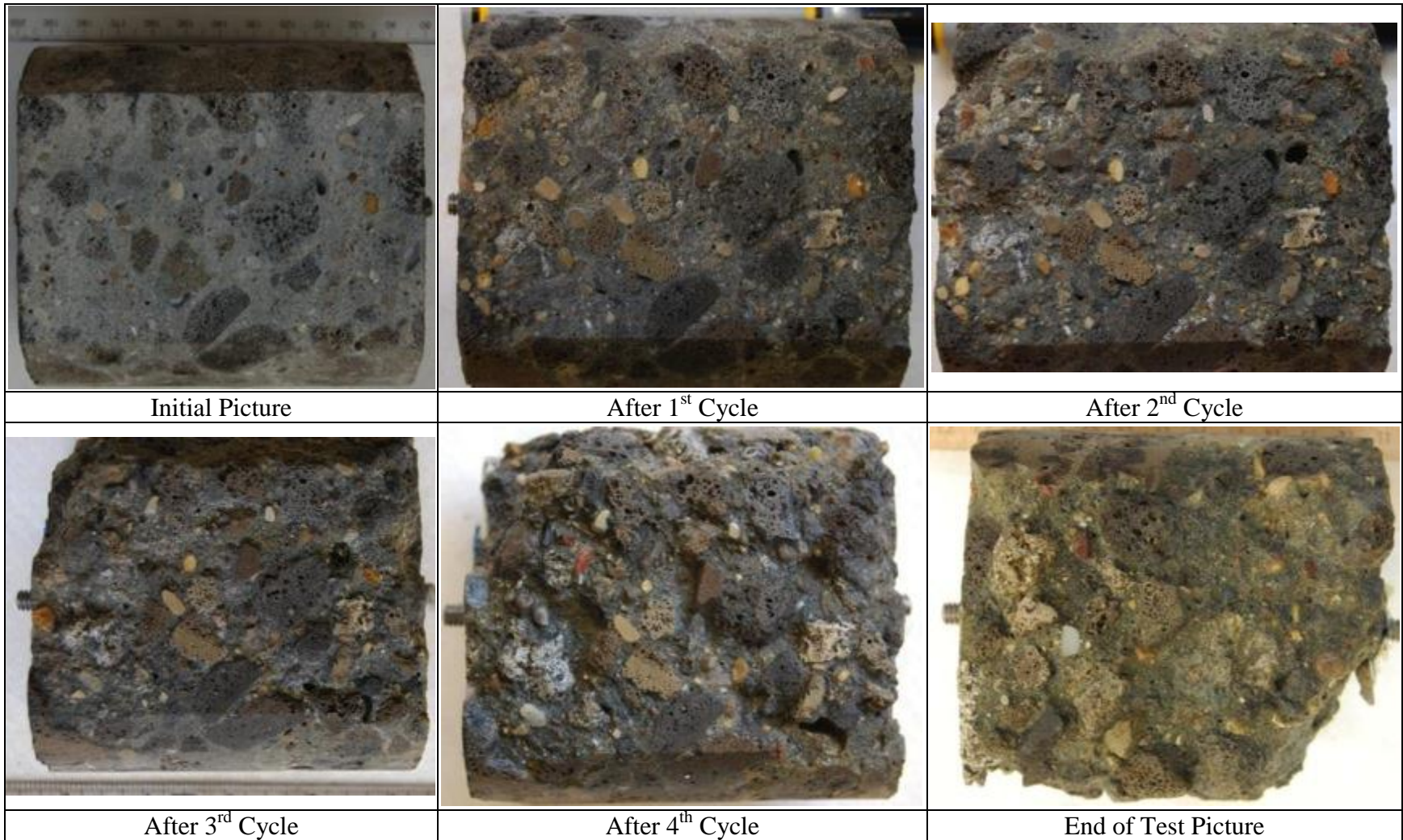


Figure 64: Visual Record of Airport V Runway Core 2 (6.4M KAc) During the Freeze Thaw Testing

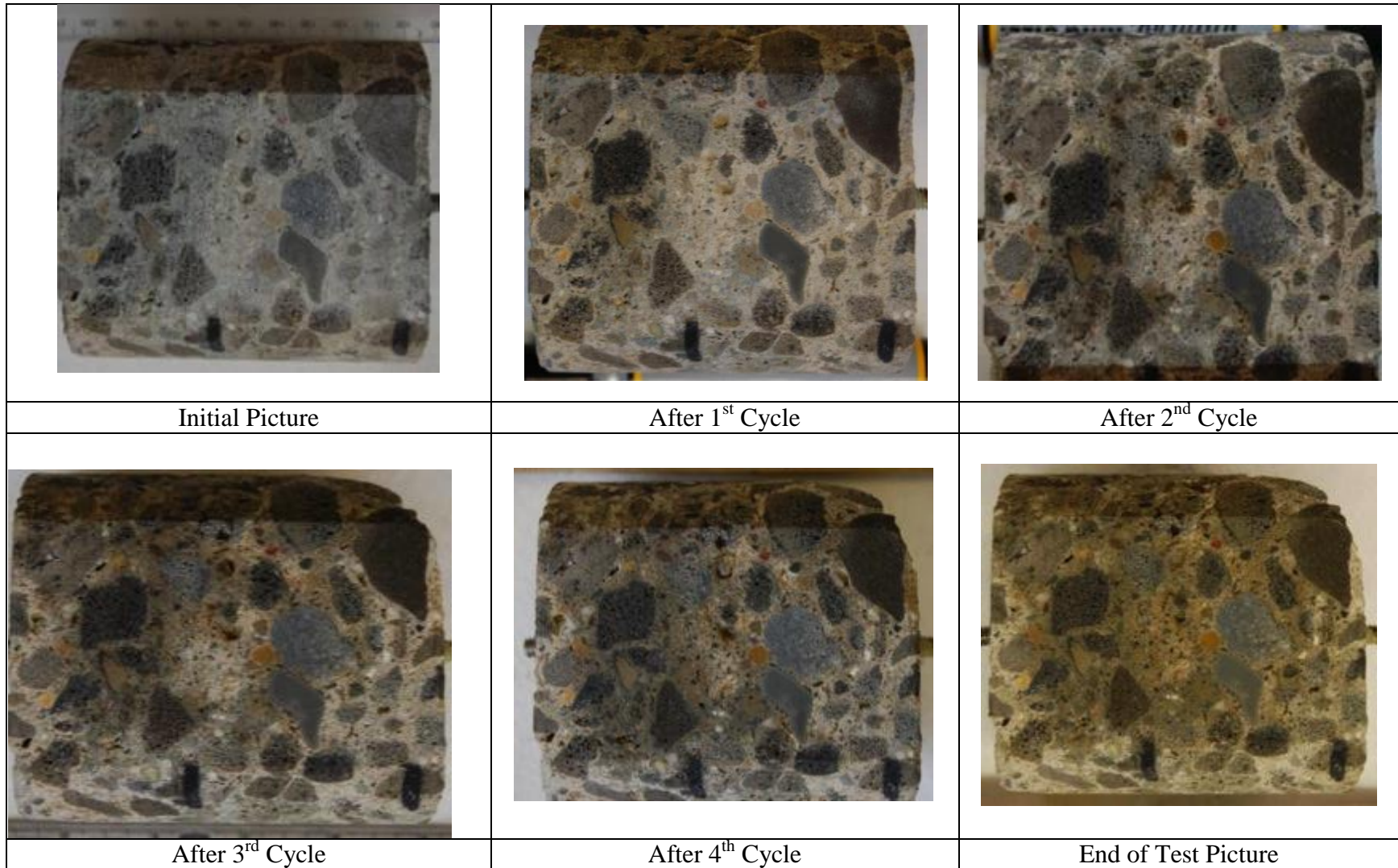


Figure 65: Visual Record of Airport V Runway Core 6 (Control) During the Freeze Thaw Testing

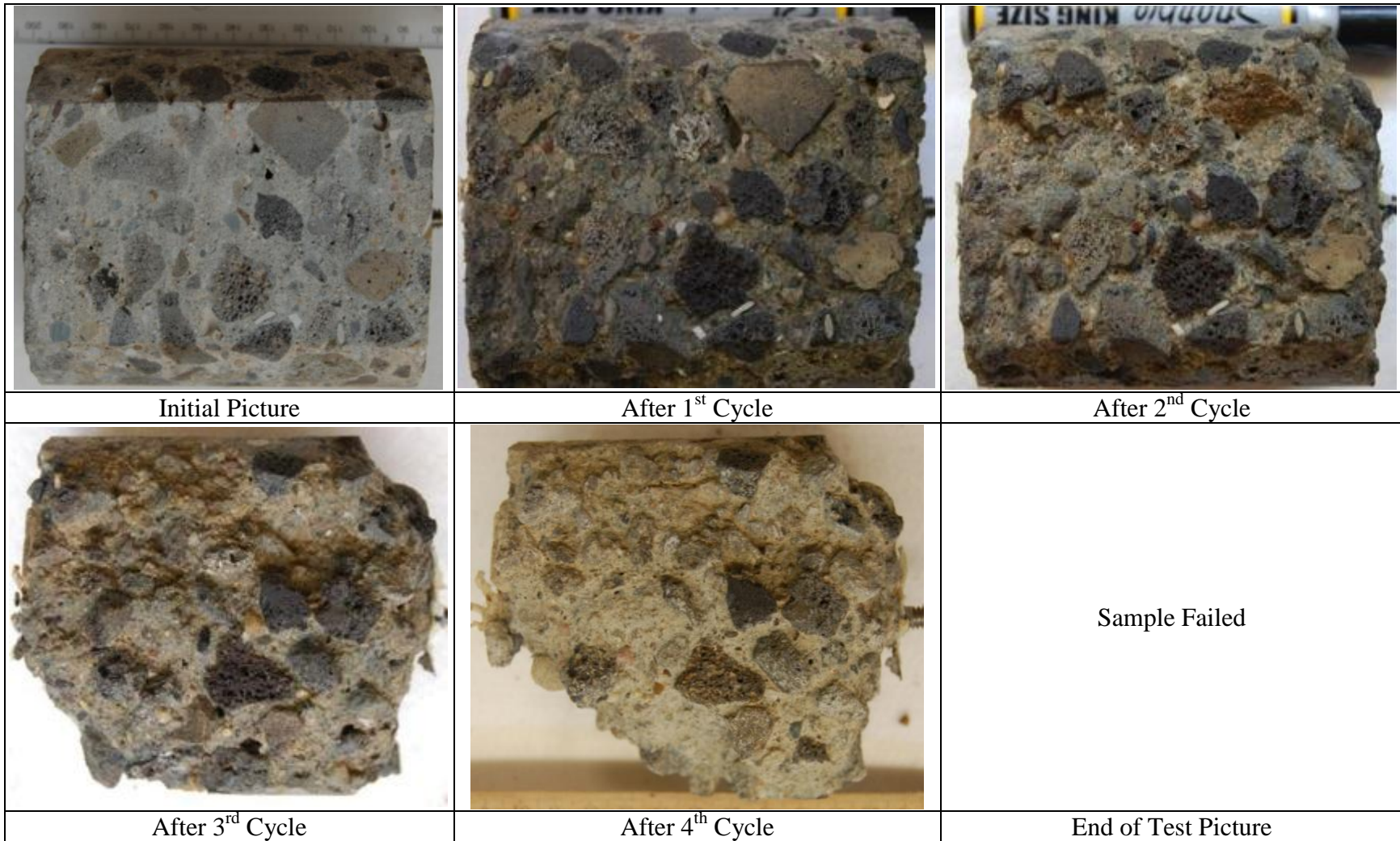


Figure 66: Visual Record of Airport V Runway Core 6 (6.4M KAc) During the Freeze Thaw Testing

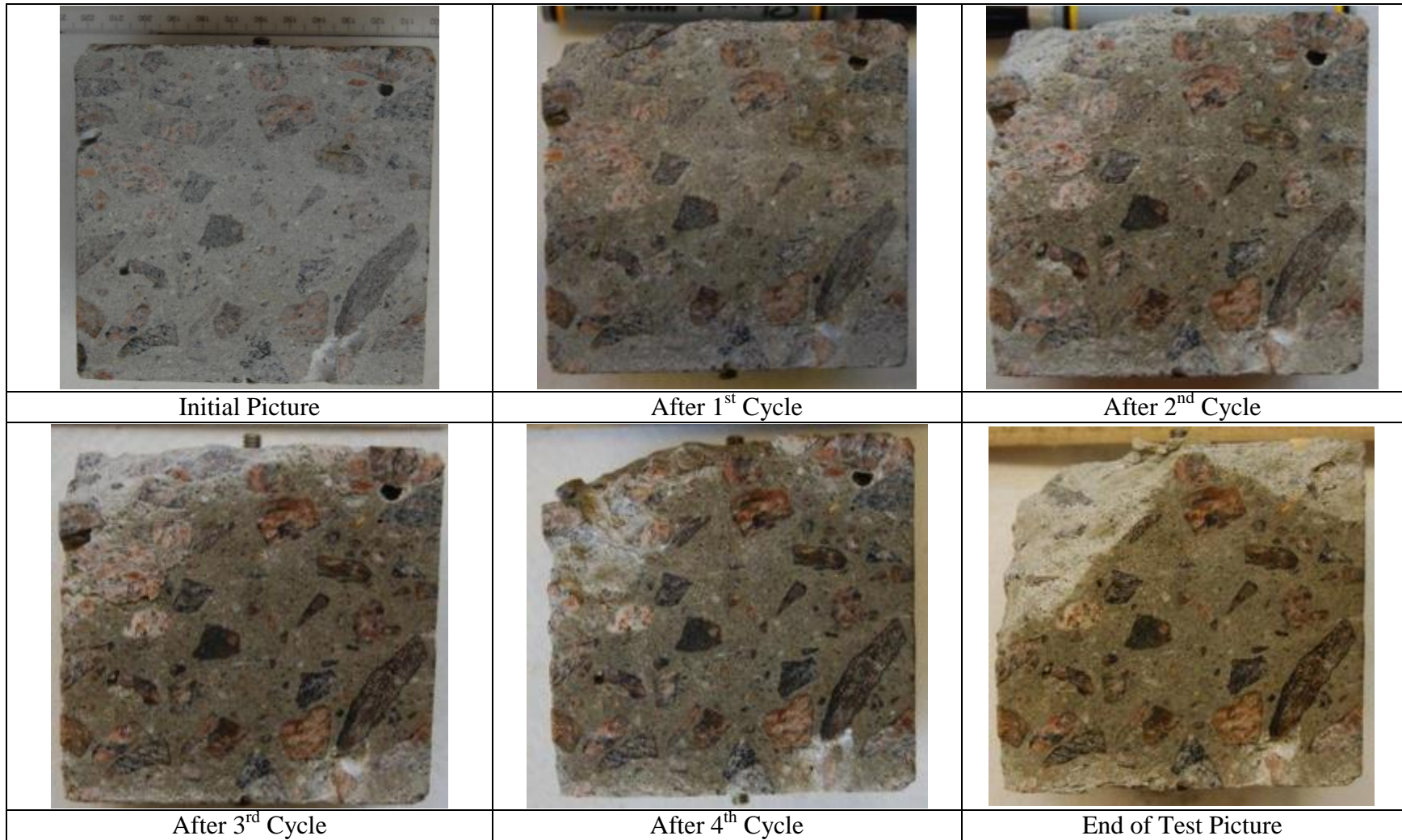


Figure 67: Visual Record of Airport VI Runway Core 7 (Control) During the Freeze Thaw Testing



		
Initial Picture	After 1 st Cycle	After 2 nd Cycle
	Sample Failed	Sample Failed
After 3 rd Cycle	After 4 th Cycle	End of Test Picture

Figure 68: Visual Record of Airport VI Runway Core 7 (6.4M KAc) During the Freeze Thaw Testing

Conclusion

The visual examination and pulse velocity results from the freeze thaw testing both supports the hypothesis that the potassium acetate deicer reduces the freeze thaw durability of the concrete system. The visual results show a failure of the mortar fraction of the concrete surface surrounding the coarse aggregates.

Known properties of KAc such as its reduction of freezing point temperatures and ability to decrease evaporation rates due to its hydrophilic nature coupled with the preliminary Cryogenic Dilatometer results show that there is a pessimum concentration of KAc at which more damage occurs in mortar samples. This point is where there is enough moisture left in the system to form the volume of ice needed to cause the cracking, and also the freezing point has not been depressed enough to prevent ice formation all together.

Part 5: Reactivity Testing of Airport Aggregates

Introduction

Aggregates were collected from Airports I – III. These aggregates were either used or were potentially used in the construction of the pavements in which the cores were selected. This section will present the results of 9 aggregates (made up of coarse and fine aggregates) being tested in the standard ASTM C 1260 test and the standard and modified versions of the ASTM 1293 Test. Airport I had six aggregates that were tested in this study (four coarse aggregates and two fine aggregates), Airport II had only one aggregate (coarse aggregate), and Airport III had two aggregates (one coarse and one fine aggregate). These aggregates were further studied for their aggregate reactivity, the results can be found in the Fundamental Investigation Appendix)

Method

ASTM C 1260 Test

The test was done according to ASTM C 1260 In this test method, mortar bars (25mm X 25mm X 285 mm) with gauge studs embedded at the ends were cast and moist cured for 24 hours in a curing room. After demolding, the bars were cured at 80°C for 24 hours in a water bath. After curing in the water bath, the bars were kept in 1N NaOH soak solution, which was preheated to 80°C for 24 hours. Periodic length change measurements were taken at regular intervals for 14 days, and percent expansion were calculated. The expansions of mortar bars less than 0.1% at 14 days were considered to be non-reactive aggregates, expansions in range from 0.1% and 0.2% were considered for additional confirmation by petrography, concrete prism tests (ASTM C 1293), or past field performance. Expansions of mortar bars over 0.2% were considered as reactive aggregates.

Standard and Modified ASTM C 1293 Test

This standard test was done according to the ASTM C 1293 Test, *Standard Test Method for Determination of Length Change of Concrete Due to Alkali-Silica Reaction*, which specifies storing the specimens vertically in a container with a small water reservoir that is not in contact with the prisms at 38°C. Modifications to this test were also incorporated, with the modified part of the test involving storing prisms in solutions of 1N NaOH and potassium acetate, similar to the ASTM C 1260 procedure. A additional modification was also tested which incorporated the use of an Air Entraining Agent to increase the air content from the standard 2.5% to the range of 6% to simulate field conditions. The use of 1N NaOH was to ensure that the Na_2O_e in the bars was still equivalent to 1.25% at all times during the test, due to the fact that some of the alkalis will leach out reducing the Na_2O_e in the standard ASTM C 1293 test. The modification using potassium acetate solution was done to determine the added effect of using a deicer, which is an external supply of alkalis, on the reactivity of the aggregates tested. “Pre-Removal” indicates that these samples were the ones that the aggregates were

removed from. These samples, having a cross section of 3"x3", were made with the respected aggregate and left to cure overnight in a 100% relative humidity room. The next day the samples were removed and initial comparator readings were taken and then the prisms were placed in their respected solution (1N NaOH or potassium acetate). These solutions were then placed in a 38°C room and readings were taken according to the schedule in ASTM C 1293. All of these readings were converted into percentage increases and then compared to the limit of 0.04% at one year, which indicates potentially deleterious reactive aggregate above this limit.

Results

Table 2: Airport Aggregate Labels and Reactivity Classification

Aggregate Source	Aggregate Label	Alternative Label	Reactivity
Airport I	CA-1	AGG-20	Non-Reactive
	CA-2	AGG-18	Reactive
	CA-3	AGG-19	Slightly Reactive
	CA-4	AGG-17	Reactive
	FA-1	AGG-21	Reactive
	FA-2	AGG-22	Reactive
Airport II	CA-1	AGG-29	Non-Reactive
Airport III	CA-1	AGG-27	Reactive
	FA-1	AGG-28	Reactive

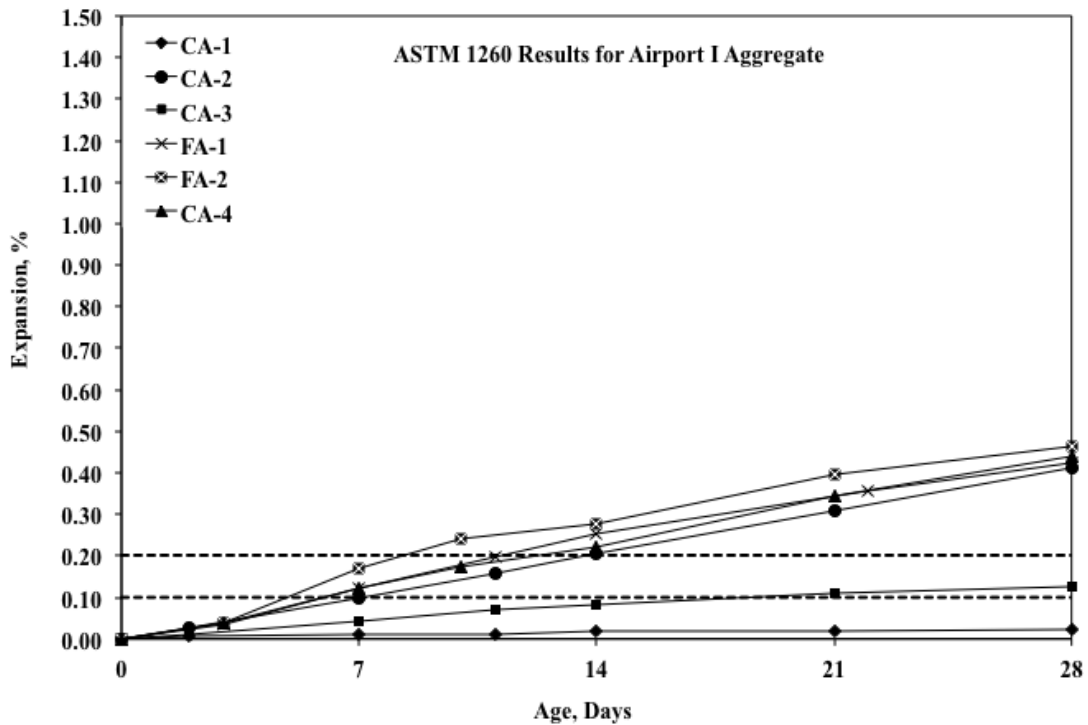


Figure 69: ASTM C 1260 Results for Airport I Aggregates

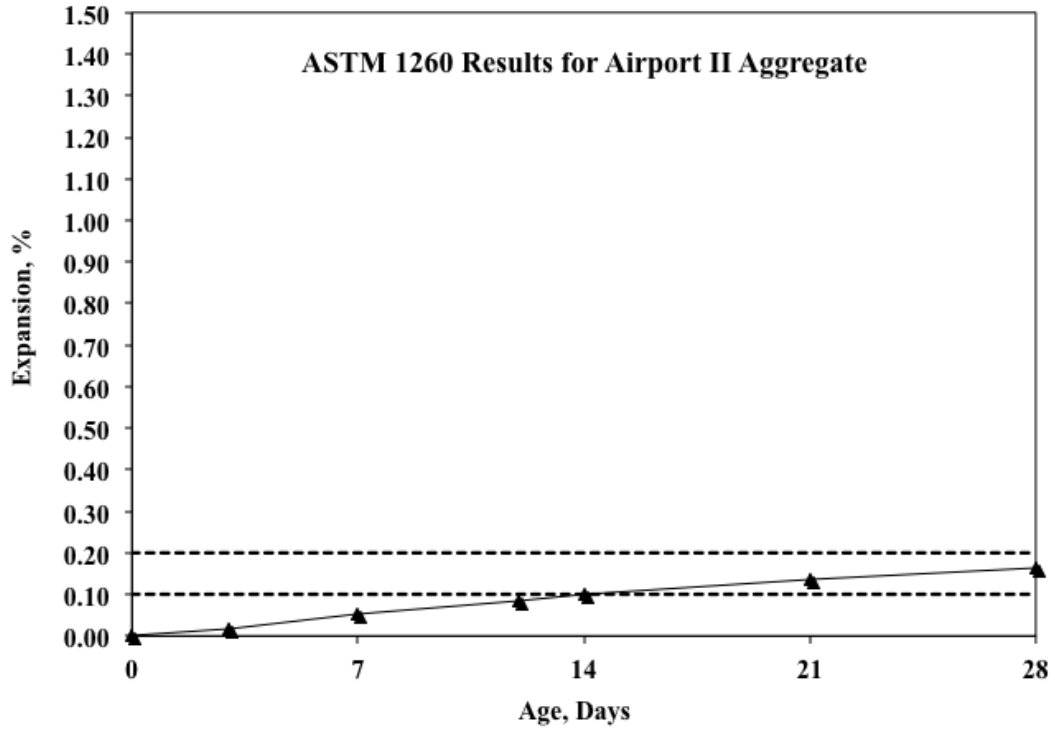


Figure 70: ASTM C 1260 Results for Airport II Aggregate

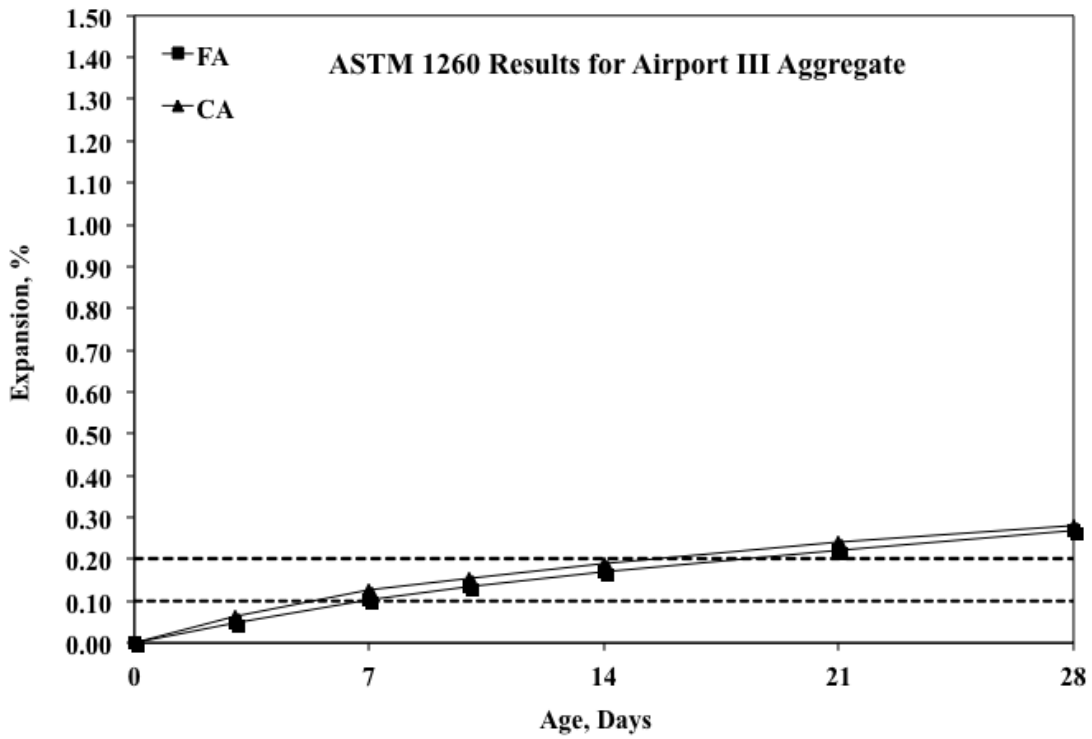


Figure 71: ASTM C 1260 Results for Airport III Aggregates

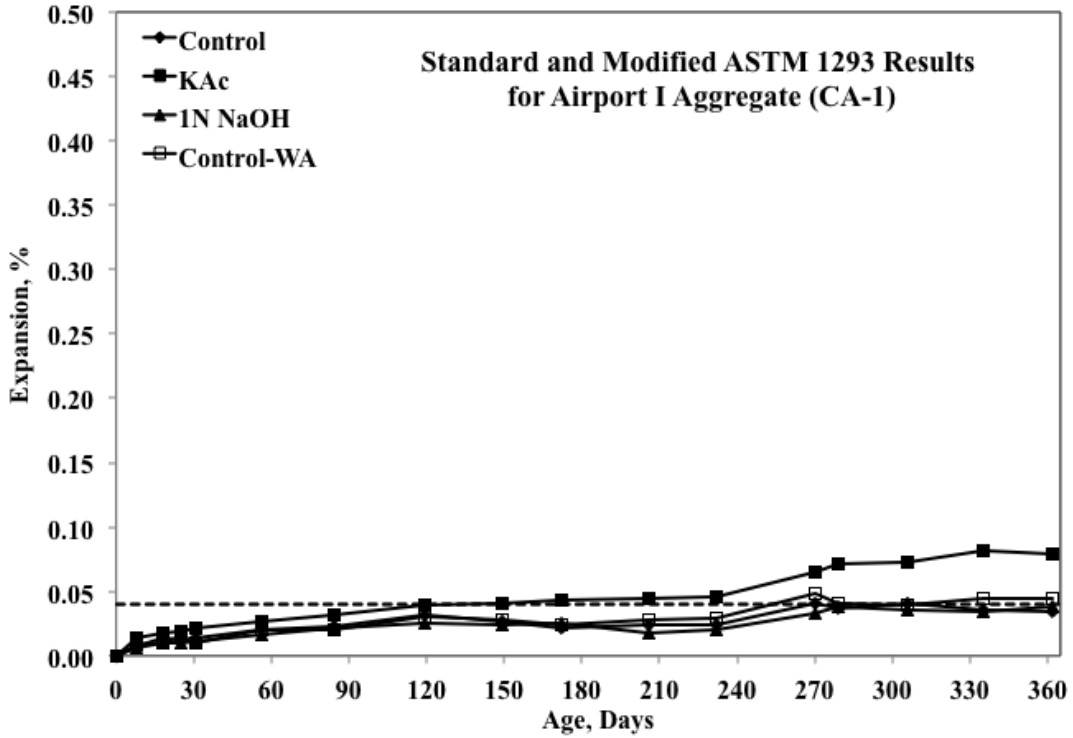


Figure 72: Standard and Modified ASTM C 1293 Results for Airport I Aggregate CA-1

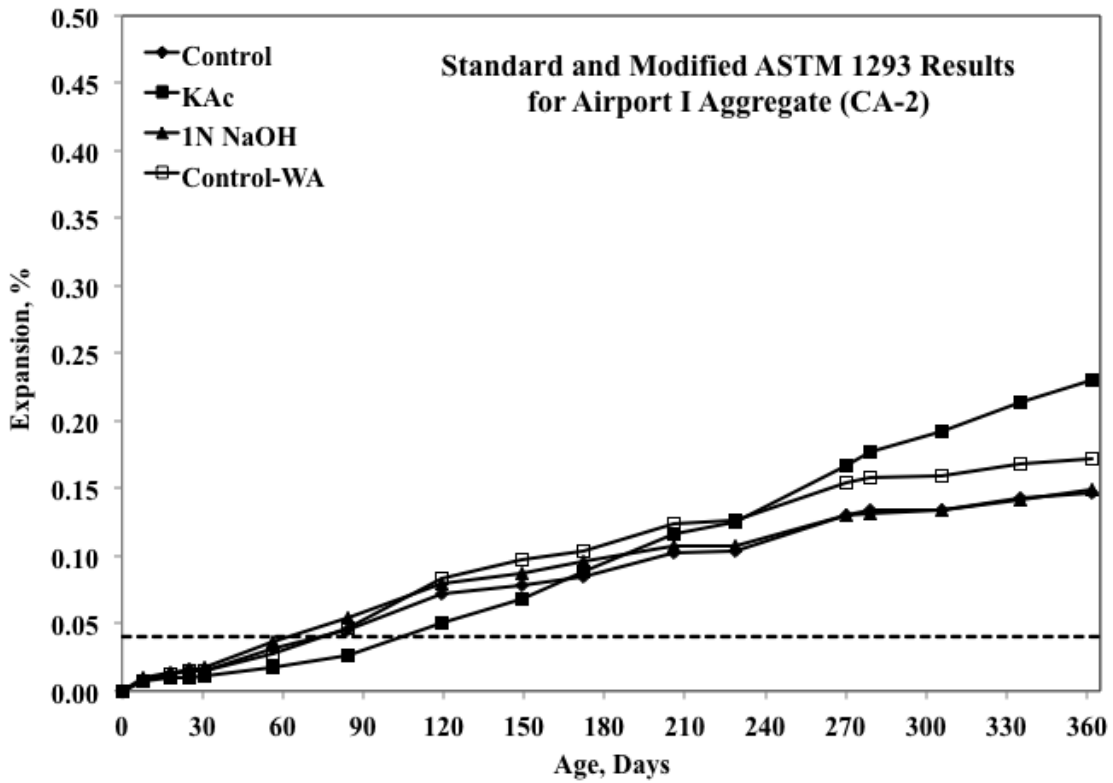


Figure 73: Standard and Modified ASTM C 1293 Results for Airport I Aggregate CA-2

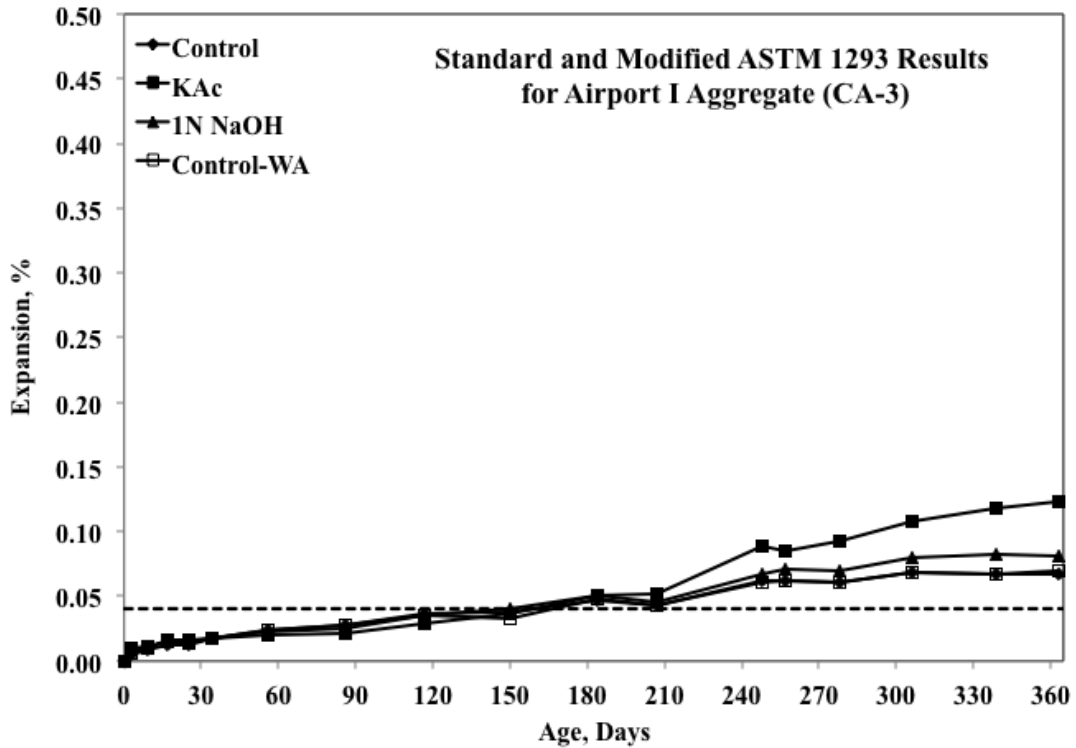


Figure 74: Standard and Modified ASTM C 1293 Results for Airport I Aggregate CA-3

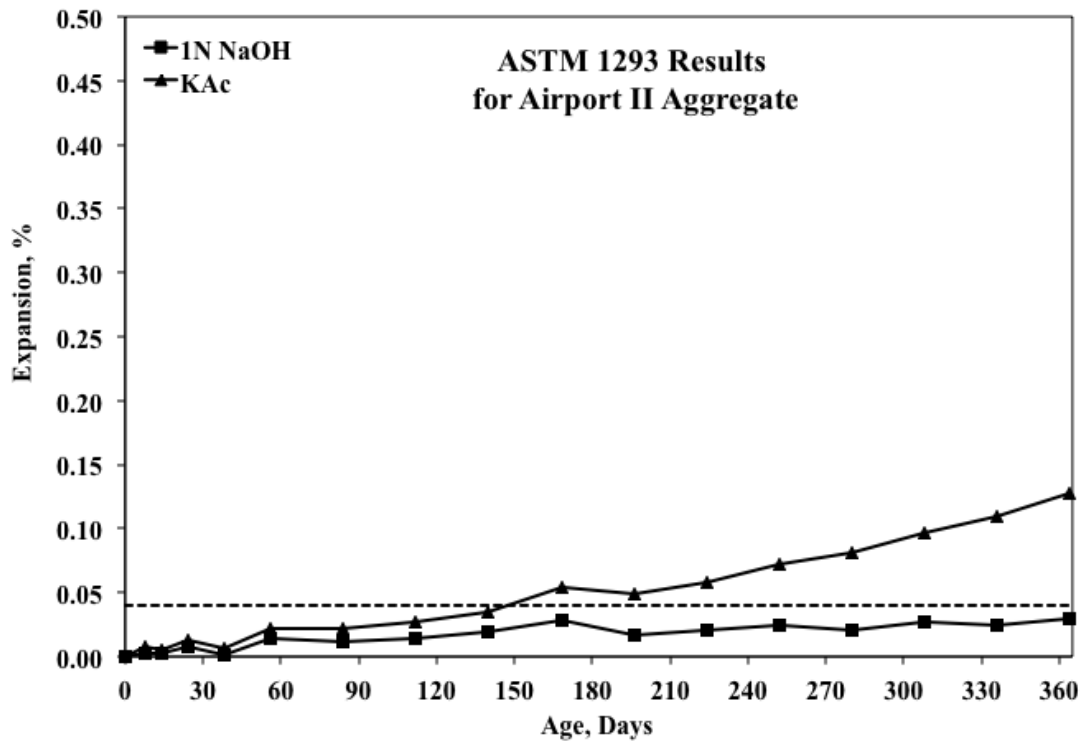


Figure 75: Modified ASTM C 1293 Results for Airport II Aggregate

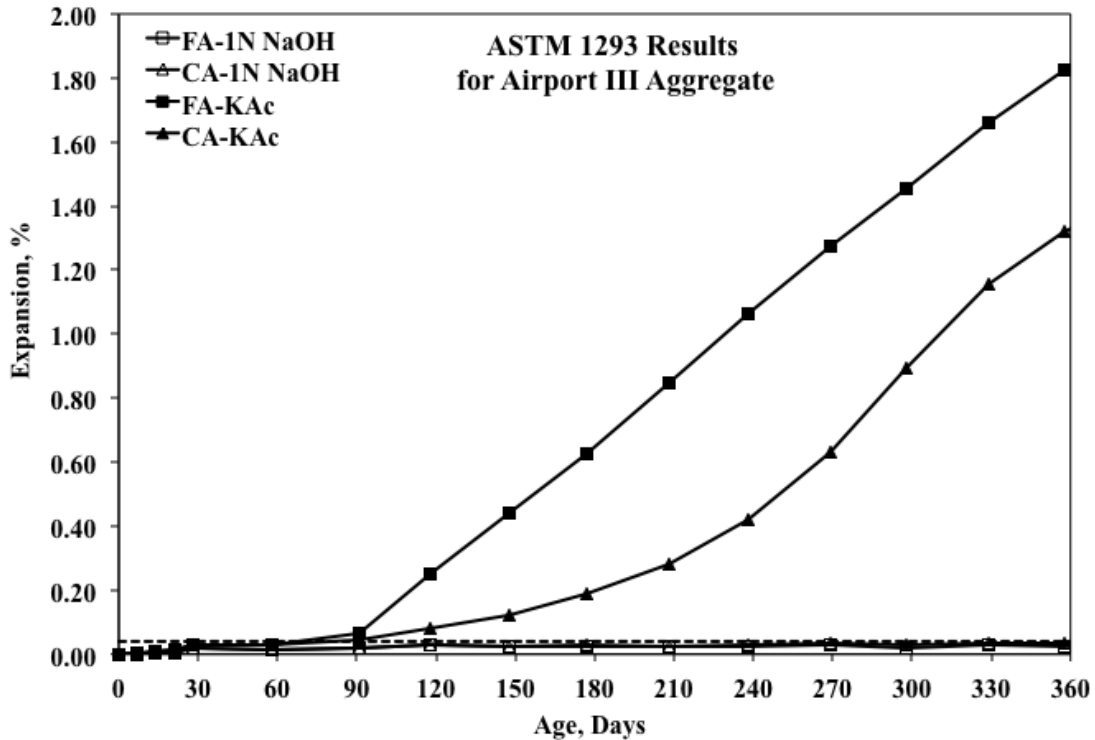


Figure 76: Modified ASTM C 1293 Results for Airport III Aggregates

The reactivity classification of the airport aggregates can be seen in Table 2. If the reactivity was close to 0.1% in the ASTM C 1260 test, the ultimate decision of whether or not it was reactive was determined through the ASTM C 1293 test. This only had an effect on two of the aggregates (Airport I CA-3 and Airport II CA-1). The modified ASTM C 1293 tests showed that some of the aggregates were more reactive in the presence of deicers and also that the additional air content did not aid in the reduction of the expansions.

Conclusion

Of the nine aggregates tested only two of the aggregates were deemed non-reactive. This made mitigation measure selection a necessity in the design of the pavements. From the Field Survey Data Appendix it can be seen that an attempt was made to mitigate these reactive aggregates, but mitigation measure selection and usage rates were inadequate to reduce these reactions. This will further be discussed in the Petrographic Examination Appendix and the Fundamental Investigation Appendix.